University of California at Davis
California Department of Transportation

DESIGN AND ANALYSIS OF AN AUTOMATED MECHANICAL SYSTEM FOR THE REPLACEMENT OF RAISED PAVEMENT MARKERS

Paul Sherrill, George Burkett, Professor Steven A. Velinsky: Principal Investigator, Duane Bennett: Chief Engineer

Report Number: CA08-0945

AHMCT Research Report:

UCD-ARR-07-06-30-02

Final Report of Contract: 65A0210, T.O. 07-10

AHMCT

Advanced Highway Maintenance and Construction Technology Research Center

Department of Mechanical and Aeronautical Engineering
Division of Research and Innovation

Technical Documentation Page

1. Report No. CA08-0945	2. Government Accession No.	3. Recipient's Catalog No.
4. Title and Subtitle Design and Analysis of an Automated Mechanical System for the Replacement of Raised Pavement Markers FINAL REPORT		5. Report Date June 30, 2007
		6. Performing Organization Code AHMCT
7. Author(s): Paul Sherrill, George Burkett, Duane A. Bennett, Steven A. Velinsky		8. Performing Organization Report No. UCD-ARR-07-06-30-02
9. Performing Organization Name and Address AHMCT Research Center Dept of Mechanical & Aeronautical Engineering, Univ. of California Davis, California 95616-5294		10. Work Unit No. (TRAIS)
		11. Contract or Grant IA 65A0210, T.O. 07-10
12. Sponsoring Agency Name and Address California Department of Transportation P.O. Box 942873, MS#83 Sacramento, CA 94273-0001		13. Type of Report and Period Covered Final Report July 2005 – June 2007
		14. Sponsoring Agency Code CALTRANS

15. Supplementary Notes

16. Abstract

    Raised pavement markers are used to delineate roadways because they provide excellent visual, tactile, and auditory feedback to drivers. However, over time markers can become dull or detach from the road, which necessitates their replacement. New markers must be placed relative to the existing installation, and this has traditionally been done by hand while riding in a specially-equipped truck.

    In order to improve cost efficiency and worker safety, this report presents an alternative method of marker replacement. The alternative is a machine designed to automate the replacement process. The ultimate product is described in general terms, but the main focus of this report is to describe the current prototype stage.

    The device will be carried by some vehicle. It is designed to allow for marker placement while the vehicle is in motion. To accomplish this, the primary installation equipment is mounted to a linear slide. The installation equipment is stationary with the road while placing a new marker, yet the vehicle can continue moving forward. A laboratory prototype has been developed and fabricated using a conveyor belt to simulate the relative motion of the road. The prototype can place a marker while the conveyor is at any speed up to 0.9 m/s (2 mph). The next stage of development will be a vehicle-mounted unit for field testing, and most of the current prototype can be transplanted for that purpose.

17. Key Words Automation, RPM, raised pavement marker, highway maintenance	18. Distribution Statement No restrictions. This document is available to the public through the National Technical Information Service, Springfield, Virginia 22161.		
20. Security Classif. (of this report) Unclassified	20. Security Classif. (of this page) Unclassified	21. No. of Pages 206	22. Price

Form DOT F 1700.7 (8-72)   Reproduction of completed page authorized
(PF V2.1, 6/30/92)

California AHMCT Research Center
University of California at Davis
California Department of Transportation

DESIGN AND ANALYSIS OF AN AUTOMATED MECHANICAL SYSTEM FOR THE REPLACEMENT OF RAISED PAVEMENT MARKERS

Paul Sherrill
George Burkett
Duane Bennett
Steven A. Velinsky

ABSTRACT

Raised pavement markers are used to delineate roadways because they provide excellent visual, tactile, and auditory feedback to drivers. However, over time markers can become dull or detach from the road, which necessitates their replacement. New markers must be placed relative to the existing installation, and this has traditionally been done by hand while riding in a specially-equipped truck.

In order to improve cost efficiency and worker safety, this report presents an alternative method of marker replacement. The alternative is a machine designed to automate the replacement process. The ultimate product is described in general terms, but the main focus of this report is to describe the current prototype stage.

The device will be carried by some vehicle. It is designed to allow for marker placement while the vehicle is in motion. To accomplish this, the primary installation equipment is mounted to a linear slide. The installation equipment is stationary with the road while placing a new marker, yet the vehicle can continue moving forward. A laboratory prototype has been developed and fabricated using a conveyor belt to simulate the relative motion of the road. The prototype can place a marker while the conveyor is at any speed up to 0.9 m/s (2 mph). The next stage of development will be a vehicle-mounted unit for field testing, and most of the current prototype can be transplanted for that purpose.

EXECUTIVE SUMMARY

Raised pavement markers are useful for road safety, as they provide superb visual, tactile, and auditory feedback to drivers. When RPMs become damaged or missing, they must be replaced. The current method for this replacement is suboptimal in terms of worker safety and cost effectiveness, leading to efforts at improving the replacement process through mechanical innovation.

Attempts have been made by other agencies to solve these problems, but no adequate solution has emerged. Therefore, this project aims to design an automated machine for the replacement of raised pavement markers. The machine will increase safety by removing the worker from a dangerous position and will increase cost effectiveness by speeding the rate of dot placement without adding excessive costs.

This report first describes the form and function of the final product as it is currently envisioned. The first field-deployable prototype is expected to use a trailer as its foundation, being towed by any standard automobile. It will sense existing raised pavement markers and place a new marker directly in front of the old. Deployment of the main apparatus will be accomplished with horizontal and vertical actuators, and the horizontal actuators will furthermore enable lateral targeting. For longitudinal targeting, precise actuation timing will position the dot placer at the correct point on the road, and the foot will secure this position by physically gripping the road surface. The linear slide allows the placement equipment to be stationary with the road while the vehicle is in motion, achieving proper placement and high average vehicle speed.

In addition to this ultimate vision, a laboratory prototype has already been developed. Its purpose is to enable the completion of the next step by proving the longitudinal targeting concept. Furthermore, the laboratory prototype can be transplanted onto the field-deployable prototype, aiding in cost efficiency.

The laboratory prototype of the marker placement device is then discussed. It consists of a carriage on a linear slide, actuated with a pneumatic band cylinder. It places dots onto a conveyor that simulates the relative motion of a road. On the carriage, there is a pneumatic foot to grip the conveyor, an adhesive dispenser, and a dot placer. First, the dot placer picks up a dot from a reservoir and thereby is ready for a target. When the system senses a magnet embedded at one point in the conveyor belt, it targets the new dot relative to that position. When conditions are right, it accelerates the carriage to match road speed and descends the foot to ensure a steady position. The adhesive dispenser actuates, the dot placer puts down the dot, and then the carriage returns to its home position to repeat the cycle.

The targeting process requires a deterministic response because of the infeasibility of feedback. As such, a calibration procedure is necessary to ensure that the control system takes into account the realistic response of the actuators. A special calibration routine is used to measure carriage acceleration. From those measurements, curve fits are made and inserted back into the control code. For the foot, a simple program measures the time necessary for the foot to fully descend, and this time is likewise inserted into the code. Finally, testing indicates that the

longitudinal targeting error is less than 1.3 cm (0.50 in) at speeds ranging from 0.2 m/s (0.5 mph) to 0.9 m/s (2 mph). This level of precision is adequate for field operation.

Of course, before testing of the prototype, various analysis techniques were utilized to ensure proper operation and ability of the device and these are summarized in the document. One is a dynamic pneumatic simulation that approximates the motion of the carriage. This simulation can be used to test various scenarios without spending the additional time and money that would be required to test them on the physical prototype.

Another analytical method is an energy-based determination of the linear slide's deformation under load. This can be used to verify that deformations are within acceptable bounds. Furthermore, the analysis can aid the optimization of beam design later.

Finally, a calculation was made for the worst-case lateral displacement of the carriage during marker placement. Such lateral movement can potentially result in targeting error and damage to the apparatus, but the targeting error is likely to be insignificant in most cases, and serious damage will not occur if the force of the foot is properly limited.

Analysis has also been performed for an alternative speed-matching method in which sophisticated pneumatic control is used instead of the road-grabbing foot. Whether it is ultimately worthwhile to remove the foot remains to be seen. However, it is assuredly possible according to the routine described herein. Future work will determine the final course of action.

In summary, this report presents the description and justification of a device for the automated placement of raised pavement markers. The premise for ultimate completion has been outlined, and complete details for the current stage of the project. Currently, there is a laboratory prototype of the main functional elements. The prototype is such that it can be transplanted onto a moving vehicle for field testing.

All information currently available indicates that the final product is feasible and will result in numerous benefits, the most notable of which are cost efficiency and safety.

TABLE OF CONTENTS

TABLE OF FIGURES

TABLE OF TABLES

DISCLAIMER

The research reported herein was performed as part of the Advanced Highway Maintenance and Construction Technology (AHMCT) Research Center, within the Department of Mechanical and Aeronautical Engineering at the University of California, Davis and the Division of Research and Innovation at the California Department of Transportation. It is evolutionary and voluntary. It is a cooperative venture of local, state and federal governments and universities.

The contents of this report reflect the views of the author(s) who is fare and responsible for the facts and the accuracy of the data presented herein. The contents do not necessarily reflect the official views or policies of the STATE OF CALIFORNIA or the FEDERAL HIGHWAY ADMINISTRATION or the UNIVERSITY OF CALIFORNIA. This report does not constitute a standard, specification, or regulation

CHAPTER 1

INTRODUCTION

On California roadways, raised pavement markers (RPMs or simply "dots") are frequently used to delineate lane divisions. In addition to being normally visible, they add tactile and auditory feedback to drivers when the vehicles' tires pass over the dots. Furthermore, some dots are reflective for excellent night visibility. In terms of size, a typical RPM measures approximately 10.16 x 10.16 cm (4 x 4 inches) at the base and 1.78 cm (0.7 inches) in height. They are made primarily of ceramic, but other materials are often used to improve surface properties. This is the case with reflective dots, which feature a reflective metal pattern overlayed with translucent plastic. RPMs are affixed to a roadway's surface by means of hot-melt bituminous adhesive.

Although durable, RPMs eventually fail. One way is when a dot separates from the road surface, exacerbated by the oscillatory force applied by vehicle tires passing over. Once disengaged from the road, the dot travels from its intended location and obviously cannot serve its proper function. The second common failure occurs when a dot's surface becomes dirty and worn, losing visible distinction from the surrounding road surface. This is especially detrimental for reflective dots, whose reflective boon becomes nullified. For either of these cases, RPM replacement is called for. For a missing dot, a new dot should be placed approximately in the evacuated location. For a dot with a worn surface, a new specimen can be placed just ahead of the old one. Removal is unnecessary.

Task Definition

It is clear that dot replacement is desired, but the exact method of accomplishing that is less certain. The first criterion for success is obviously the requirement that the result be adequate. If the method does not achieve a useful and durable RPM placement, it is unacceptable. Additionally, as with all things economical, monetary concerns are among the foremost. It is best to minimize the overall cost per benefit. In this case, the unit of cost is monetary expenditure, and the unit of benefit is a dot placed upon the road. Thus, cost effectiveness is best expressed as money per dot. Finally, the safety of human life is also vital. Although some risk is inevitable, law and good conscience mandate effort to minimize such risk.

Basic Requirements

Any method for RPM replacement must fulfill certain basic requirements. Because RPMs have undergone extensive engineering and refinement, it is unreasonable in the scope of this discussion for a replacement method to dictate the use of alternate dot technologies. The dots themselves should be utilized in their standard forms, and the method of attaching the dots to the surface should also be standard. In doing so, the probability of success is high, investment for development is minimized, and the final product is more likely to be adopted.

Another requirement is that a new dot be positioned correctly. It should be placed in the evacuated position of a missing dot or directly before a damaged dot. If the dot has directional

properties, it should also be oriented properly. Doing these tasks will allow the new dot to satisfy the function of the dot that is being replaced.

Cost Effectiveness

Cost

Consider the various monetary costs that are likely to be incurred by RPM replacement. Replacement will require some specialized equipment, so the purchasing cost of that equipment is one. That equipment will require maintenance, which will incur its own costs. Likewise, the equipment will require staff to operate it. Consumables will also be necessary. The most obvious consumables are the adhesive and RPMs themselves. Beyond this, fuels of various kinds are required and fuel efficiency of the system can minimize the associated expenditure. There are also indirect costs such as when a highway lane closure is necessary because the RPM placement vehicle moves slowly. The type and cost of lane closure can vary depending on the speed of the vehicle.

Naturally, there are many more indirect costs, but their relevance is likely to decrease with decreased proximity to the replacement method itself. Thus, due to presumption of complexity and irrelevancy, such indirect costs will be ignored hereafter. Furthermore, some of the aforementioned costs may not be effective differentiators between methods. If all methods incur a certain cost, that cost is irrelevant to method selection. If a cost is unique but it is insignificant relative to other costs, it can likewise be neglected.

It is assumed that the method will use an internal combustion vehicle. The directly associated costs in equipment, maintenance, and fuel are functionally identical among all methods considered. It is assumed that all methods consume the same amount of fuels, so the cost of fuels need not be addressed in evaluation. The operator staff is also assumed to be uniform among all methods. Thus the only costs to be considered for every method are the purchasing price of equipment and the cost of lane closure. If a method possesses a unique aspect that challenges these cost assumptions, it can be addressed on an individual basis.

Benefit

As mentioned previously, the unit of benefit is the successful placement of a dot onto a road. The total benefit of a method is the total number of dots it can place, expressed in placement rate and total quantity over lifetime.

Rate is relevant for a variety of reasons, the foremost being that it allows a minimal stock of equipment at any given time. It is generally beneficial to accomplish a task with one piece of equipment rather than two, unless there are exceptional cost differences to justify the equipment increase.

Here, the rate of RPM output will be determined by two factors: the typical speed of the placement operation itself, and process bottlenecks. The first factor is self explanatory indeed. If a method can place dots rapidly, its overall production rate is likely to be high. Process bottlenecks can reduce overall production by halting this normal operation of the method. For example, an adhesive melter may need to be refilled, which may temporarily halt production. Another bottleneck relates to equipment reliability. That is, equipment under repair is unable to

perform its function and its average production suffers. It is far preferable for a method to be reliable and avoid this "down time."

A final consideration that directly affects cost effectiveness is the expected lifetime of the equipment in terms of RPMs placed. Naturally, extra expense is justified for a system that can place more dots in its lifetime.

Safety

At all times, the safety of human life must be protected. First, the equipment must be safe for use by its operators. Second, in a busy roadway situation, traffic accidents are a major risk. As RPM replacement takes place at slow speed, the speed difference between the placement equipment and passing traffic is significant and hazardous. A typically feared scenario is one in which a vehicle runs into the rear or side of the dot placement equipment. This case must certainly be addressed in any method consideration, endeavoring to protect the equipment operators, the occupants of the colliding vehicle, and surrounding traffic.

However, it must be noted that serious injuries related to dot placement are rare. During the two years of 2001 and 2002 in California, injury costs related to the maintenance of raised pavement markers totaled about $3900, with no apparent permanent injuries [1]. Furthermore, most injuries were not associated with being exposed to traffic, although this exposure may seem dangerous. For this reason, safety improvements in that regard are not sufficient for justifying large increases in cost.

Traditional Method

The traditional method of RPM replacement in California involves a specialized truck (Figure 1). The truck contains a stock of adhesive and dots. It also has a small suspended sidecar on either side. The driver of the truck positions a sidecar near the point of dot replacement, and a worker sitting in the sidecar places a dot (Figure 2). He or she is equipped with an adhesive dispenser and a supply of dots. The worker dispenses about 240 mL (8.0 fluid ounces) of adhesive at the desired point and then places a dot, pressing the dot momentarily with approximately 36 N (8.0 pounds) of force. It is important for the worker to press enough for the adhesive to distribute evenly, but it is also important to not press too much as that would result in an excessively thin layer of adhesive. With less cushioning in the adhesive layer, the placed dot would be more likely to detach from the road surface after repeated loading by vehicle tires.

- 3 -

Figure 1: A traditional RPM placement vehicle

Figure 2: The traditional RPM placement action

There are several problems with this approach to dot replacement. A striking aspect is that the worker in the sidecar is placed in close proximity to traffic—a matter of inches, as vehicles pass in the adjacent lane. For safety, it would certainly be advantageous to remove this worker from this position, bringing him or her into the truck's interior, better protected from traffic.

- 4 -

Regarding cost, the use of a dedicated truck has several ramifications. It is an integrated system, so when one important part of it fails, the entire system becomes inoperable. For example, engine trouble completely prevents dot replacement, even though all the replacement-specific equipment may be operational. A decoupling of the vehicular and replacement functions is therefore desirable. Integrated systems are also typically more expensive initially. In addition to safety and cost issues, the rate of dot placement is lackluster. It is nearly as efficient as any hand-placement system could be, but it is still a far stretch from being mechanically optimal: the placement operation itself is limited by the speed of the individual placing the dot, and the truck must stop completely at every replacement point. An automated system could accelerate the placement process itself and also contrive some means for the truck to remain in motion during the placement.

Some goals for improvement over this method include improving worker safety, increasing the speed of the placement operation, and allowing the vehicle to remain in motion during placement. These objectives are the most likely to decrease injury rates and increase cost effectiveness.

Historical Development

Previous AHMCT Version

About 1992, AHMCT produced a prototype system for the automated replacement of RPMs. It had an adhesive dispenser and a dot placement device affixed to a carriage. This carriage would travel along an actuated linear slide such that the placement equipment could be stationary with the road even when the vehicle was moving. That is, a vehicle traveling at a given speed would have the carriage travel backward at that same speed. Through this approach, dots could be placed at speeds up to 16 kph (10 mph). The carriage would then travel again to its forward position, thereupon being ready for a new cycle of placement. See Figure 3.

Figure 3: The previous AHMCT marker placement vehicle

This system was advantageous over the traditional method in several ways. Safety was greatly improved because of the automation. No worker was exposed to traffic. The performance

- 5 -

of the device was also impressive, being capable of placing a dot at a vehicle speed of 16 kph (10 mph).

However, the system was not without its problems. Placement at 10 mph required the linear slide to be long, making it generally cumbersome. The slide also needed to be low to the ground in order to facilitate placement, and this coupled with the extreme length made collisions with the ground a grave concern. Furthermore, the linear slide used ball bearings. The ball bearings made it slide very easily, but would require shielding to protect those bearings in a dirty roadway environment. Effective shielding over the length of the slide was problematic. Generally, the slide actuator and the slide itself were delicate. Lateral positioning of a new dot was also completely determined by the position of the vehicle. There was no lateral targeting for placement. The actuated slide used a timing belt and a servo motor for actuation, and although this technology was effective, it was expensive at approximately $12,000 cost at the time. A final noteworthy limitation is that when the device was operating at 16 kph (10 mph) continuously, it could place successive dots with spacing no less than 7.0 m (23 ft) [2].

TRPMA

In 1995, the Telerobotic Raised Pavement-Marker Applicator (TRPMA) prototype was completed by Rami Rihani and Leonhard Bernold at the North Carolina State University of Raleigh [3]. Its primary purpose was to improve worker safety by moving the worker from his sidecar position to the truck's cab. To place the dots, TRPMA utilized a system of various actuators. The driver would stop the truck at a dot replacement point. A video camera would transmit a closed-circuit television image of the road to another worker in the truck's cab. Using this image, the worker would select the lateral position for the dot placement, and the equipment would place the dot as such.

TRPMA's only virtue was the improvement in safety gained by moving the worker from the sidecar to the cab. By the creators' estimation, TRPMA had the potential to merely match the overall speed of the traditional method. Because the truck had to stop at each point and lateral targeting input was also required, improvements in speed are fundamentally precluded. Even the ability of the system to correctly position a dot is questionable, as it could only target laterally. Longitudinal positioning depended solely on the vehicle's stopped position, controlled by the driver. Even in the traditional method, the sidecar worker can compensate for small amounts of driver error in any direction. Furthermore, one may presume that the TRPMA system would be considerably more expensive than the traditional method because it incorporates a relatively complex system of structures, generators, actuators, and a computer. Being so economically disadvantageous, even claims of improved worker safety may be inadequate justification.

MRL's Attempt

The company Mark Rites Lines (MRL) has developed a machine for the placement of raised pavement markers. However, due to company secrecy, full details on MRL's device are not available. The most reliable source of information is from the photographs published on MRL's web site, shown here in Figure 4 and Figure 5.

Figure 4: MRL's RPM placement vehicle [4]

Figure 5: A closer view of the placement apparatus [4]

Figure 4 shows a side view of MRL's prototype truck, and Figure 5 shows a closer view of the area having to do with dot placement. Notice the functional resemblance between these and Figure 1 and Figure 2 featured in the description of the traditional method. Like the traditional method, the MRL device has a worker placed in a sidecar, and there is no apparent means of placing an RPM while the vehicle is in motion. Thus, the only evident advancements over the traditional method are based in safety: placing a guardrail to protect the worker and instituting a mechanism to place the adhesive and the dots so the worker need not do it by hand. The increase in safety is questionable because the worker is not far removed from traffic. With the supposed lack of performance increase as well, the expense required to accomplish this setup is economically unjustifiable.

- 7 -

The Georgia Tech Research Institute (GTRI) is currently developing a machine to place raised pavement markers. According to one article, the device is capable of placing an RPM with hot adhesive while the vehicle is moving at 8.0 kph (5.0 mph) [5]. It is also capable of 0.91 m (3.0 ft) of lateral targeting. These are impressive capabilities, but the overall usefulness of the Georgia system depends on its limitations. For example, the article states that the machine typically places RPMs 24 m (80 ft) apart. If the machine cannot achieve closer spacings, it may not be appropriate for many dot-laying tasks. GTRI has been unwilling to share information with AHMCT, so a precise evaluation of their device is impossible.

Figure 6: GTRI's placement vehicle [5]

Figure 7: GTRI's placement vehicle [5]

Figure 6 and Figure 7 display GTRI's prototype device. Clearly, it is unique from the design discussed later in this report. As such, it is extremely interesting and important. However, the inability to discern its detailed costs and benefits places AHMCT in the position to carry on regardless. While the GTRI device is a worthy concern, it is not sufficient to impede AHMCT's research.

Goals for this Project

A major goal for this project is to accomplish relatively fast vehicle speed during dot placement. By doing so, road crews can use a moving lane closure, which is much more efficient than a static lane closure. A static lane closure involves more preparation, consuming extra time of workers and equipment [2]. To accomplish the fast vehicle speed, it is necessary to enable the dot placement system to work while the vehicle is in motion. Even if the placement operation were instantaneous, the vehicle would not be able to maintain an adequate average speed if it had to stop at every replacement point. The placement must occur while the vehicle is moving.

Like any project of this nature, the worker will be removed from the sidecar to increase his safety. The magnitude of the safety improvement is difficult to determine, but a definite improvement exists. Some human life will be preserved because of this change.

It is problematic to have the vehicle and dot placement systems integrated, since the failure of either one will temporarily halt the use of the other. For this reason, one goal is to put the dot placement system onto a trailer that can be towed by non-dedicated vehicles.

Chapter Summary

Chapter 1 has outlined the foundation upon which the remainder of this report is premised. Raised pavement markers are useful for road safety, as they provide superb visual, tactile, and auditory feedback to drivers. When RPMs become damaged or missing, they must be replaced. The current method for this replacement is suboptimal in terms of worker safety and cost effectiveness, leading to efforts at improving the replacement process through mechanical innovation.

Attempts have been made by other agencies to solve these problems, but no adequate solution has emerged, with the uncertain exception of GTRI's prototype. Because the workings of GTRI's prototype are kept secret, it cannot be evaluated. Therefore, this project aims to design an automated machine for the replacement of raised pavement markers. The machine will increase safety by removing the worker from a dangerous position and will increase cost effectiveness by speeding the rate of dot placement without adding excessive costs.

CHAPTER 2

DESCIPTION OF PLANNED PRODUCT

Although the final product has not been designed in perfect detail, it is important to understand its overall goals. This gives context to present accomplishments and future work. As such, this chapter describes the basic anatomy and function of the machine as it is predicted to be in a field-deployable form.

Anatomy

The product design presented here takes the form of a trailer-based unit. However, it is noted that the basic mechanism can be easily accommodated to a truck as well, and that the trailer-based unit is used here because it will likely be the form of the first field-operational prototype. First, the anatomy of the machine is described.
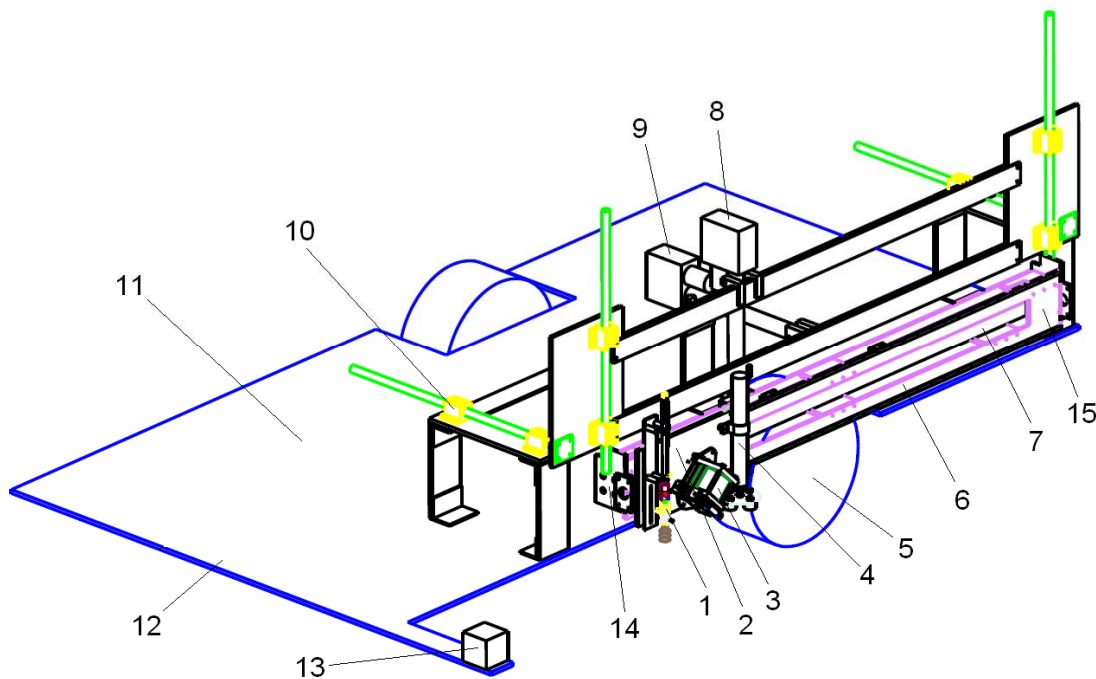
Figure 8: Isometric view of the product, annotated

- 10 -

Number	Description
1	Dot placer
2	Carriage plate
3	Adhesive dispenser
4	Foot
5	Trailer wheel
6	Linear slide
7	Band cylinder
8	Vertical actuator
9	Lateral actuator
10	Linear bearing
11	Trailer bed
12	Trailer front
13	Dot sensors
14	Home end of the linear slide
15	Far end of the linear slide

Table 1: Key for Figure 8 through Figure 11
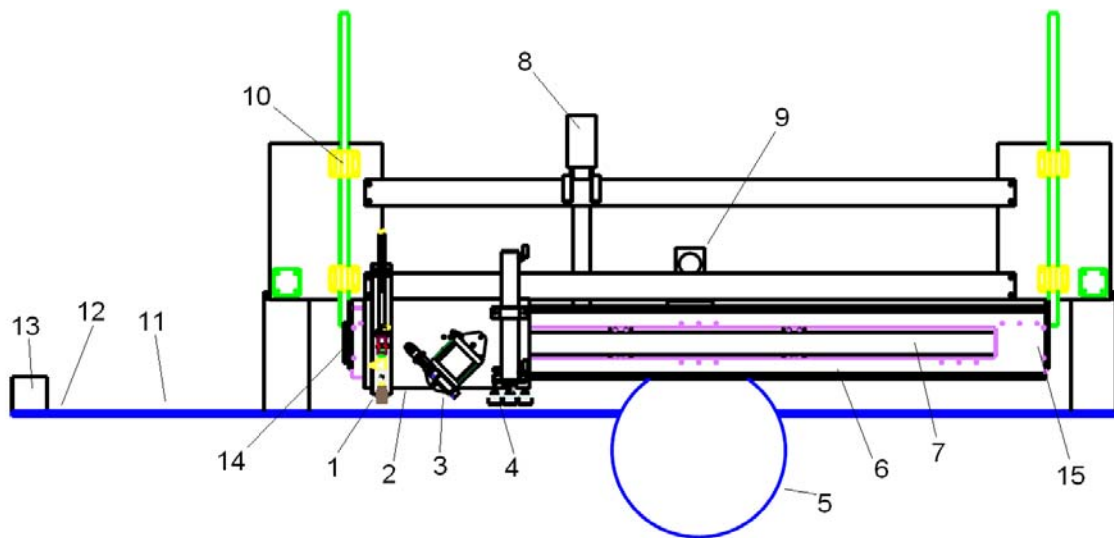
Figure 9: Side view of the product
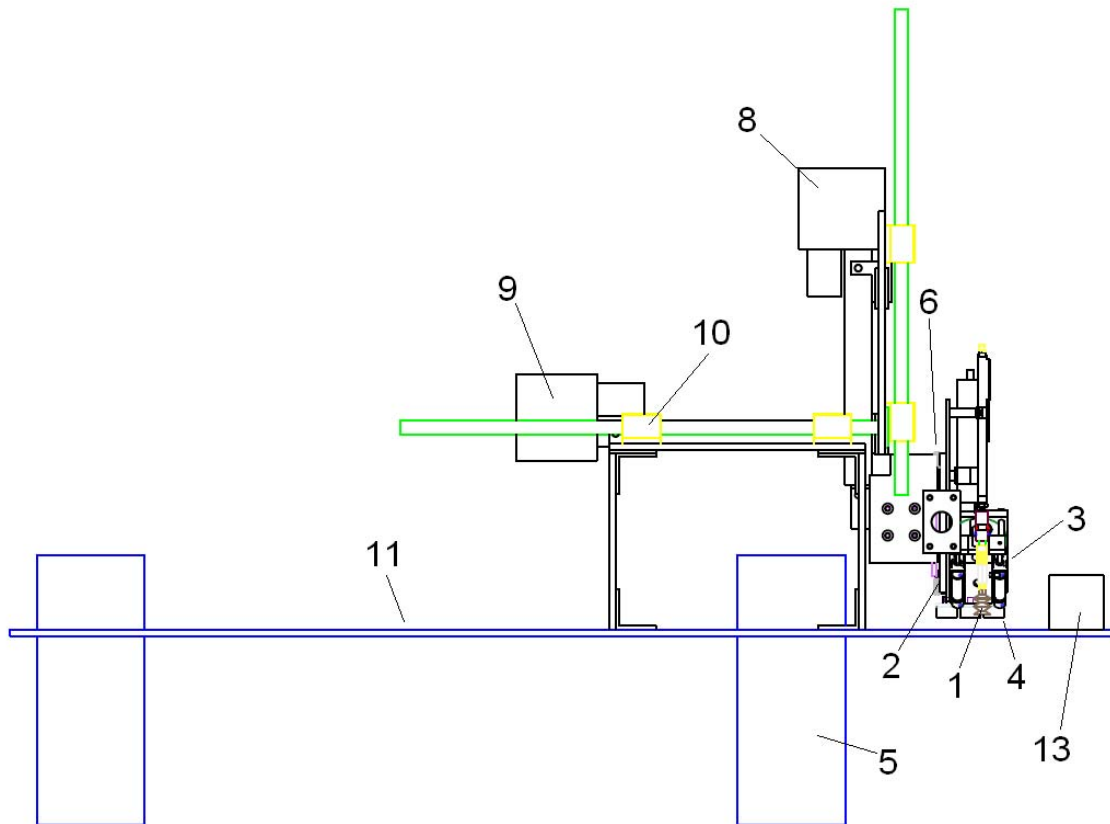
Figure 10: Front view of the product
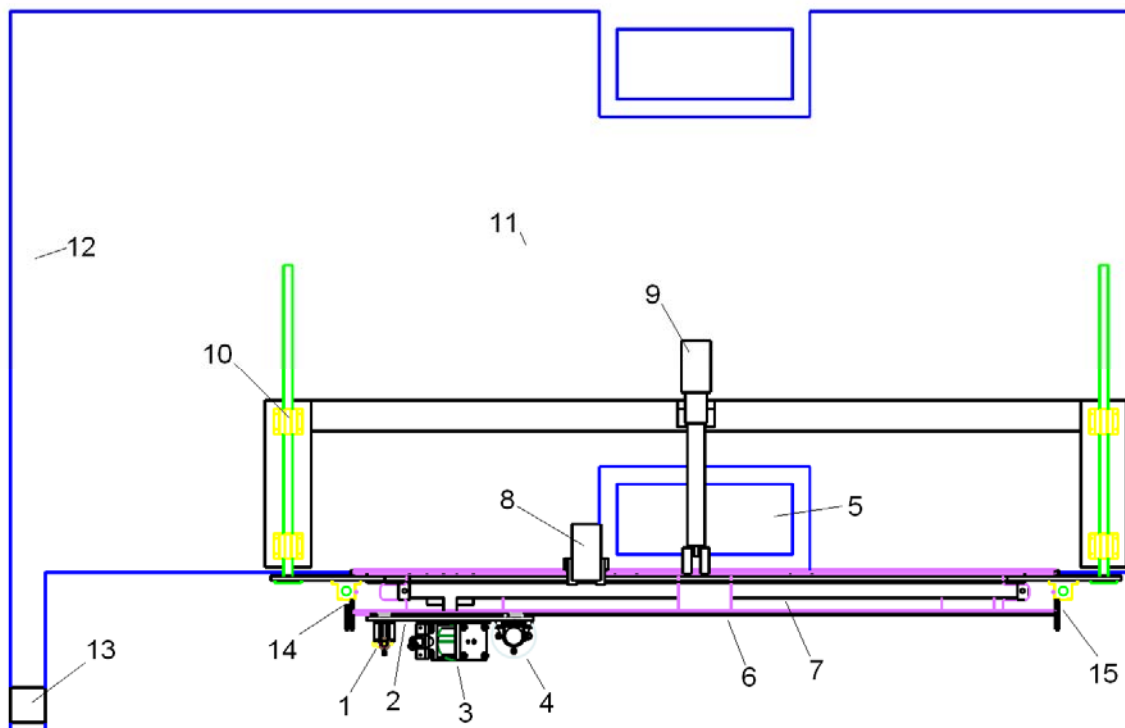
It must be noted that the device pictured in Figure 8 and on through Figure 11 is incomplete. Missing items include an air compressor, an adhesive melter, an electric generator, and a dot storage container. While necessary, these items are mundane and static. They may be omitted from further discussion without impairing the operational description.

Functional Description

The product will be described in terms of its functionality, in the sequence of actions necessary during typical operation.

Deployment

First, the linear slide deploys into a position where it has access to the roadway surface. This is accomplished by the lateral and vertical actuators, moving the linear slide outward and down. Thus the dot placer is positioned close to the road, and also in line with the dot sensors. The dot placer obtains a dot from the dot dispenser, and the system is ready.

Dot Sensing

The device's essential purpose is to place a new dot where an old dot is dirty or missing entirely. Consider the case of a dirty dot. The dot is detected by the dot sensors, which are four laser range-finders distributed laterally with 2.54 cm (1.00 inch) spacing. Due to this spacing, the sensors can only sense the dot's lateral position to within 1.27 cm (0.500 inch).
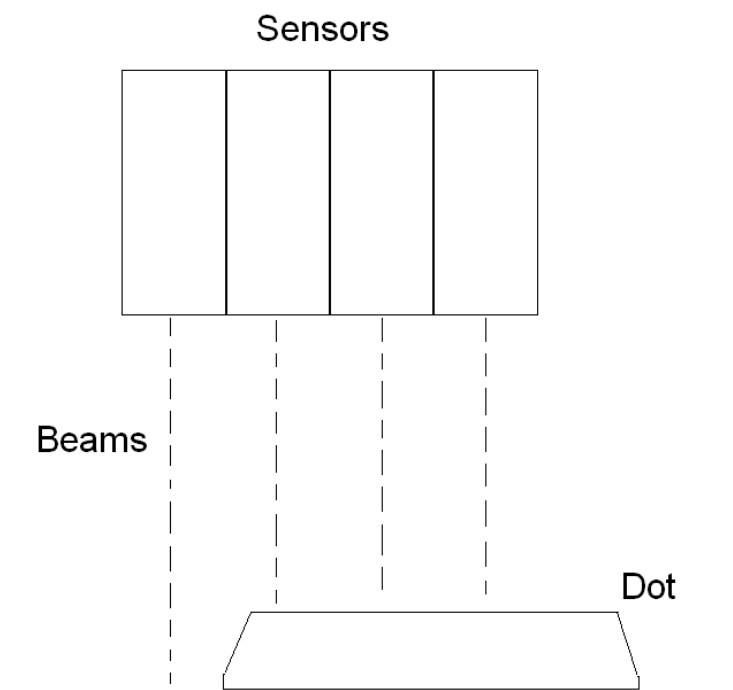
Figure 12: Dot sensors

- 13 -

In the case presented in Figure 12, three sensors detect a sudden increase in proximity when their beams reach the dot. This sudden increase in proximity is the method for sensing the dot. Furthermore, because the leftmost beam strikes only the road, it is known that the dot is positioned slightly to the right. From this lateral sensing, the lateral actuator can position the linear slide accordingly.

In addition to locating the dot laterally, the sensors locate it longitudinally. After the initial detection, an angular encoder on the trailer's wheels updates the longitudinal position of the dot as the vehicle moves forward. The goal is to place the new dot in front of the old dot by 2.54 cm (1.00 inch). By being in front of the old dot, it is visible while still maintaining the existing dot pattern. The old dot does no harm by remaining.

Missing Dot

Of course, there is also the case where the old dot is actually missing. The system must determine that a dot is missing by predicting spacing and recognizing when that spacing is violated. The system records recently observed spacings. If it detects a vacant region significantly larger than the typical spacing, it will assume that a dot is missing and place one according to the typical distribution. Spacings are not perfectly uniform even when all dots are present, so the system must be fairly tolerant of large spacings, only assuming that a dot is missing when the spacing is truly exceptional.

This presents a problem in that the dot sensors are not very far ahead of the dot placer. Thus, by the time the dot sensors have observed an exceptionally large vacant distance, the dot placer may have already passed the ideal placement point for the new dot. A solution is to position the dot sensors farther ahead of the placer, but the only way to feasibly gain a significant increase is to put the sensors at the front of the vehicle that is towing the trailer. This would involve troublesome modification of the towing vehicle. It may be more practical to simply tolerate the slightly erroneous placement that is likely to occur when a dot is missing.

Another solution is to give the operator the ability to place a dot at will. The operator knows when a dot is missing and can position the vehicle at the approximately correct location. At the press of a button the device can place a new dot where it is, or it can delay for a certain distance, depending on how the operator can best aim at a certain location. Operator-initiated placement is the most straightforward way to achieve excellent results when replacing a missing dot. As such, it warrants preliminary testing.

Speed Matching

An important goal for the device is to place a new dot while the vehicle is in motion. This is accomplished by moving the carriage rearward on the linear slide such that the carriage is stationary with respect to the road even as the vehicle is moving. At the proper moment, high pressure air is applied to the home end of the band cylinder, forcing it rearward. The foot descends such that it makes contact with the road just as the carriage matches the road speed. The acceleration of the carriage prevents shock and slippage of the foot, and the foot ensures that the carriage is stationary with the road during the placement operation.

Longitudinal Targeting

In addition to matching the speed of the road, the carriage must move such that the new dot will be placed at the proper longitudinal position. This necessitates consideration of the overall process such that the desired outcome is achieved. Namely, the foot must contact the road at the moment the carriage has matched vehicle speed and is in the proper longitudinal position to place the new dot. The derivation begins with the idea that the acceleration process requires a certain amount of time and a certain amount of displacement relative to the vehicle, and each is a function of the vehicle speed v. That is, the faster the vehicle is moving, the more time and displacement the carriage will need to achieve that speed. To achieve speed equal to v, the time and displacement required are expressed as

$$\Delta t_{acc} = f_t(v), \tag{1}$$

$$\Delta x_{acc} = f_x(v), \tag{2}$$

where $f_t(v)$ and $f_x(v)$ are known from prior measurements. Note that displacements here are relative to the vehicle. The direction from the vehicle's front to rear is considered positive, and the direction from the rear to front is negative. Thus, as the vehicle travels forward, any point on the road is undergoing positive displacement. Likewise, when the carriage moves rearward on the trailer, it is undergoing positive displacement. Next, it is assumed that the descent of the foot takes a certain amount of time as expressed by

$$\Delta t_{des} = \text{constant}. \tag{3}$$

To achieve the desired carriage speed at the proper position, acceleration must begin when the displacement to reach the target location is equal to the net displacement that will occur during acceleration, as in

$$x_{target} - x_{cup,i} = \Delta x_{acc} - v * \Delta t_{acc} \tag{4}$$

where $x_{cup,i}$ is the longitudinal position of the dot placer in the home position, and x_{target} is the position of the target location on the road. The carriage will move rearward by Δx_{acc}, but will move forward with the vehicle by $v * \Delta t_{acc}$. Depending on which effect is greater, the acceleration may begin before or after the target location has passed the dot placer. Rearranging (4), acceleration should begin when

$$x_{target} = x_{cup,i} + \Delta x_{acc} - v * \Delta t_{acc}. \tag{5}$$

Now it must be determined when the foot should descend. Similar to the speed-matching equation, the foot should begin descending when the displacement to the target location is equal to the displacement that the carriage will undergo during descent, expressed by

$$x_{target} - x_{cup,i} = \Delta x_{acc} - v * \Delta t_{des}. \tag{6}$$

Rearranging, foot descent should begin when

$$x_{target} = x_{cup,i} + \Delta x_{acc} - v * \Delta t_{des}. \tag{7}$$

Dot Placement

Once the carriage is secured to the ground by the foot, the dot placement operation begins. First, the adhesive dispenser ejects a slug of about 240 mL (8.0 fluid ounces) of hot-melted bituminous adhesive onto the target location. Then the dot placer descends, deposits the

new dot, and ascends. The foot retracts, and then the carriage is ready to return to the home position.

Carriage Return

To return the carriage to the home position, high pressure is applied at the far end of the band cylinder. The carriage quickly travels toward the home position until it passes a certain position and begins the braking procedure. Braking involves switching a valve on the home end such that air can only escape the home end through a restrictive orifice. The air trapped inside the home end cushions the carriage and then slowly escapes, allowing the carriage to gently move into place.

Chapter Summary

This chapter described the form and function of the final product as it is currently envisioned. The first field-deployable prototype is expected to use a trailer as its foundation, being towed by any standard automobile. It will sense existing raised pavement markers and place a new marker directly in front of the old. Deployment of the main apparatus will be accomplished with horizontal and vertical actuators, and the horizontal actuators will furthermore enable lateral targeting. For longitudinal targeting, precise actuation timing will position the dot placer at the correct point on the road, and the foot will secure this position by physically gripping the road surface. The linear slide allows the placement equipment to be stationary with the road while the vehicle is in motion, achieving proper placement and high average vehicle speed.

In addition to this ultimate vision, a laboratory prototype has already been developed. Its purpose is to enable the completion of the next step by proving the longitudinal targeting concept. Furthermore, the laboratory prototype can be transplanted onto the field-deployable prototype, aiding in cost efficiency.

CHAPTER 3

CURRENT PROTOTYPE

A prototype was constructed to verify the essential dot placement concepts, especially longitudinal targeting. Detailed anatomy can be found in Figure 13.

Anatomy

Herein the existing prototype is described hierarchically with photographic aid. First, a picture of the entire device is presented in Figure 13.
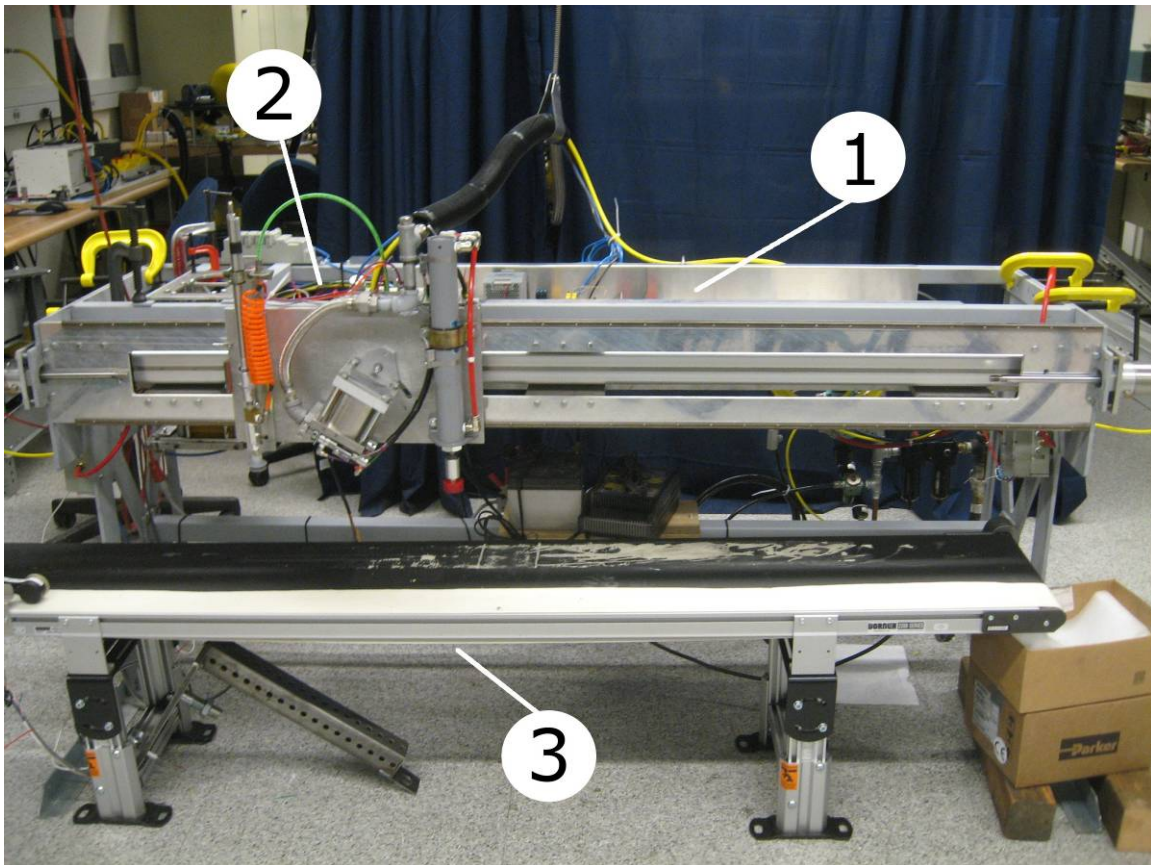
Figure 13: The current laboratory prototype

Number	Description
1	Linear slide
2	Carriage
3	Conveyor

Table 2: Key for Figure 13

The linear slide encompasses many components necessary for linear guidance. The carriage moves along the linear slide for marker placement operations, and the conveyor simulates the relative movement of the road were the RPM machine on a moving vehicle.

Linear Slide

The components of the linear slide are detailed in Figure 14.
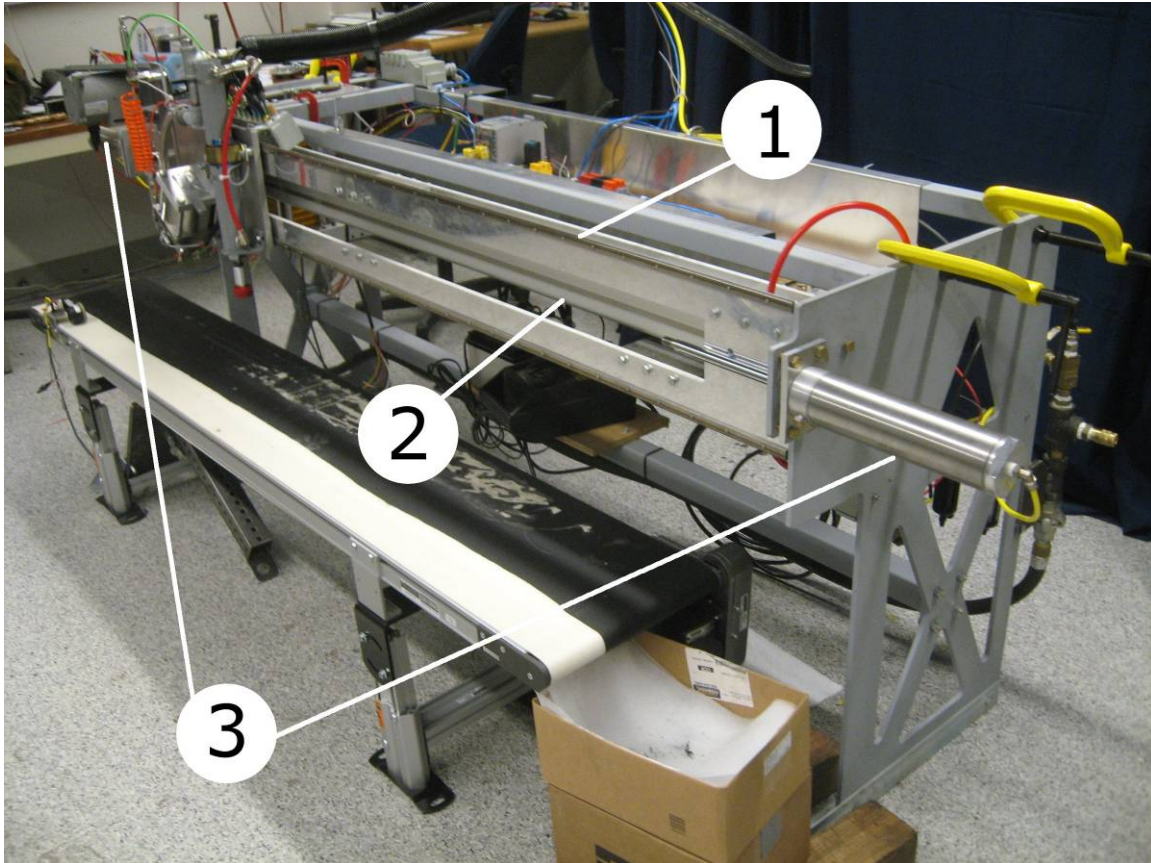
Figure 14: The linear slide assembly

Number	Description
1	Guide structure
2	Band cylinder
3	End cylinders

Table 3: Key for Figure 14

The carriage rolls along the guide structure, with the force applied by the band cylinder. The end cylinders guarantee a compliant stop if the carriage runs into the ends.

Band Cylinder Pneumatic Network

The band cylinder is subject to the pneumatic network described in Figure 15.
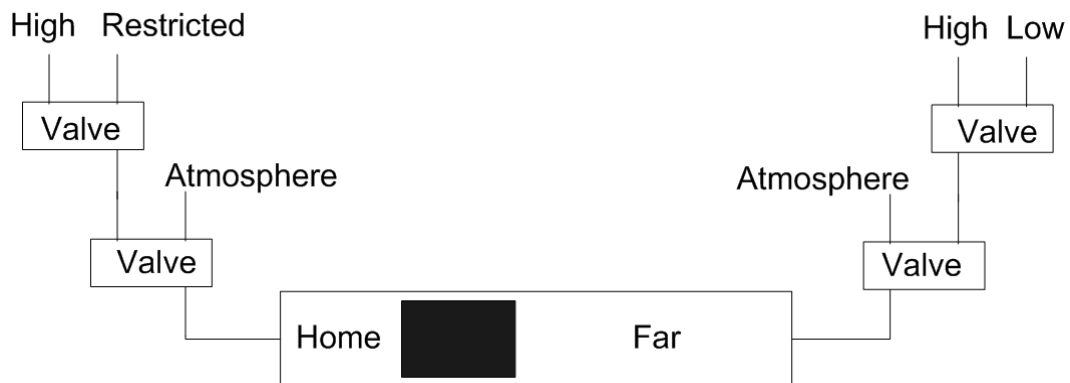
Figure 15: Pneumatic network for the band cylinder

Each valve can be set to one of two configurations, and the sum of all valve settings determines the effect on the carriage. For example, to accelerate the carriage from the home end, the home valves are set to connect the home chamber with the high pressure reservoir and the far valves are set to connect the far chamber with the open atmosphere.

Carriage

The components of the carriage are detailed in Figure 16.
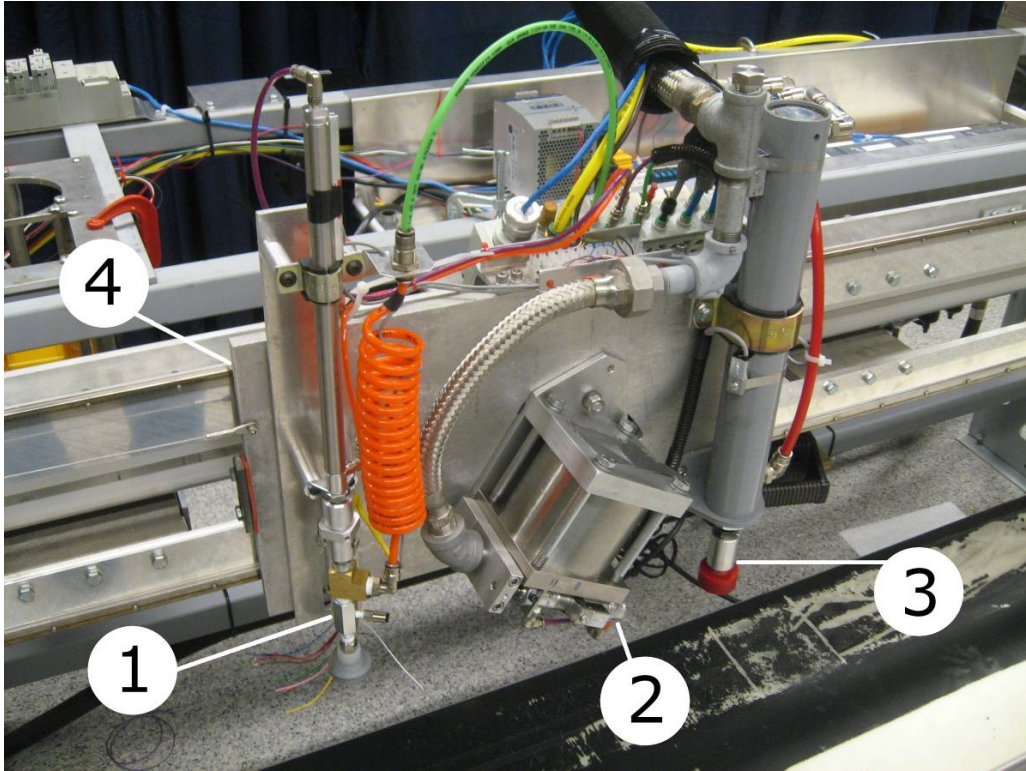
Figure 16: The carriage assembly

Number	Description
1	Dot placer
2	Adhesive dispenser
3	Foot
4	Carriage mechanism

Table 4: Key for Figure 16

The carriage contains all the primary dot installation equipment, mounted to the carriage mechanism. The carriage accelerates to match road speed, and then the foot descends to ensure that it is stationary relative to the conveyor belt. The adhesive dispenser actuates, and the dot placer extends to place a dot.

Conveyor

The components of the conveyor are detailed in Figure 17.
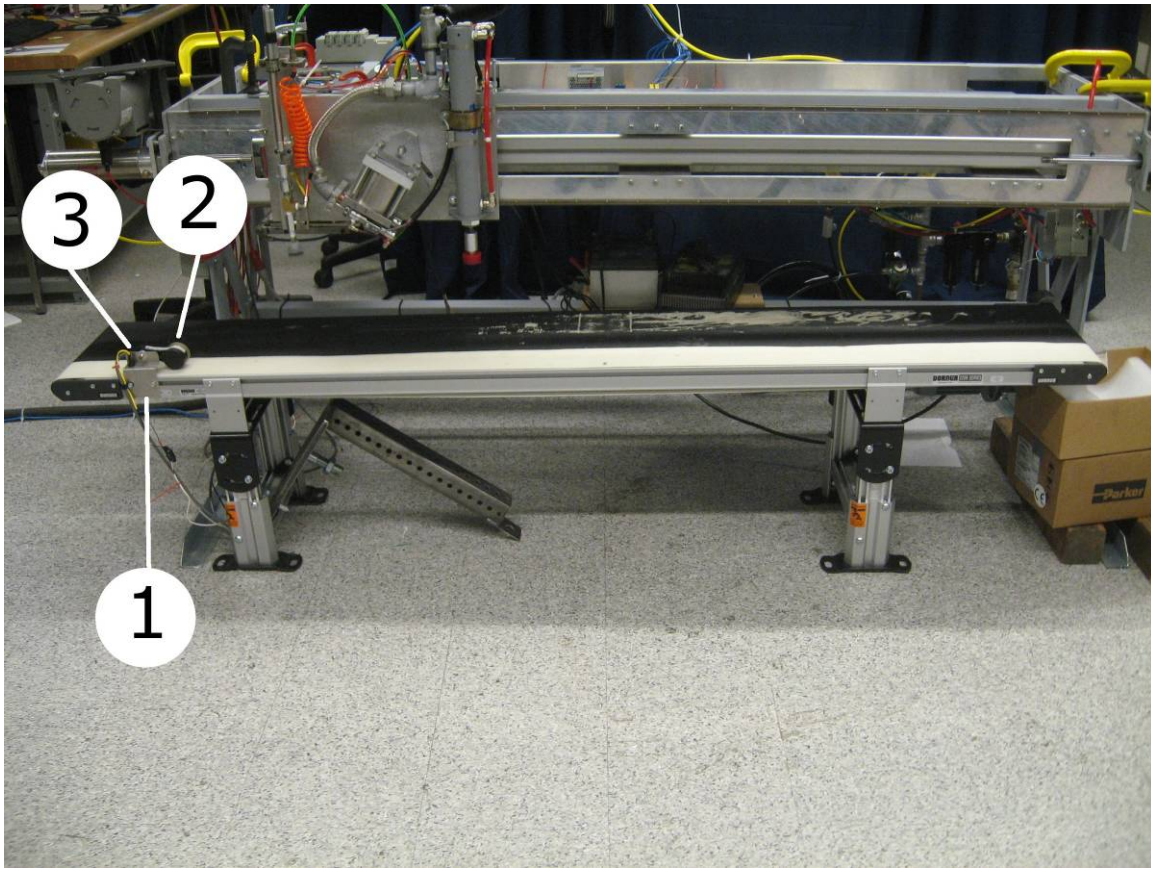
Figure 17: The conveyor assembly

Number	Description
1	Bracket
2	Measurement wheel
3	Magnetic Sensor

Table 5: Key for Figure 17

The conveyor is outfitted with some sensors. Attached to the bracket, the measurement wheel measures the movement of the conveyor belt for speed and displacement determinations. The magnetic sensor detects a magnet embedded at one point in the conveyor belt, and this is used to trigger the placement of a new dot. The new dot is targeted relative to the magnet.

Control

The prototype is governed by the control scheme outlined in Figure 18.
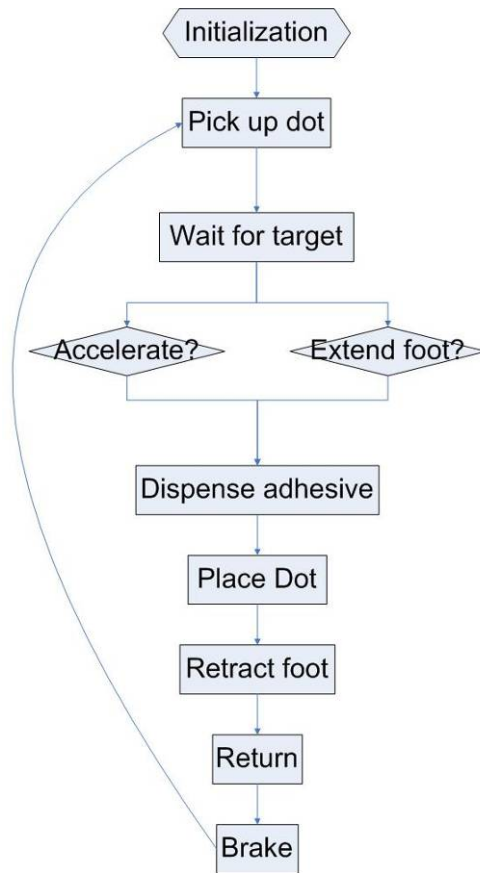
Figure 18: Prototype control scheme

When the prototype is first activated, it enters an initialization stage in which the system is prepared for operation. The carriage then picks up a dot from the dot dispenser. At this point, the system is prepared to perform the placement operation, so it waits for its cue to do so. In the scenario of an existing dot, the detection of such is the cue. Upon detection of the existing dot, the system performs repeated checks to determine when carriage acceleration and foot extension should begin. After both actions have been performed and the carriage is attached to the road, adhesive is dispensed. A dot is placed onto the adhesive, whereupon the foot retracts and the carriage begins its return to the home position. When the carriage nears the home position, pneumatic braking slows the carriage to a gentle stop. The cycle then repeats. The control code is included in Appendix D.

Initialization

The initialization stage sets all outputs to appropriate values, ensuring that the system is ready for subsequent stages. It is also responsible for preparing the controller, performing such tasks as memory allocation.

Pick Up Dot

To pick up a dot from the dot dispenser, the dispenser tray is first extended to position the proper dot directly underneath the dot placer. The dot placer then descends to the dot, grabs it

- 22 -

with the vacuum, and ascends. Finally, the dispenser tray retracts. Sensors and the control code prevent damaging interference of the tray and placer.

Wait for Target

Assuming that an old dot still exists on the road, the goal of the final device is to place a new dot directly before it. Thus, it waits to sense a dot. In the case of the prototype, the role of the existing dot is played by the magnet embedded in the conveyor belt, which is detected by the magnetic sensor as it passes. This establishes the target position on the belt.

Accelerate and Extend Foot

Once a target location has been determined, the system waits until the proper moment to start accelerating the carriage and start the foot descent. The measurements of conveyor belt displacement and speed are used for this purpose. The acceleration and the descent are conducted independently, but each is directed such that they will achieve the desired final state together. Namely, the foot will contact the belt at the moment when the carriage has accelerated enough to be stationary relative to the belt, and at the proper longitudinal position. The scheme to achieve this is described in Section 0.

Dispense Adhesive

As soon as the carriage has become stationary with the road, the adhesive dispenser actuates such that it would eject adhesive onto the target location. However, the adhesive dispenser on the prototype does not actually use adhesive or any liquid substitute due to the infeasibility of such in the laboratory setting. Any liquid would pose a danger to the conveyor, require extensive cleanup, and necessitate additional resources. However, a mitigating factor is that a similar adhesive dispensing design was previously field tested by AHMCT and verified. Although the current prototype dispenser has not been verified, its operating principles are sound.

Place Dot

Once the adhesive has been dispensed, the dot placer descends to the conveyor belt. It presses the dot momentarily, deactivates its vacuum, and ascends, leaving the dot behind.

Retract Foot

As soon as the dot placer is not in contact with the dot, the foot ascends.

Return

When the foot has left the ground, the carriage can begin moving back to the home position.

Brake

When the carriage is within a certain distance to the home position, the home end of the cylinder is switched to a narrow aperture vent. This restricts outward flow from the home end, resulting in a high pressure as the carriage compresses it. The high pressure slows the carriage, but the slow flow allows the carriage to ultimately settle at the home position in a gentle, controlled manner.

Calibration for Longitudinal Targeting

As mentioned in Equations (1) and (2), the displacement and time required for the carriage to reach road speed can be considered functions of that speed. However, the functions must be known before the RPM machine can operate. These functions should be determined empirically so as to most accurately reflect the system, in a process of calibration.

The process begins by gathering acceleration data from the apparatus. The carriage is attached to some kind of linear displacement sensor; in the case of the prototype it is a cable extensometer. The carriage is then accelerated and the linear displacement is measured over time. An example of the carriage's displacement over time is displayed in Figure 19 and the carriage's velocity over time is shown in Figure 20.

Carriage Displacement vs Time
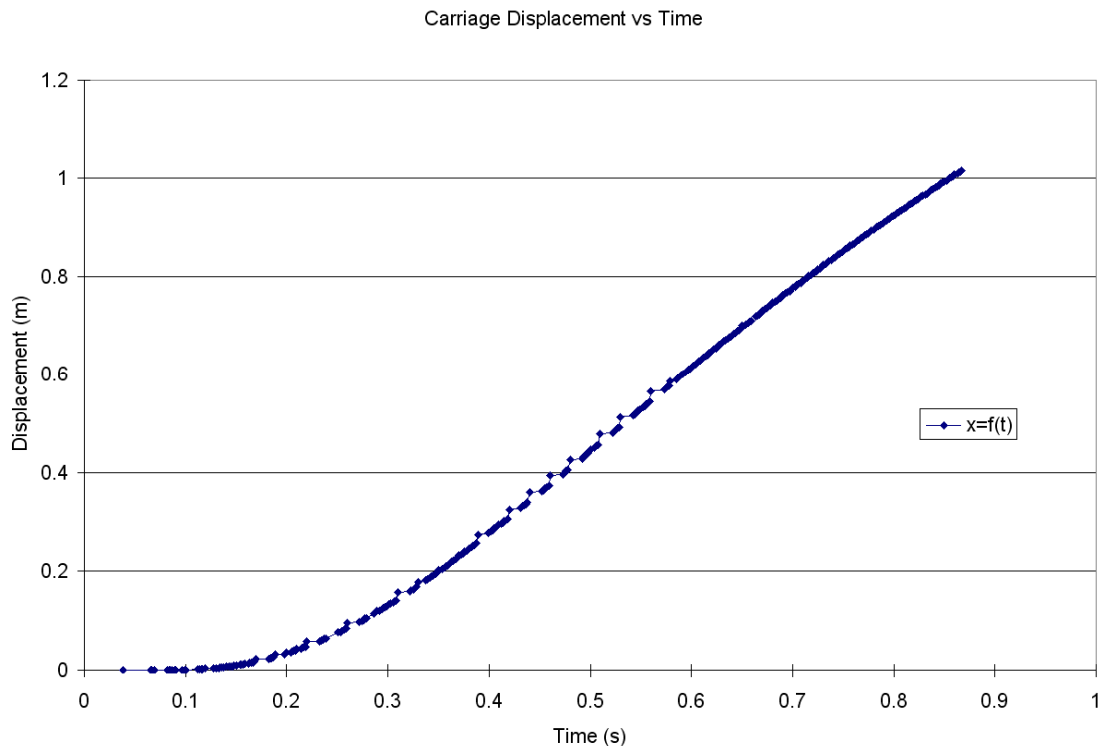
Figure 19: Carriage Displacement vs. Time during acceleration

- 24 -
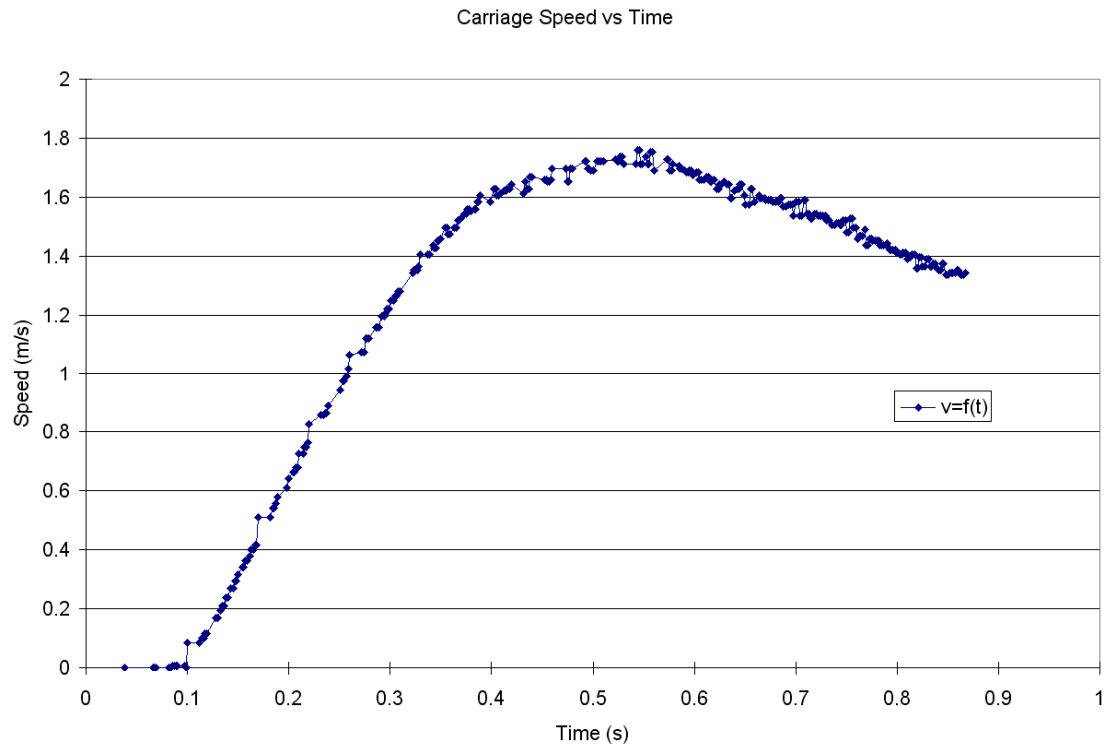
Figure 20: Carriage Speed vs. Time during acceleration

Through simple rearrangement of the data, time and displacement may be presented as functions of speed, as in Figure 21 and Figure 22.

Time vs Carriage Speed

$$y = 0.1713x^6 - 0.5592x^5 + 0.4356x^4 + 0.3095x^3 - 0.5451x^2 + 0.369x + 0.0786$$
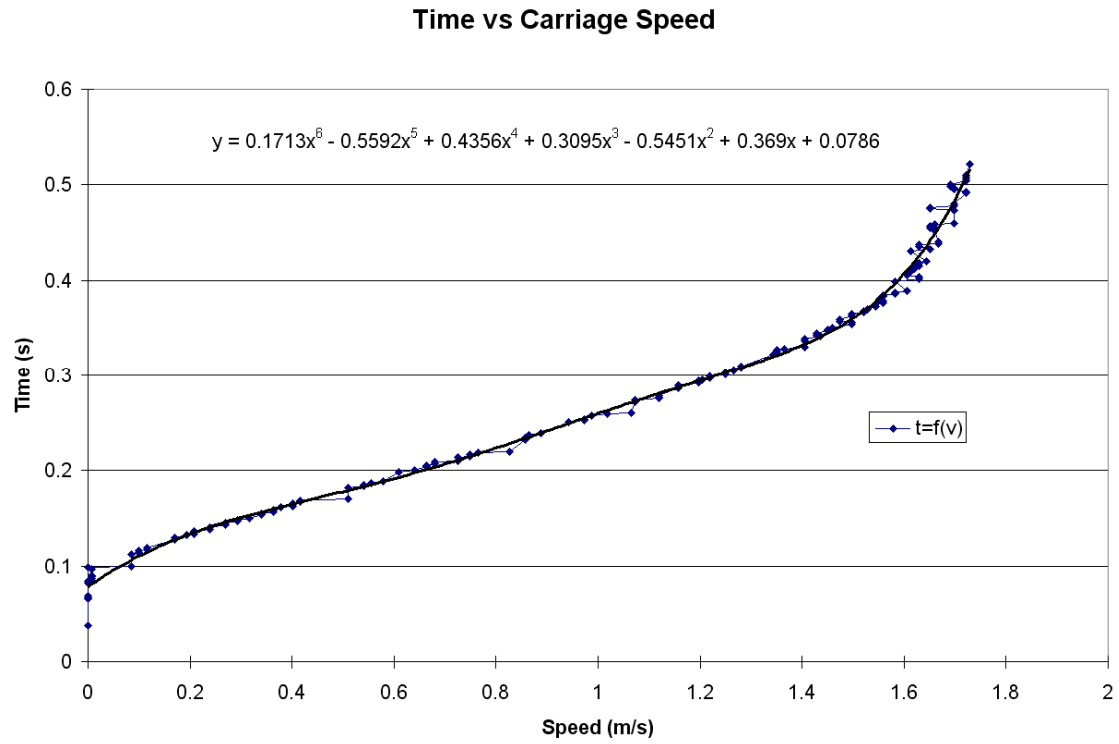
Figure 21: Time as a function of desired carriage speed

Displacement vs Speed

$$y = 0.5208x^6 - 2.2724x^5 + 3.717x^4 - 2.7759x^3 + 0.9953x^2 - 0.0998x + 0.0011$$
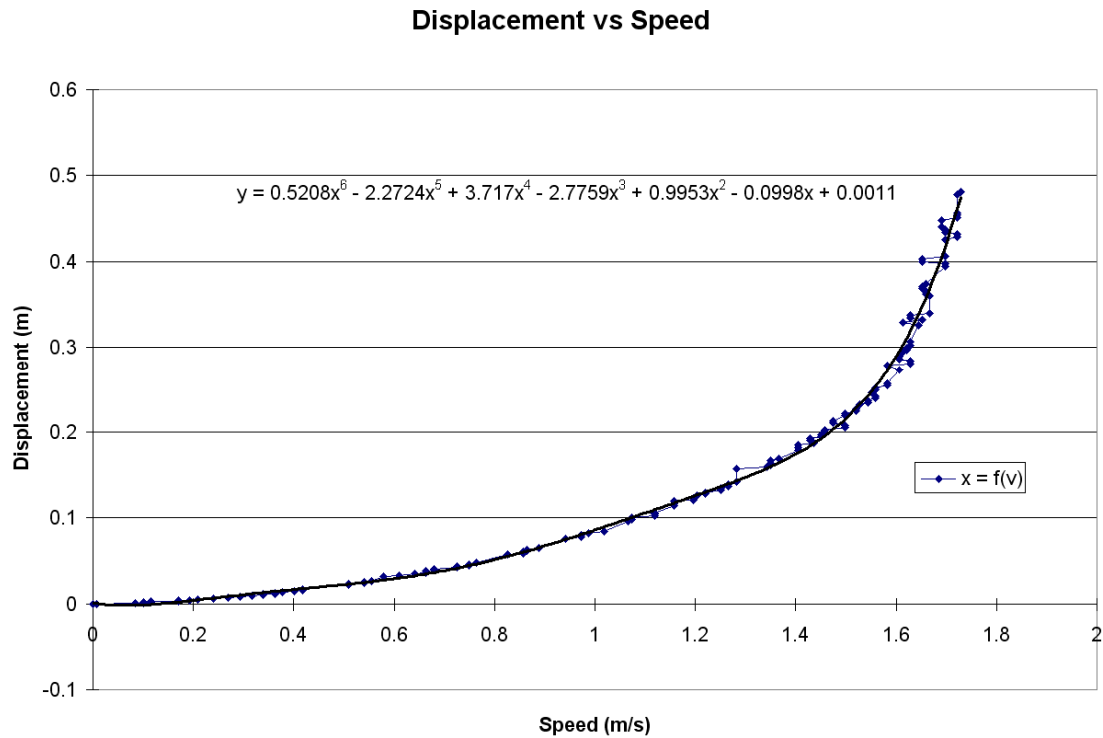
Figure 22: Displacement as a function of desired carriage speed

Thus the necessary functions have been determined empirically, presented as 6th order polynomial curve fits in Figure 21 and Figure 22. If the 6th order polynomials are too computationally intensive, they can be replaced with simplified functions or a discretized lookup table.

Testing of Longitudinal Targeting

One of the primary reasons to construct a prototype was to confirm the effectiveness of longitudinal targeting through real tests. Such testing is described herein.

Calibration

The control procedure assumes a deterministic system response, so the response must be measured and incorporated into the control code. This is necessary for the processes of carriage acceleration and foot descent.

Carriage Acceleration

The carriage was accelerated five times within the span of a few minutes, and the response was measured for each. The measured gauge pressures are 2.9 E5 Pag (42 psig) for the high band cylinder pressure and 1.6 E5 Pag (23 psig) for the low band cylinder pressure.

Carriage Speed vs Time, 5 Trials
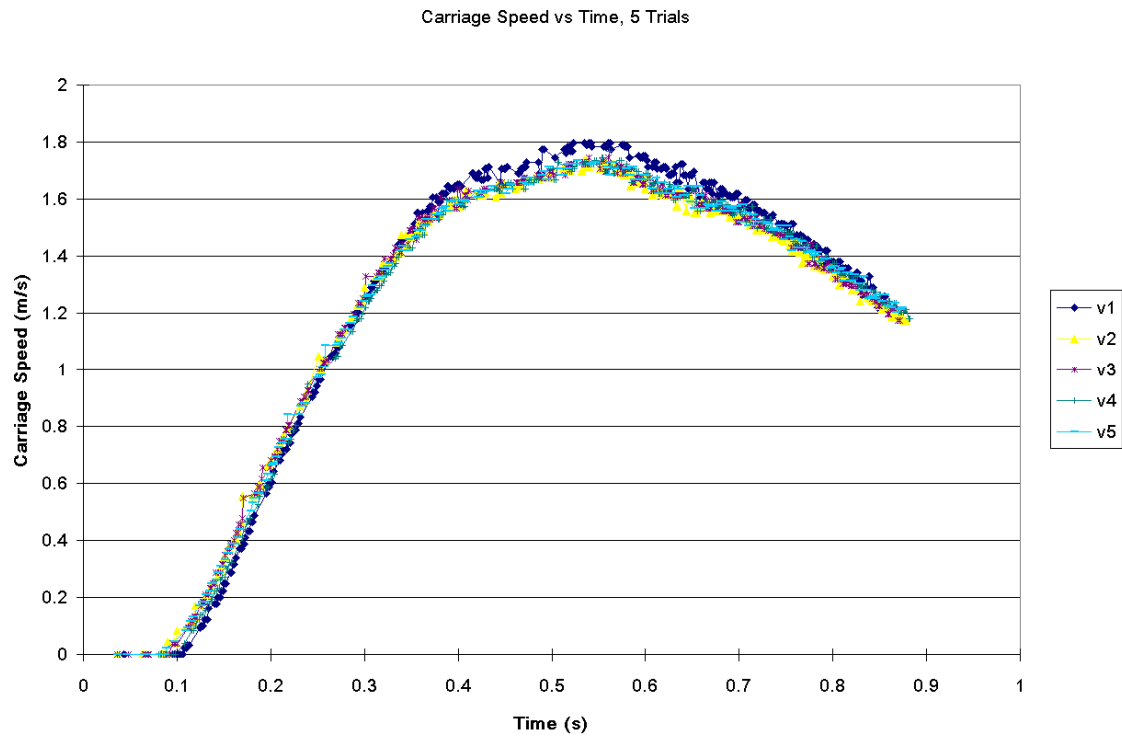
Figure 23: Carriage Speed vs. Time, 5 Trials

Carriage Position vs Time, 5 Trials
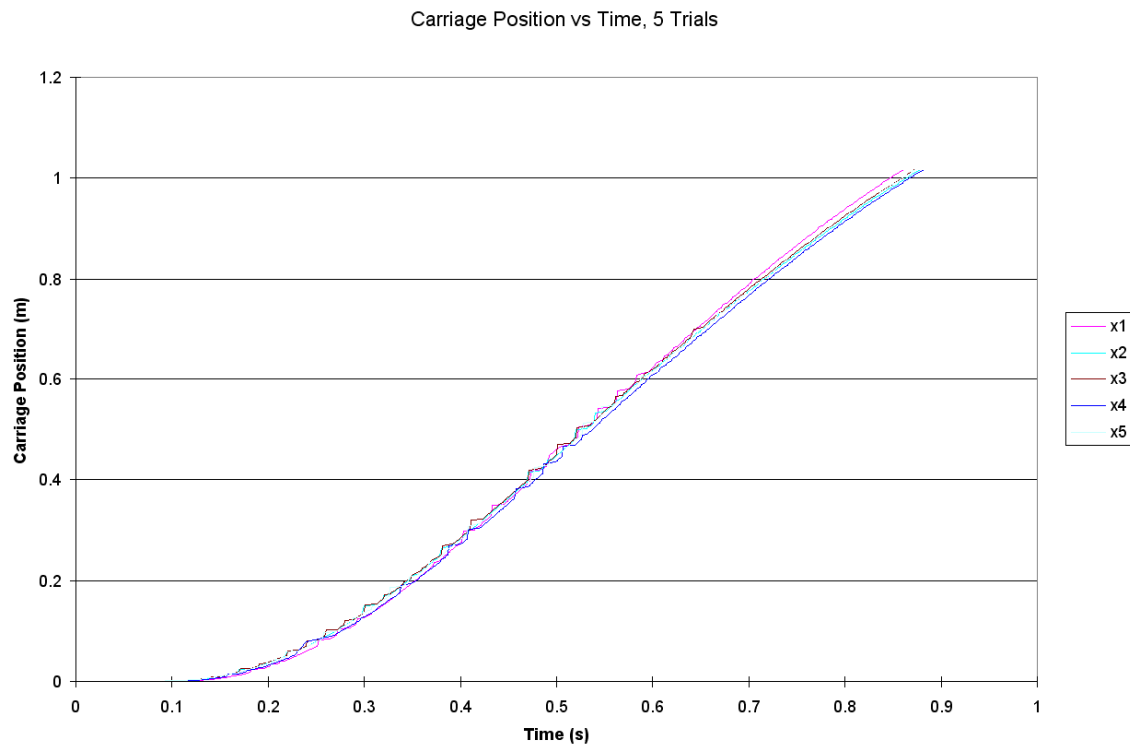
Figure 24: Carriage Position vs. Time, 5 Trials

- 28 -

Figure 23 displays the carriage speed throughout acceleration, and Figure 24 shows the position. The results are very similar, as one might expect, so visually distinguishing between the data sets is difficult and mostly unnecessary. The only unusual result was in the first trial. The carriage started moving slightly later than in any of the others, and it reached a higher speed at its peak. This is probably because it was the first carriage acceleration of the day. As such, the carriage may have been subject to some extra friction from uneven lubrication or other unknown factors. In operation, the device executes many times in a short period, so the first trial's result are incongruent with operating conditions. The fifth trial's results were used for calibration.

In order to minimize computation time, the data was simplified before curve fitting. Initially, the speed data is nearly linear. Extraneous points were removed to achieve the result in Figure 25.

Linear Portion of Speed Plot

$y = 6.2953x - 0.6116$
$R^2 = 0.9976$
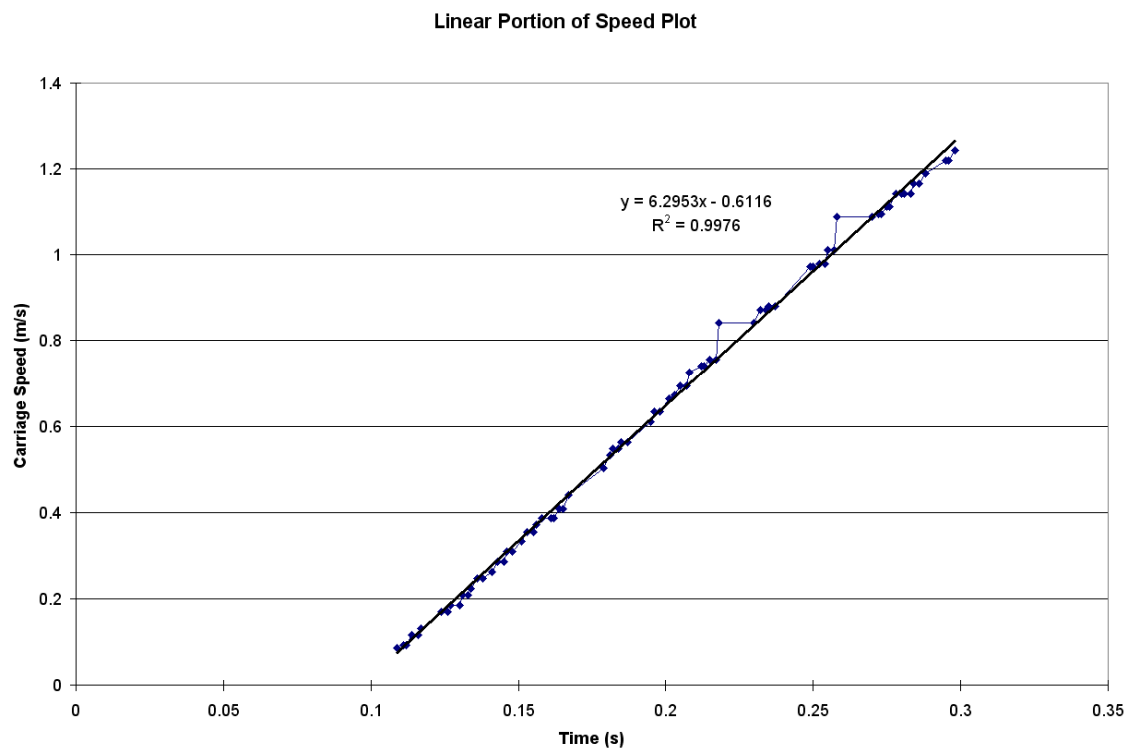
Figure 25: Linear Portion of Speed Plot

Because the speed plot is linear in this range, the corresponding plot of position is a second-order polynomial.
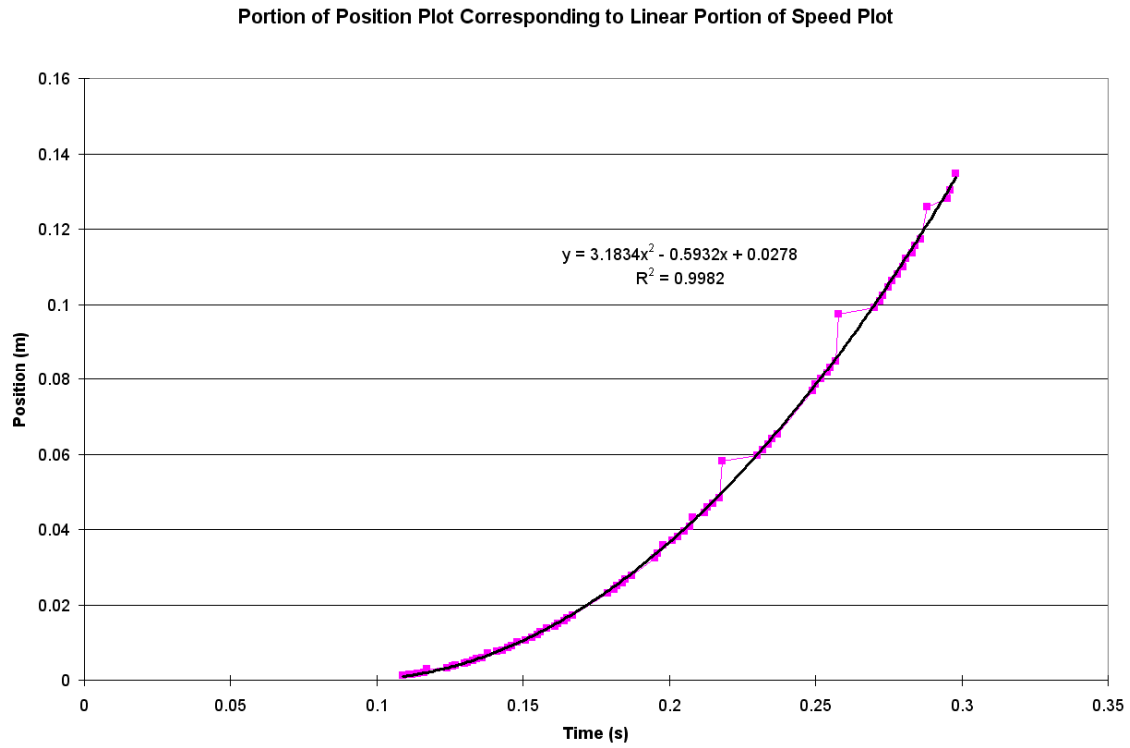
Figure 26: Portion of Position Plot Corresponding to Linear Portion of Speed Plot

Now, the data is rearranged to the form required by the control system, as described in Equations (1) and (2).
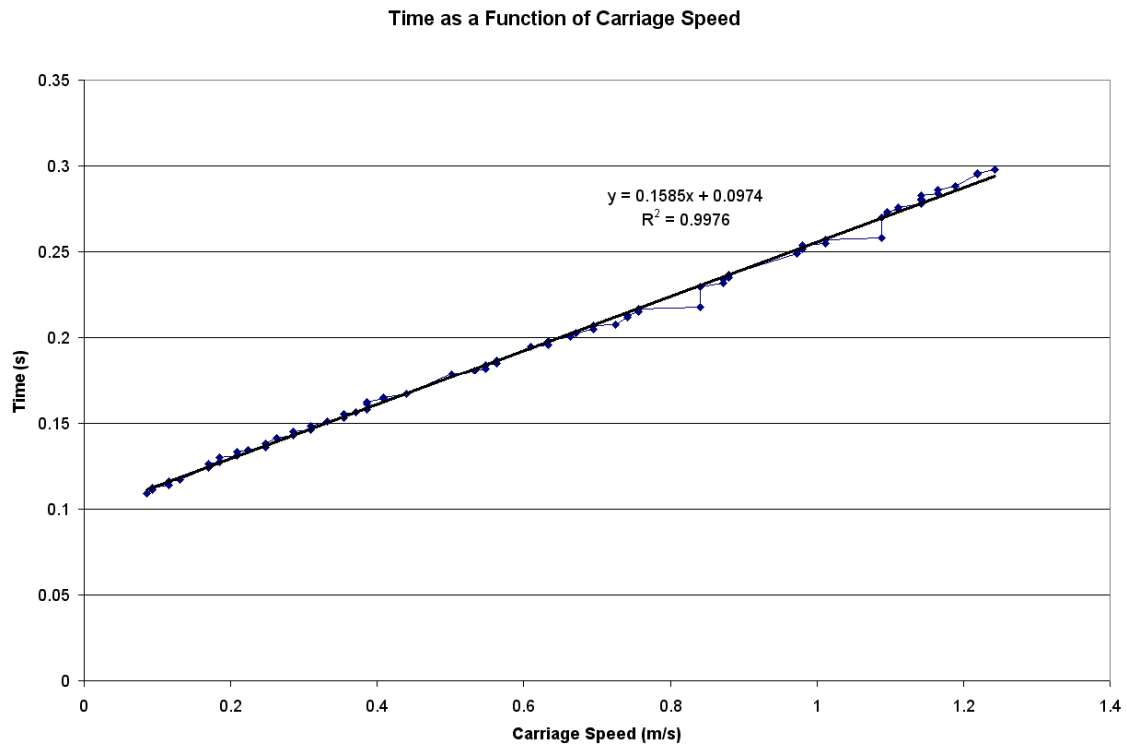
Figure 27: Time as a Function of Carriage Speed

Position as a Function of Carriage Speed

$$y = 0.0915x^2 - 0.01x + 0.0031$$
$$R^2 = 0.9986$$
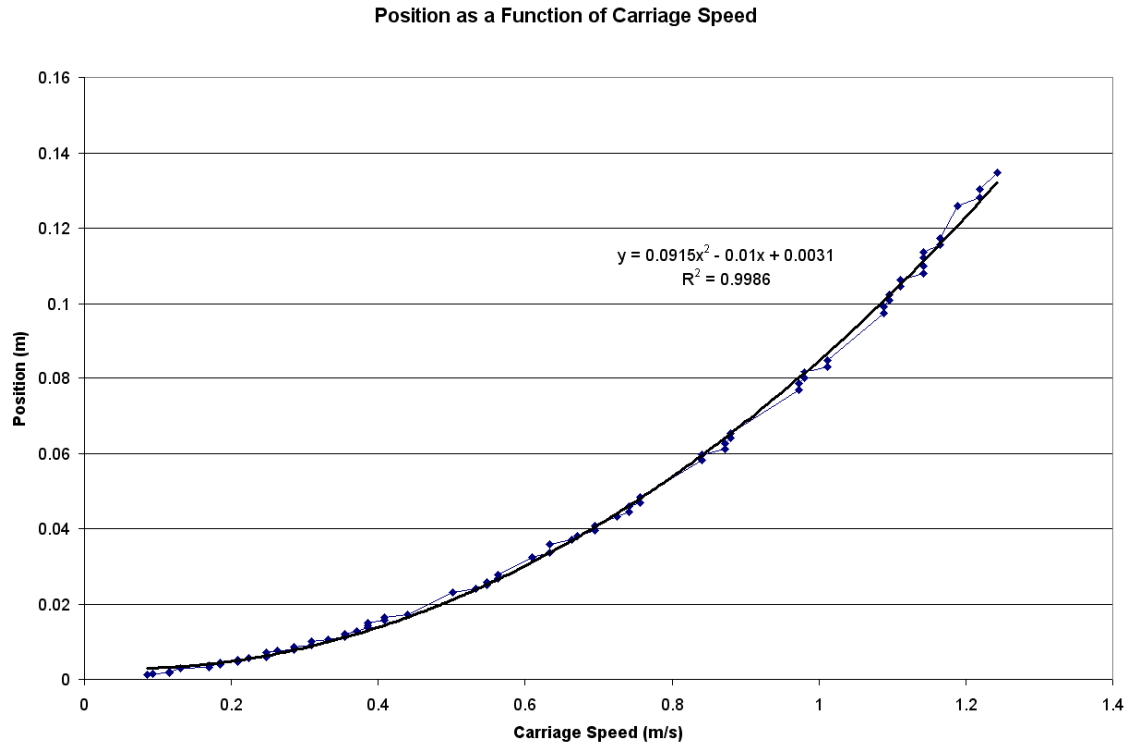
Figure 28: Position as a Function of Carriage Speed

From the R-squared values in Figure 27 and Figure 28, these curve fits are excellent. They are also simple for the sake of computational efficiency.

Foot Descent

The time required for the foot to descend is determined using a sensor at the bottom of the foot's travel and a specialized program. The program commands the descent of the foot and measures the time until sensor activation. The foot was supplied with a gauge pressure of 5.2 E5 Pag (76 psig). In five attempts, the times were 95, 96, 96, 95, and 95 ms. The program was therefore set to use 95 ms.

Of course, the foot descent time depends on how much distance the foot must travel to reach the road or conveyor belt. If the distance varies, as it might in real-world situations, the descent time will change. However, it is hoped that the great speed of the foot will make such small variations irrelevant.

Testing Method and Result

For longitudinal targeting, two aspects are important: consistency and adaptability. At any given speed, the targeting must be consistent to a certain location. The targeting must also adapt to different vehicle speeds. To accomplish this, the placement location was measured repeatedly at a low speed of 0.23 m/s (0.51 mph) and at a high speed of 0.907 m/s (2.03 mph).

- 32 -

Of course, the final location of the dot placer is the important parameter, but since it is fixed relative to the foot, the position of the foot can also be used in testing. The conveyor belt was marked with lateral lines 2.54 cm (1.00 inch) apart. The system was set to target a certain location relative to the conveyor's embedded magnet, and the actual location of the placed foot was measured visually using the marked lines. The placement location never exceeded an error of 1.3 cm (0.50 in), at either the low speed or the high speed, proving adaptability and consistency within an acceptable range.

Chapter Summary

This chapter discussed the laboratory prototype of the marker placement device. It consists of a carriage on a linear slide, actuated with a pneumatic band cylinder. It places dots onto a conveyor that simulates the relative motion of a road. On the carriage, there is a pneumatic foot to grip the conveyor, an adhesive dispenser, and a dot placer. First, the dot placer picks up a dot from a reservoir and thereby is ready for a target. When the system senses a magnet embedded at one point in the conveyor belt, it targets the new dot relative to that position. When conditions are right, it accelerates the carriage to match road speed and descends the foot to ensure a steady position. The adhesive dispenser actuates, the dot placer puts down the dot, and then the carriage returns to its home position to repeat the cycle.

The targeting process requires a deterministic response because of the infeasibility of feedback. As such, a calibration procedure is necessary to ensure that the control system takes into account the realistic response of the actuators. A special calibration routine is used to measure carriage acceleration. From those measurements, curve fits are made and inserted back into the control code. For the foot, a simple program measures the time necessary for the foot to fully descend, and this time is likewise inserted into the code. Finally, testing indicates that the longitudinal targeting error is less than 1.3 cm (0.50 in) at speeds ranging from 0.23 m/s (0.51 mph) to 0.907 m/s (2.03 mph). This level of precision is adequate for field operation.

Of course, before testing of the prototype, various analysis techniques were utilized to ensure proper operation and ability of the device.

CHAPTER 4

ANALYSIS

Dynamic Pneumatic Simulation

A major challenge of this project is to use pneumatic actuation to achieve a carriage speed that matches that of the vehicle. Pneumatic actuation is generally regarded as inexpensive and strong, but also as being rather uncontrollable. To aid in the achievement of this control, a computer simulation of the carriage was made.

Mathematical Model

The computer simulation is based on the model presented in Figure 29. It depicts the band cylinder, divided by the inner piston. The piston is attached to the remainder of the carriage, and the piston is considered to be part of the carriage for mass concerns.
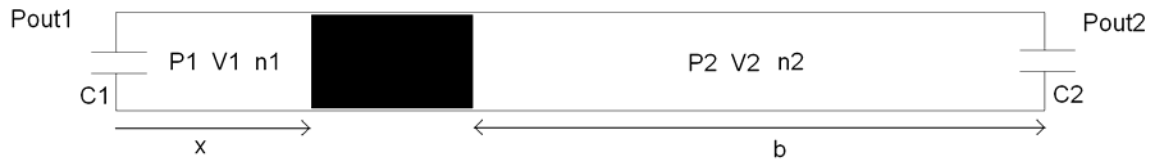
Figure 29: Illustration of the model used for simulation

Symbol	Description	Units
P_{out1}	Absolute pressure supplied to the home side	Pa
C_1	Net flow conductance between the outer pressure reservoir and the home chamber.	mol/s/Pa
P_1	Absolute pressure in the home chamber	Pa
P_{up1}	The upstream pressure at the home end. Equals P_1 or P_{out1}.	Pa
V_1	Volume of the home chamber	m³
n_1	Moles of air in the home chamber	mol
x	Length of the home chamber, and position of carriage	m
$\dot{x}$ or v	Speed of carriage	m/s
$\ddot{x}$ or a	Acceleration of carriage	m/s²
T_1	Temperature of the air in the far chamber	K
P_{out2}	Absolute pressure supplied to the far side	Pa
C_2	Net flow conductance between the outer pressure reservoir and the far chamber	mol/s/Pa
P_2	Absolute pressure in the far chamber	Pa
P_{up2}	The upstream pressure at the far end. Equals P_2 or P_{out2}.	Pa
V_2	Volume of the far chamber	m³
n_2	Moles of air in the far chamber	mol

- 34 -

b	Length of the far chamber	m
T_2	Temperature of the air in the far chamber	K
$F_{f,static}$	Static Coulomb friction acting on the carriage	N
$F_{f,kinetic}$	Kinetic Coulomb friction acting on the carriage	N
m	Total mass of the carriage	kg
A	Cross-sectional area of the band cylinder chamber	m²
L	Length of the total band cylinder chamber minus piston length. Equal to the nominal travel of the band cylinder	m
R	Universal gas constant	J/mol/K

Table 6: Nomenclature of the Model

Flow Rate

   At either end, the obstruction between the outer reservoir and the inner chamber is considered to act like an orifice plate, which is governed by the set of equations for compressible fluids to follow.

$$\dot{m} = CYA\sqrt{2\rho_1(P_{out1} - P_1)} \tag{8}$$

   The nomenclature presented in this equation need not be explained here. Suffice it to say that the mass flow rate $\dot{m}$ is proportional to the molar flow rate, and that all constants can be encapsulated in C_1 and C_2. These are empirical values that include the following properties: obstruction geometry, fluid molar mass, and fluid expansion factor. Any value of C_1 or C_2 is therefore only valid as long as the aforementioned properties remain unchanged. Consolidating the constants results in

$$\frac{dn_1}{dt} = C_1\sqrt{\rho_{up}}\sqrt{P_{out1} - P_1} \tag{9}$$

where ρ_{up} is the upstream fluid density. From the ideal gas law stated in Equation (12), density is directly proportional to pressure if temperature is constant (an approximation here). Thus,

$$\rho_{up} \propto P_{up} \tag{10}$$

   Density is assumed proportional to pressure, so upstream pressure can replace upstream density (with modification to the value of C_1). P_{up} may equal P_{out1} or P_1, depending on the direction of the flow. The molar flow rate equations are finally

$$\frac{dn_1}{dt} = C_1\sqrt{P_{up1}}\sqrt{P_{out1} - P_1}$$
$$\frac{dn_2}{dt} = C_2\sqrt{P_{up2}}\sqrt{P_{out2} - P_2} \tag{11}$$

- 35 -

Ideal Gas Law

Air is approximated as an ideal gas, so the Ideal Gas Equation can be used.

$$P_1 A x = n_1 R T_1$$
$$P_2 A b = n_2 R T_2$$

(12)

Equation of Motion

The carriage is assumed to be subject to the following forces: the pressure force at the home side, the pressure force at the far side, and friction. Coulomb friction is assumed.
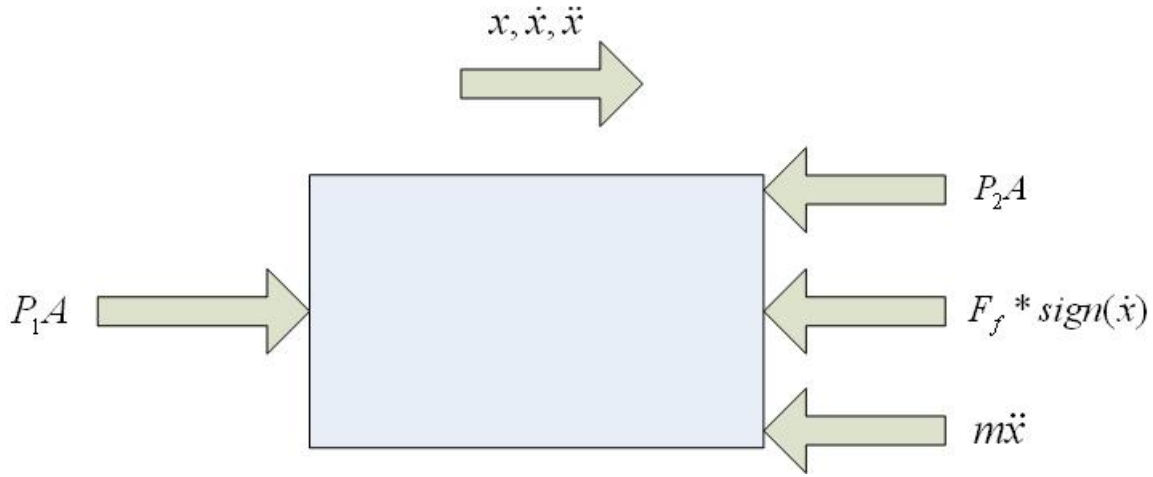
Figure 30: Free body diagram for the carriage

From Figure 30, the equation of motion is

$$(P_1 - P_2)A - F_f * sign(\dot{x}) - m\ddot{x} = 0$$

(13)

Also, by definition, speed is the time derivative of position

$$\dot{x} = \frac{dx}{dt}$$

(14)

and acceleration is the time derivative of speed.

$$\ddot{x} = \frac{d\dot{x}}{dt}$$

(15)

Simulation Algorithm

To simulate the time evolution of the carriage movement in a variety of scenarios, the following algorithm is used for each uniform time step of 0.0001 s:

1. Update P_{up1} and P_{up2} according to pressure differences.

2. Update n_1 and n_2 .according to Equation (11).

3. Update P_1 and P_2 according to Equation (12).

4. Update a according to Equation (13)).

5. Update v according to Equation (15).

6. Update x according to Equation (14).

- 36 -

The interested reader is referred to Appendix B for the complete algorithm.

Verification of Simulation Against Measurements

In order to verify that the simulation is accurate, simulation results were compared against measurements taken from the prototype itself. The scenario being examined is that in which the carriage is accelerated from the home position. The initial conditions used in the simulation are described in Table 7, and Table 8 contains the values that were considered constant.

Symbol	Value	Source
P_1	1.01e5 Pa	Assumed (open to atmosphere, near sea level)
P_2	1.01e5 Pa	Assumed (open to atmosphere, near sea level)
x	0.145 m	Measured
v	0 m/s	Assumed (stationary)
a	0 m/s^2	Assumed (stationary)

Table 7: Initial conditions in simulation

Symbol	Value	Source
P_{out1}	3.77e5 Pa	Measured
P_{out2}	1.01e5 Pa	Assumed (open to atmosphere, near sea level)
C_1	3.6e-7 mol/s/Pa	Empirical
C_2	1.5e-6 mol/s/Pa	Empirical
T_1	298 K	Assumed (comfortable room temperature, neglecting compression/expansion effects)
T_2	298 K	Assumed (comfortable room temperature, neglecting compression/expansion effects)
A	0.00114 m^2	Component documentation
L	1.524 m	Component documentation
$F_{f,static}$	53 N	Measured
$F_{f,kinetic}$	44 N	Measured
m	16 kg	Empirical
R	8.314 J/mol/K	Literature

Table 8: Constants in simulation
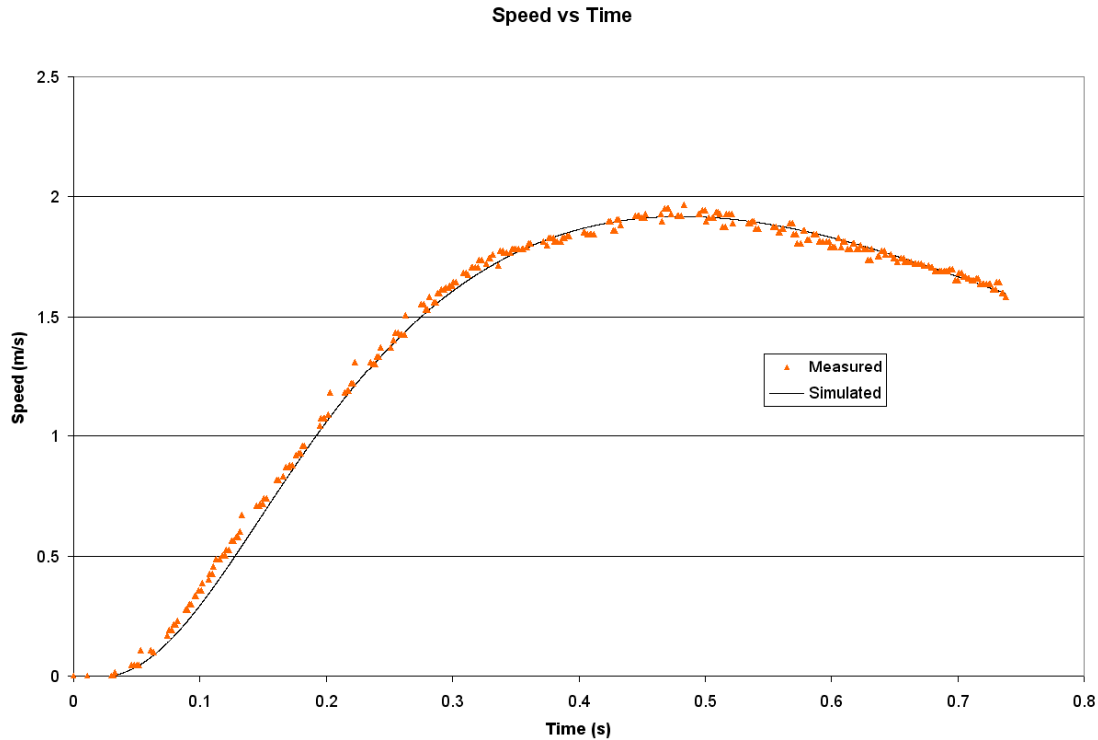
Figure 31: Carriage acceleration, simulated and measured results

Carriage acceleration was performed according to the aforementioned parameter values, both in simulation and in experimentation with the prototype. The simulated and measured results were very similar, as shown in Figure 31. This indicates that the simulation is physically accurate. As such, the simulation should be capable of accurately predicting the movement of the carriage under a wide variety of conditions. For example, it should be accurate for more complex acceleration schemes and for the return of the carriage to the home position.

Beam Deflection from Transverse Loading

The design described in this report uses a linear slide, which entails the travel of a carriage upon a beam with ends that may be considered fixed. The carriage undergoes a transverse load from its own weight and/or from the force of the foot, and the load is in turn applied to the beam. Deformation of the beam must be limited in order to preserve proper functioning of the linear slide, but the transverse load will cause some deformation. Thus arises the necessity of determining the deformation of the beam.

Model

Consider the linear slide to be a simple beam with fixed ends, illustrated in Figure 32. Of course, the linear slide guide structure is much more complex than a simple beam, but a portion of it may be approximated in this way. This is a conservative approximation because only a portion of the guide structure is considered to bear all of the load.

- 38 -
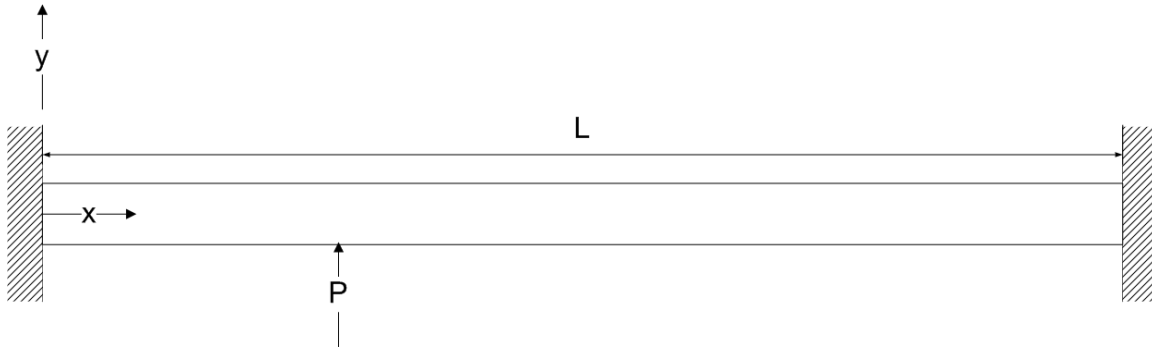
Figure 32: A model of the linear slide as a beam

Assumptions

 The following assumptions apply to this problem:

1. No point on the beam's centroidal axis undergoes any horizontal displacement.
2. The beam's material is homogeneous and isotropic throughout.
3. All beam properties are uniform throughout its length.
4. The load is applied at a point.
5. The displacement and slope of the beam are continuous at the point of load application.

Nomenclature

 The nomenclature in Table 9 applies to this problem.

- 39 -

Symbol	Unit	Description
x	m	horizontal position on the centroidal axis relative to the left end of the beam
y	m	vertical position on the centroidal axis relative to the centroidal axis of the undeformed beam
x_2	m	horizontal position on the centroidal axis relative to the right end of the beam
I	m^4	second moment of area about the z-axis for the cross-section of the beam
E	N/m^2	Young's modulus of the beam
L	m	length of the beam
P	N	force applied to the beam
x_p	m	value of x at which P is applied
U	N-m	potential energy of a given system
F, F_1, F_2	N	$\frac{1}{2}EIy''^2$
g	N-m	$-Py(x_p)$
g_1	N-m	$-V_1 y(x_p)$
g_2	N-m	$-V_2 y(L-x_p)$
C_1, C_2, C_3, C_4	N, N-m, N-m^2, N-m^3	integration constants
M	N-m	internal moment of the beam
V	N	internal shear force (general)
V_1	N	internal shear force at $0 < x < x_p$
V_2	N	internal shear force at $x_p < x < L$

Table 9: Nomenclature for beam deformation analysis

Discontinuity at Load

A beam element at the point of load application is subject to vertical forces as shown in Figure 33.

- 40 -
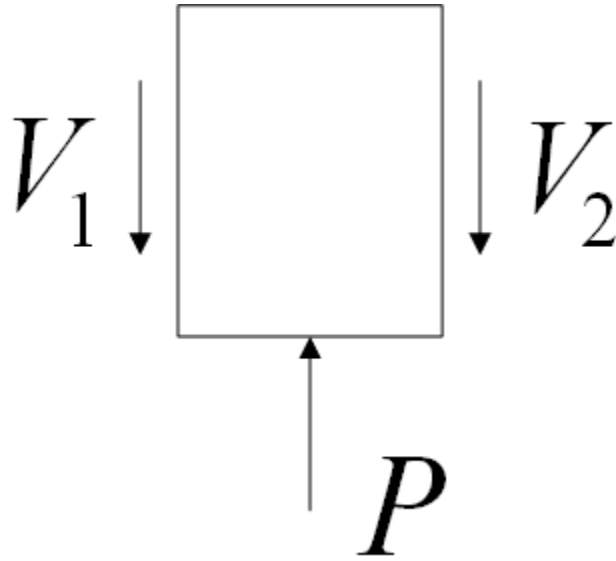
Figure 33: Vertical forces affecting a beam element at the point of load application

In most loading cases, $V_1 \neq V_2$. Assuming this to be the case, the point of load application constitutes a discontinuity that prohibits a unified solution for the whole beam. Thus, a separate solution will be determined for each side about the load.

Solution of the Left Side
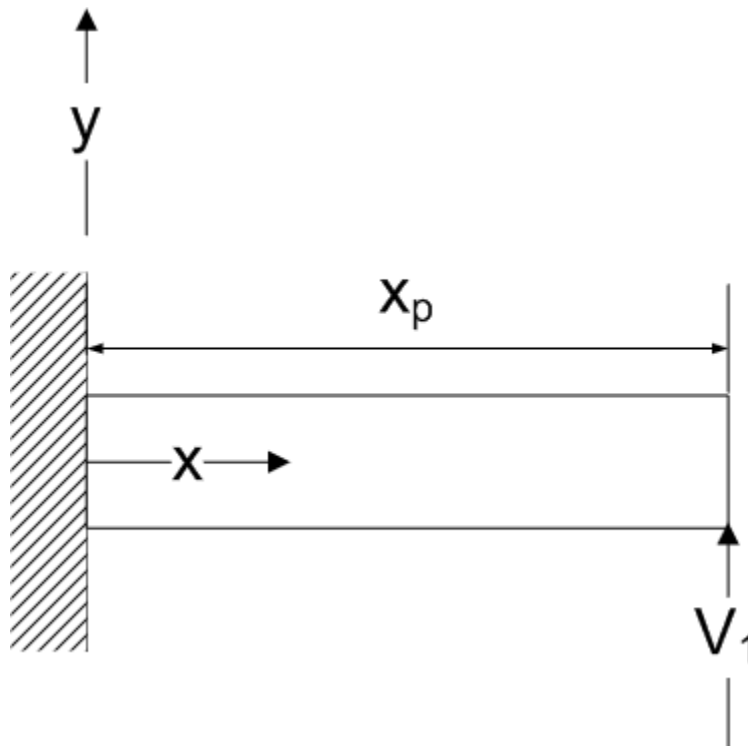
Figure 34: A simple model of the linear slide's left side

<u>Potential Energy of the System</u>

Potential energy of the system consists of strain energy and the energy of the transverse load, and is expressed as

$$U = \int_0^{x_p} \tfrac{1}{2} EIy''^2 \, dx - V_1 y(x_p) \,. \tag{16}$$

Let $\tfrac{1}{2} EIy''^2$ be denoted as F_1 and $-V_1 y(x_p)$ as g_1.

<u>Application of the Euler-Lagrange Equation</u>

The Euler-Lagrange equation is applicable to this problem, starting with the generic form

$$F_y - \tfrac{d}{dx} F_{y'} + \tfrac{d^2}{dx^2} F_{y''} = 0 \,. \tag{17}$$

Substitution of F_1 yields

$$0 - \tfrac{d}{dx}(0) + \tfrac{d^2}{dx^2} EIy'' = 0 \tag{18}$$

and

$$EIy_L{}^{IV} = 0 \,. \tag{19}$$

Successively integrating (19) with respect to x in order to solve for y gives

$$EIy_L''' + C_{L1} = 0 \,, \tag{20}$$

$$EIy_L'' + C_{L1}x + C_{L2} = 0 \,, \tag{21}$$

$$EIy_L' + \tfrac{1}{2} C_{L1}x^2 + C_{L2}x + C_{L3} = 0 \,, \tag{22}$$

$$EIy_L + \tfrac{1}{6} C_{L1}x^3 + \tfrac{1}{2} C_{L2}x^2 + C_{L3}x + C_{L4} = 0 \,. \tag{23}$$

<center>Solution of the Right Side</center>
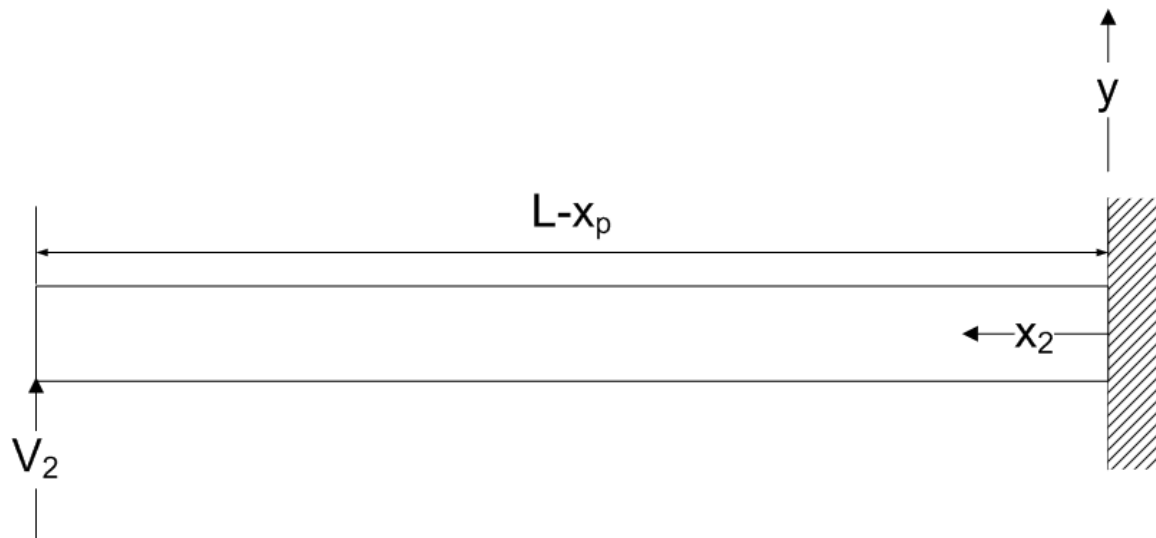
Figure 35 A simple model of the linear slide's right side

In Figure 35, the Right Side model of the beam is displayed. Note the alternate coordinate system used, with x_2 proceeding from the right end to the left.

<center>- 42 -</center>

This problem is mathematically identical to that of the Left Side if the following equivalencies are observed:

$$\text{Load: } V_1 \rightarrow V_2, \tag{24}$$

$$\text{Length: } x_p \rightarrow L - x_p, \tag{25}$$

$$\text{Horizontal position: } x \rightarrow x_2 = L - x. \tag{26}$$

Using x_2 as the horizontal coordinate, the equations of beam deformation result as

$$EIy_R{}^{IV} = 0, \tag{27}$$

$$EIy_R{}''' + C_{R1} = 0, \tag{28}$$

$$EIy_R{}'' + C_{R1}x_2 + C_{R2} = 0, \tag{29}$$

$$EIy_R{}' + \tfrac{1}{2}C_{R1}x_2^2 + C_{R2}x_2 + C_{R3} = 0, \tag{30}$$

$$EIy_R + \tfrac{1}{6}C_{R1}x_2^3 + \tfrac{1}{2}C_{R2}x_2^2 + C_{R3}x_2 + C_{R4} = 0. \tag{31}$$

Now, $x_2 = L - x$, which can be used to unify the coordinate systems of the left and right sides. However, an important note is that the direction of x_2 is opposite to that of x. When the independent variable is changed from x_2 to x, the sign of every odd derivative also changes. For example, if the slope of the beam is positive in one direction, it is negative in the other. Using x as the coordinate, Equations (27) to (31) become

$$EIy_R{}^{IV} = 0, \tag{32}$$

$$EIy_R{}''' - C_{R1} = 0, \tag{33}$$

$$EIy_R{}'' + C_{R1}(L - x) + C_{R2} = 0, \tag{34}$$

$$EIy_R{}' - \tfrac{1}{2}C_{R1}(L - x)^2 - C_{R2}(L - x) - C_{R3} = 0, \tag{35}$$

$$EIy_R + \tfrac{1}{6}C_{R1}(L - x)^3 + \tfrac{1}{2}C_{R2}(L - x)^2 + C_{R3}(L - x) + C_{R4} = 0. \tag{36}$$

Application of Geometric Boundary Conditions

The geometric boundary conditions are

$$y_L(0) = 0, \tag{37}$$

$$y_L{}'(0) = 0, \tag{38}$$

$$y_R(L) = 0, \tag{39}$$

$$y_R{}'(L) = 0, \tag{40}$$

$$y_L(x_p) = y_R(L - x_p), \tag{41}$$

$$y_L{}'(x_p) = y_R{}'(L - x_p). \tag{42}$$

Solution of the Fourth Integration Constants

From (37) and (23),

$$EI(0) + \tfrac{1}{6}C_{L1}(0)^3 + \tfrac{1}{2}C_{L2}(0)^2 + C_{L3}(0) + C_{L4} = 0, \tag{43}$$

which yields

$$C_{L4} = 0. \tag{44}$$

From (39) and (36),

$$EI(0) + \tfrac{1}{6}C_{R1}(0)^3 + \tfrac{1}{2}C_{R2}(0)^2 + C_{R3}(0) + C_{R4} = 0, \tag{45}$$

likewise yielding

$$C_{R4} = 0. \tag{46}$$

Solution of the Third Integration Constants

From (38) and (22),

$$EI(0) + \tfrac{1}{2}C_{L1}(0)^2 + C_{L2}(0) + C_{L3} = 0, \tag{47}$$

which gives

$$C_{L3} = 0. \tag{48}$$

From (40) and (35)

$$EI(0) - \tfrac{1}{2}C_{R1}(0)^2 - C_{R2}(0) - C_{R3} = 0, \tag{49}$$

which gives

$$C_{R3} = 0. \tag{50}$$

Solution of the First Integration Constants

The Euler-Bernoulli equation may be applied to this problem as

$$\frac{\partial^2 y}{\partial x^2} = \frac{M}{EI}. \tag{51}$$

Differentiation with respect to x yields

$$\frac{\partial^3 y}{\partial x^3} = \frac{1}{EI}\frac{dM}{dx}. \tag{52}$$

Substituting the general internal shear force V for $\dfrac{dM}{dx}$ leads to

$$y''' = \frac{V}{EI}. \tag{53}$$

Substituting (53) into (20) and (33) gives

$$V + C_{L1} = 0 \text{ and } V - C_{R1} = 0. \tag{54}$$

From Figure 34, $V = -V_1$ for the left side, and $V = V_2$ for the right. Therefore,

$$C_{L1} = V_1 \text{ and } C_{R1} = V_2. \tag{55}$$

Solution of the Second Integration Constants

From the solution thus far, Equations (22), (23), (35), (36), (41), and (42) evaluated at x_p become

$$EIy_L'(x_p) + \tfrac{1}{2}V_1 x_p^2 + C_{L2}x_p = 0, \tag{56}$$

$$EIy_L(x_p) + \tfrac{1}{6}V_1 x_p^3 + \tfrac{1}{2}C_{L2}x_p^2 = 0, \tag{57}$$

$$EIy_R'(L - x_p) - \tfrac{1}{2}V_2(L - x_p)^2 - C_{R2}(L - x_p) = 0, \tag{58}$$

$$EIy_R(L - x_p) + \tfrac{1}{6}V_2(L - x_p)^3 + \tfrac{1}{2}C_{R2}(L - x_p)^2 = 0, \tag{59}$$

$$y_L(x_p) = y_R(L - x_p), \tag{60}$$

$$y_L'(x_p) = y_R'(L - x_p). \tag{61}$$

- 44 -

To eliminate all unknowns except C_{L2}, begin by solving (57) for $y_L(x_p)$ to get

$$y_L(x_p) = \frac{-\frac{1}{6}V_1 x_p^3 - \frac{1}{2}C_{L2} x_p^2}{EI}.$$ (62)

Substituting into (60) yields

$$y_R(L - x_p) = \frac{-\frac{1}{6}V_1 x_p^3 - \frac{1}{2}C_{L2} x_p^2}{EI}.$$ (63)

Substituting into (59) and solving for C_{R2} gives

$$C_{R2} = \frac{\frac{1}{3}V_1 x_p^3 + C_{L2} x_p^2 - \frac{1}{3}V_2(L - x_p)^3}{(L - x_p)^2}.$$ (64)

Substituting into (58) and solving for $y_R{}'(L - x_p)$ gives

$$y_R{}'(L - x_p) = \frac{\frac{1}{2}V_2(L - x_p)^2}{EI} + \frac{\frac{1}{3}V_1 x_p^3 + C_{L2} x_p^2 - \frac{1}{3}V_2(L - x_p)^3}{EI(L - x_p)}.$$ (65)

Substituting into (61) yields

$$y_L{}'(x_p) = \frac{\frac{1}{2}V_2(L - x_p)^2}{EI} + \frac{\frac{1}{3}V_1 x_p^3 + C_{L2} x_p^2 - \frac{1}{3}V_2(L - x_p)^3}{EI(L - x_p)}.$$ (66)

Finally, substituting into (56) and solving for C_{L2} achieves the solution

$$C_{L2} = \frac{-\frac{1}{6}V_2(L - x_p)^3 - \frac{1}{6}V_1 x_p^2(3L - x_p)}{x_p L}.$$ (67)

Substituting into (64) yields

$$C_{R2} = \frac{-\frac{1}{6}V_1 x_p^3 - \frac{1}{6}V_2(L - x_p)^2\left(2L + x_p\right)}{L(L - x_p)}.$$ (68)

Applying the Integration Constants

Substitution of all the integration constants into Equations (19)-(23) and (32)-(36) yields

$$EIy_L{}^{IV} = 0,$$ (69)

$$EIy_L{}''' + V_1 = 0,$$ (70)

$$EIy_L{}'' + V_1 x - \frac{\frac{1}{6}V_2(L - x_p)^3 + \frac{1}{6}V_1 x_p^2(3L - x_p)}{x_p L} = 0,$$ (71)

$$EIy_L{}' + \frac{1}{2}V_1 x^2 - \frac{\frac{1}{6}V_2(L - x_p)^3 + \frac{1}{6}V_1 x_p^2(3L - x_p)}{x_p L}x = 0,$$ (72)

$$EIy_L + \frac{1}{6}V_1 x^3 - \frac{1}{2}\frac{\frac{1}{6}V_2(L - x_p)^3 + \frac{1}{6}V_1 x_p^2(3L - x_p)}{x_p L}x^2 = 0,$$ (73)

$$EIy_R{}^{IV} = 0,$$ (74)

$$EIy_R{}''' - V_2 = 0,$$ (75)

$$EIy_R{}'' + V_2(L - x) - \frac{\frac{1}{6}V_1 x_p^3 + \frac{1}{6}V_2(L - x_p)^2\left(2L + x_p\right)}{L(L - x_p)} = 0,$$ (76)

- 45 -

$$EIy_R' - \tfrac{1}{2}V_2(L-x)^2 + \frac{\tfrac{1}{6}V_1 x_p^3 + \tfrac{1}{6}V_2(L-x_p)^2(2L+x_p)}{L(L-x_p)}(L-x) = 0, \tag{77}$$

$$EIy_R + \tfrac{1}{6}V_2(L-x)^3 - \tfrac{1}{2}\frac{\tfrac{1}{6}V_1 x_p^3 + \tfrac{1}{6}V_2(L-x_p)^2(2L+x_p)}{L(L-x_p)}(L-x)^2 = 0. \tag{78}$$

Finding V_1 and V_2

Substituting (73) and (78) into (60) yields

$$-V_1 x^3 + \tfrac{1}{2}\frac{V_2(L-x_p)^3 + V_1 x_p^2(3L-x_p)}{x_p L}x^2 =$$
$$-V_2(L-x)^3 + \tfrac{1}{2}\frac{V_1 x_p^3 + V_2(L-x_p)^2(2L+x_p)}{L(L-x_p)}(L-x)^2 \tag{79}$$

which is then solved for V_2. Note that x and x_p are considered separate, and the limit will be taken as x approaches x_p.

$$V_2 = V_1 \frac{2Lx^3 + \dfrac{x_p^3}{(L-x_p)}(L-x)^2 - x_p(3L-x_p)x^2}{2L(L-x)^3 + \dfrac{(L-x_p)^3}{x_p}x^2 - (L-x_p)(2L+x_p)(L-x)^2}. \tag{80}$$

Evaluating the limit results in

$$V_2 = V_1 \frac{2Lx_p^3 + Lx_p^3 - 3Lx_p^3 - x_p^4 + x_p^4}{2L(L-x_p)^3 + (L-x_p)^3 x - (L-x_p)^3(2L+x_p)}, \tag{81}$$

which ultimately adopts the indeterminate form $\dfrac{0}{0}$. L'Hopital's rule can be applied, differentiating the numerator and the denominator to get

$$V_2 = V_1 \frac{6Lx^2 - 2\dfrac{x_p^3}{(L-x_p)}(L-x) - 2x_p(3L-x_p)x}{-6L(L-x)^2 + 2\dfrac{(L-x_p)^3}{x_p}x + 2(L-x_p)(2L+x_p)(L-x)}. \tag{82}$$

Evaluation of the limit results in

$$V_2 = V_1 \frac{6Lx_p^2 - 2x_p^3 - 2x_p^2(3L-x_p)}{-6L(L-x_p)^2 + 2(L-x_p)^3 + 4L(L-x_p)^2 + 2x_p(L-x_p)^2}, \tag{83}$$

which again ends in the form $\dfrac{0}{0}$. Applying l'Hopital's rule once more, the result is

- 46 -

$$V_2 = V_1 \frac{12Lx + 2\frac{x_p^3}{(L-x_p)} - 2x_p(3L - x_p)}{12L(L-x) + 2\frac{(L-x_p)^3}{x_p} - 2(L-x_p)(2L+x_p)}. \tag{84}$$

Evaluation finally achieves the acceptable form

$$V_2 = V_1 \frac{3Lx_p + x_p^2\left(\frac{1}{(L-x_p)} + 1\right)}{2L(L-x_p) + L^2\frac{(L-x_p)}{x_p}}. \tag{85}$$

Because the beam element illustrated in Figure 33 is in equilibrium,
$$V_1 + V_2 = P. \tag{86}$$

Substituting (85) into (86) gives

$$V_1 + V_1 \frac{3Lx_p + x_p^2\left(\frac{1}{(L-x_p)} + 1\right)}{2L(L-x_p) + L^2\frac{(L-x_p)}{x_p}} = P. \tag{87}$$

The solution for V_1 is then

$$V_1 = \frac{P}{1 + \frac{3Lx_p + x_p^2\left(\frac{1}{(L-x_p)} + 1\right)}{2L(L-x_p) + L^2\frac{(L-x_p)}{x_p}}}. \tag{88}$$

Similarly,

$$V_2 = \frac{P}{1 + \frac{2L(L-x_p) + L^2\frac{(L-x_p)}{x_p}}{3Lx_p + x_p^2\left(\frac{1}{(L-x_p)} + 1\right)}}. \tag{89}$$

Final Solution

For the portion of the beam on the left of the load,
$$y_L = \frac{-\frac{1}{6}V_1}{EI}x^3 + \frac{\frac{1}{12}V_2(L-x_p)^3 + \frac{1}{12}V_1x_p^2(3L - x_p)}{EILx_p}x^2. \tag{90}$$

For the portion of the beam on the right of the load,
$$y_R = \frac{-\frac{1}{6}V_2}{EI}(L-x)^3 + \frac{\frac{1}{12}V_1x_p^3 + \frac{1}{12}V_2(L-x_p)^2(2L+x_p)}{EIL(L-x_p)}(L-x)^2 \tag{91}$$

- 47 -

where

$$V_1 = \cfrac{P}{1 + \cfrac{3Lx_p + x_p^2\left(\cfrac{1}{(L-x_p)}+1\right)}{2L(L-x_p)+L^2\cfrac{(L-x_p)}{x_p}}} \ ,$$

(92)

$$V_2 = \cfrac{P}{1 + \cfrac{2L(L-x_p)+L^2\cfrac{(L-x_p)}{x_p}}{3Lx_p + x_p^2\left(\cfrac{1}{(L-x_p)}+1\right)}} \ .$$

(93)

Solution Example and Illustration

Parameter Values

Parameter values are approximated from the prototype itself. To find the beam's second moment of area I, the cross-section in Figure 36 is used, which represents the continuous beam portion of the guide structure. The neutral axis is assumed to coincide with the geometric center of the section.
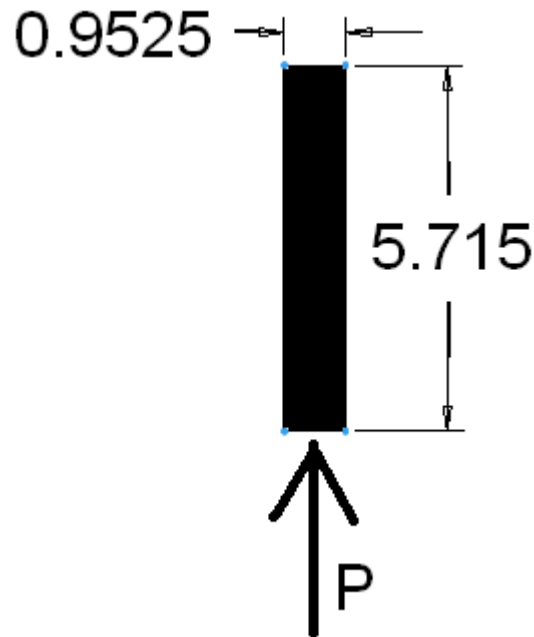
Figure 36: Cross-section of the beam, cm units

For this section,

- 48 -

$$I = \frac{bh^3}{12}$$

$$I = \frac{(0.9525)(5.715)^3}{12} \quad \text{(values in cm)}$$

$$I = 14.8\,\text{cm}^4 = 1.48E - 7\,\text{m}^4$$

(94)

Symbol	Value	Source
I	1.48 E-7 m^4	Geometry of cross-section
E	7 E10 Pa	Nominal for aluminum
L	2 m	Measured (Precise: 2.03 m)
P	800 N	Worst-case transverse load, from foot
x_p	0.5 m	Arbitrary

Table 10: Values used in deflection example

Illustration of Beam Shape

With the values described in Table 10, the beam shape is as described in Figure 37.
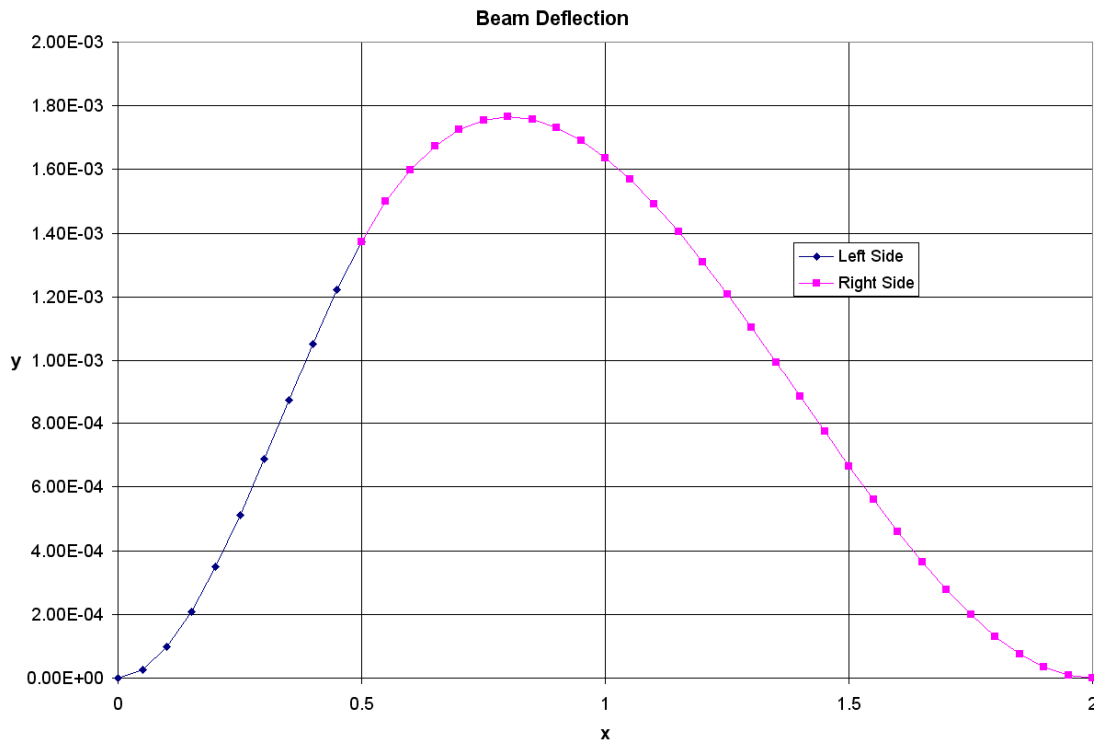
Figure 37: Chart depicting the theoretical beam shape under transverse load at x = 0.5 m

- 49 -

Figure 37 visually verifies all the characteristics of the beam deformation that one would expect. The endpoints are fixed at zero displacement and zero slope, there is no geometric discontinuity at the point of load application, and the peak deformation is off-center when the load is off-center. Worst-case loading, however, occurs when the load is applied at the center of the beam.
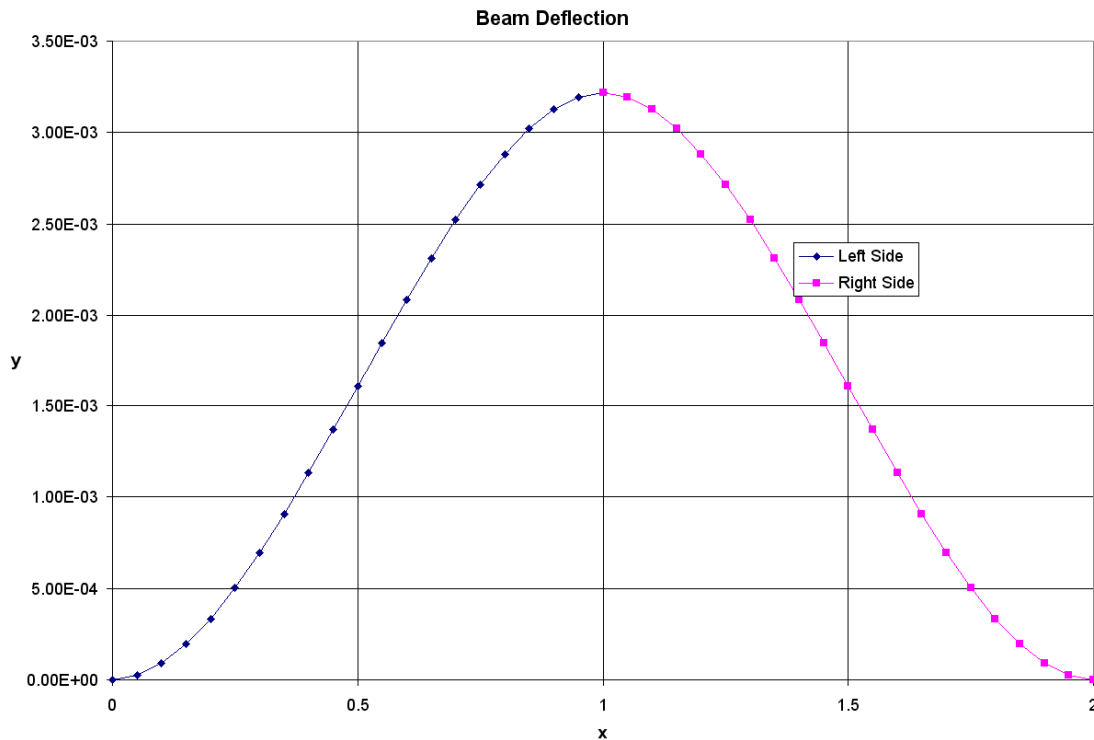
Figure 38: Chart depicting the theoretical beam shape under transverse load at x = 1 m

Under the worst-case loading depicted in Figure 38, the maximum deflection of the beam is predicted to be 3.2 mm. Although this value is approximate and the ramifications of deformation have not been extensively analyzed, it seems insignificant to the functioning of the linear slide.

The resulting description of beam deformation presented here is consistent with similar conclusions found in other works. For example, it agrees with Roark's result for maximum displacement, with only minor discrepancy no doubt owing to different assumptions made in the analytical process [6]. The solution presented here has the notable advantage of describing the beam shape at all points, rather than just at the point of maximum displacement.

Lateral Displacement of Carriage During Dot Placement in a Curve

One of the basic principles of operation on which the RPM machine relies is that the carriage should remain fixed to a single point on the road during marker placement. However, this is not the case when the vehicle is moving on a curved path. As the carriage travels along the

- 50 -

linear slide, its lateral position changes relative to the road, assuming that the bond to the vehicle is absolute.

Consider the case in which the apparatus resides upon a single-axle trailer. The travel of the carriage is centered about said axle in order to minimize the lateral displacement that will soon be quantified. The carriage moves 0.762 m (2.50 ft) along the linear slide from its home position to the axle. The vehicle moves in an arc, and the center of the linear slide thereby moves in an arc of 15.24 m (50.00 ft). This is visualized in Figure 39, which is exaggerated in proportion to emphasize the lateral displacement.
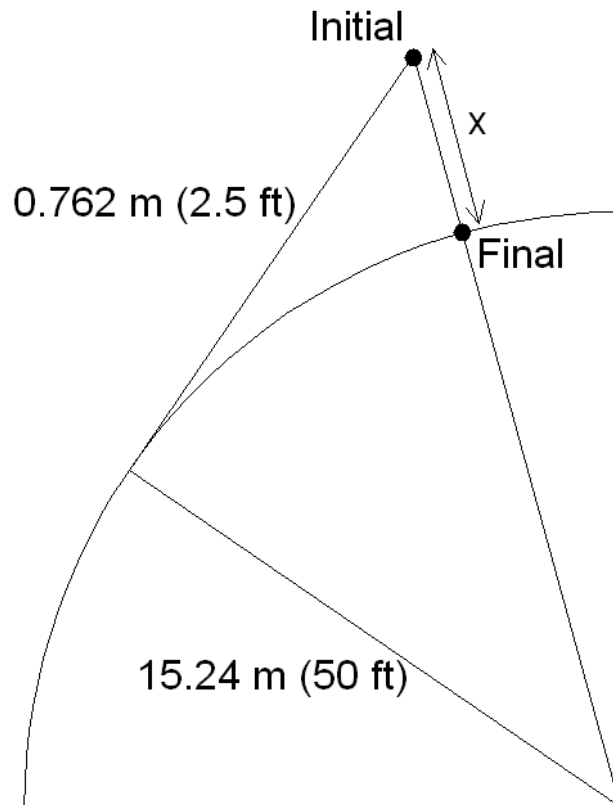
Figure 39: Lateral Displacement in a Curve

The carriage attaches to the road at the Initial position, and then follows the linear slide as the trailer moves in the specified arc. However, moving along the linear slide brings the carriage closer to the arc's center by the radial x, forcing the carriage to move laterally relative to the road despite its attachment. To find this value, the initial radial distance is to be compared against the final value. The initial radial distance is equal to the hypotenuse of the right triangle with 0.762 m and 15.24 m as the minor sides. By the Pythagorean Theorem,

$$\text{Initial radial distance} = \sqrt{(0.762)^2 + (15.24)^2} = 15.259 \text{ m} . \qquad (95)$$

As the final radial distance must be 15.24 m, the radial or lateral translation of the carriage is 0.019 m (0.75 inch). This may be considered the worst-case value.

- 51 -

There is currently no allowance made for this lateral displacement on curved lanes. Naturally, this is less of an issue when the curvature of the road is less severe, but lateral displacement must be addressed if the system is to be capable of placement on curved lanes. An important problem of lateral displacement is that it makes the final lateral position of the new marker uncertain. Depending on vehicle speed, the carriage may undergo lateral displacement in any amount from zero to maximum. Ideally, lateral targeting would predict the displacement and compensate for it, but this would require knowledge of the turning radius, which is heretofore unmeasured and whose measurement would be difficult to achieve. The most efficient response may be to tolerate small lateral displacements, and minimize them by reducing vehicle speed in curves.

However, even small lateral displacements may cause damage to the apparatus. Namely, if the foot is fixed to the road but then forced to move laterally, various damages may occur. The foot may become worn from being dragged across the road, or if the foot does not slip, the rest of the apparatus must accommodate the deformation, possibly resulting in structural bending or separation of parts. Assuming foot wear to be the lesser of two evils, the force of the foot should be limited such that it will slide along the road before damaging the rest of the device.

Chapter Summary

This chapter has described three of the analytical methods applied to the device. One is a dynamic pneumatic simulation that approximates the motion of the carriage. This simulation can be used to test various scenarios without spending the additional time and money that would be required to test them on the physical prototype.

Another analytical method is an energy-based determination of the linear slide's deformation under load. This can be used to verify that deformations are within acceptable bounds. Furthermore, the analysis can aid the optimization of beam design later.

Finally, a calculation was made for the worst-case lateral displacement of the carriage during marker placement. Such lateral movement can potentially result in targeting error and damage to the apparatus, but the targeting error is likely to be insignificant in most cases, and serious damage will not occur if the force of the foot is properly limited.

Analysis has also been performed for an alternative speed-matching method in which sophisticated pneumatic control is used instead of the road-grabbing foot. By applying the correct pneumatic inputs, the carriage can quickly match road speed without the foot.

CHAPTER 5

CURRENT ALTERNATIVE DESIGN WITH NO FOOT

In the current design, a foot descends from the carriage in order to ensure that the carriage is stationary relative to the road. However, this may not be necessary. Pneumatic control alone may be adequate to achieve constant carriage speed matched to the vehicle's speed such that the carriage is stationary relative to the road. The challenge for this arises due to the compressibility of air. That is, the carriage is desired to accelerate quickly to match the vehicle speed, but it is also desired to stop accelerating at that point and become steady. These two goals are contradictory. The first requires a large influx of air into the band cylinder's chamber, but if too much air is squeezed in, the expansion of that air will accelerate the carriage beyond the desired speed. Thus, the acceleration process must be controlled with the final state in mind.

Condition for Steady Speed

A steady, final speed is desired. In this case, the force balance on the carriage is zero. Assuming friction to be constant at constant speed, the net pressure on the carriage's piston must also be constant, just enough to overcome that friction. The desired pressure must be achieved at the home side, and the flow must be correct such that this pressure is maintained as the carriage moves and the volume at the home side thereby becomes larger. The force balance equation when the speed of the carriage is steady, assuming that the carriage is moving away from the home end, is

$$P_1 = \frac{F_f}{A} + P_2 . \tag{96}$$

Solving Equation (12) for P_1 yields

$$P_1 = \frac{n_1 RT}{V_1} . \tag{97}$$

P_1 must have a constant value during steady state. Because R and T are considered constant at all times, the ratio $\frac{n_1}{V_1}$ must also be constant. Therefore, when the carriage moves an infinitesimal amount, the added volume dV_1 must be filled with an equivalent number of moles dn_1. Thus $\frac{dn_1}{dV_1}$ can be substituted for $\frac{n_1}{V_1}$ to get

$$P_1 = \frac{dn_1}{dV_1} * RT . \tag{98}$$

Substituting for dn_1 using Equation (11) and replacing dV_1 with Adx yields

$$P_1 = \frac{C_1 \sqrt{P_{out1}} \sqrt{P_{out1} - P_1} dt}{Adx} * RT . \tag{99}$$

Because speed $v = \frac{dx}{dt}$,

$$P_1 = \frac{C_1 \sqrt{P_{out1}} \sqrt{P_{out1} - P_1}}{Av} * RT . \tag{100}$$

Squaring the equation yields

$$P_1^2 = \left(\frac{RT_1 C_1}{Av}\right)^2 P_{out1} (P_{out1} - P_1). \tag{101}$$

Rearrangement yields

$$P_1^2 + \left(\frac{RT_1 C_1}{Av}\right)^2 P_{out1} P_1 - \left(\frac{RT_1 C_1}{Av}\right)^2 P_{out1}^2 = 0 . \tag{102}$$

Solving using the Quadratic Formula achieves

$$P_1 = \frac{-\left(\frac{RT_1 C_1}{Av}\right)^2 P_{out1} + \sqrt{\left(\frac{RT_1 C_1}{Av}\right)^4 P_{out1}^2 + 4\left(\frac{RT_1 C_1}{Av}\right)^2 P_{out1}^2}}{2} . \tag{103}$$

Next is the derivation of steady-speed P_2, which is very similar to that of P_1. It begins by solving Equation (12) for P_2 to get

$$P_2 = \frac{n_2 RT}{V_2} . \tag{104}$$

P_2 must have a constant value during steady state. Because R and T are considered constant at all times, the ratio $\frac{n_2}{V_2}$ must also be constant. Therefore, when the carriage moves an infinitesimal amount, the added volume dV_2 must be filled with an equivalent number of moles dn_2. Thus $\frac{dn_2}{dV_2}$ can be substituted for $\frac{n_2}{V_2}$ to get

$$P_2 = \frac{dn_2}{dV_2} * RT . \tag{105}$$

Substituting for dn_2 using Equation (11) and replacing dV_2 with $-Adx$ yields

$$P_2 = -\frac{C_2 \sqrt{P_2} \sqrt{P_2 - P_{out2}} \, dt}{Adx} * RT . \tag{106}$$

Because speed $v = \frac{dx}{dt}$,

$$P_2 = -\frac{C_2 \sqrt{P_2} \sqrt{P_2 - P_{out2}}}{Av} * RT . \tag{107}$$

Squaring the equation yields

$$P_2^2 = \left(\frac{RT_2 C_2}{Av}\right)^2 P_2 (P_2 - P_{out2}). \tag{108}$$

Rearranging and dividing by P_2 results in

$$\left[1-\left(\frac{RT_2C_2}{Av}\right)^2\right]P_2 + \left(\frac{RT_2C_2}{Av}\right)^2 P_{out2} = 0. \tag{109}$$

Solving expressly for P_2 yields

$$P_2 = \frac{P_{out2}}{1-\left(\dfrac{Av}{RT_2C_2}\right)^2}. \tag{110}$$

Substituting Equations (110) and (103) into (96) yields

$$\frac{-\left(\dfrac{RT_1C_1}{Av}\right)^2 P_{out1} + \sqrt{\left(\dfrac{RT_1C_1}{Av}\right)^4 P_{out1}^2 + 4\left(\dfrac{RT_1C_1}{Av}\right)^2 P_{out1}^2}}{2} = \frac{F_f}{A} + \frac{P_{out2}}{1-\left(\dfrac{Av}{RT_2C_2}\right)^2}. \tag{111}$$

Finally, the solution for P_{out1} is

$$P_{out1} = \frac{\dfrac{2F_f}{A} + \dfrac{2P_{out2}}{1-\left(\dfrac{Av}{RT_2C_2}\right)^2}}{-\left(\dfrac{RT_1C_1}{Av}\right)^2 + \left(\dfrac{RT_1C_1}{Av}\right)\sqrt{\left(\dfrac{RT_1C_1}{Av}\right)^2 + 4}}. \tag{112}$$

Equation (112) describes the conditions that must be met for the carriage to move at a steady speed.

Uniform Application of Steady Conditions

The most direct approach to reach a steady speed is to apply the control inputs necessary for steady speed from the very beginning of carriage acceleration. Thus, the carriage should reach the steady speed eventually. Steady control inputs will now be applied in simulation, using values from Section CHAPTER 0: , with the exception that P_{out1} will take on alternate values meant to achieve certain speeds according to Equation (112).

v (m/s)	P_{out1} (Pa, abs)
0.25	1.533 E5
0.5	1.863 E5
1	2.810 E5
1.5	4.137 E5
2	6.227 E5

Table 11: Pressure values to achieve certain constant speeds

- 55 -
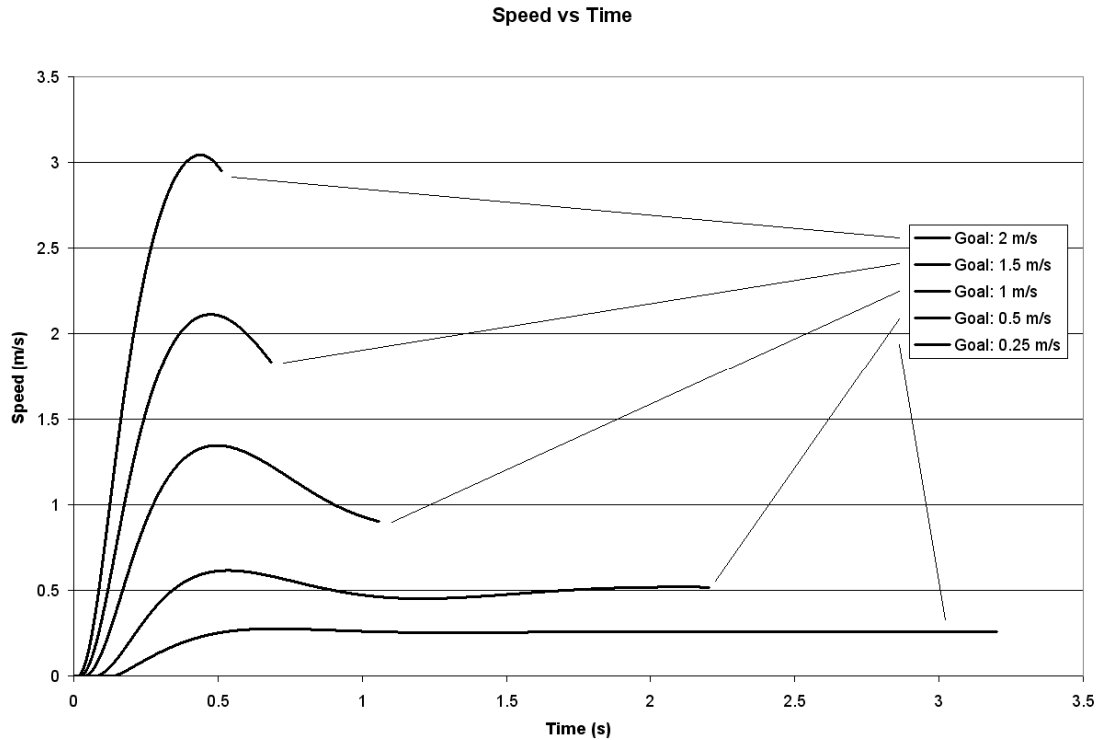
Figure 40: Speed vs. time when carriage is subjected to steady inputs

The simulation yields the results displayed in Figure 40. Clearly, there is concern regarding overshoot and settling time of the carriage response. When applying low pressure in order to achieve a low steady speed, these issues are minor, but they become unacceptable when attempting to reach higher speeds. For example, the attempt to reach a steady 2 m/s (4.47 mph) resulted in an overshoot greater than 50%. Furthermore, the carriage speed does not have a chance to settle, because it reaches the end of the linear slide too quickly.

The cause of this oscillatory motion is the compressibility of air. When the carriage is at rest in the home position and pressure is suddenly applied to it, an excessive pressure builds up that is far greater than what is required for steady speed. The expansion of this compressed air, coupled with continuous flow, accelerates the carriage past its steady speed. This phenomenon can be called "overfill." It is addressed in Chapter 5, High Performance Routine.

High Performance Routine

Optimally, the carriage should undergo rapid acceleration followed by constant speed. Rapid acceleration is easy to achieve, as it simply involves the application of high-pressure and/or unrestricted air flow to the carriage. However, transitioning from acceleration to constant speed is problematic. During acceleration, the home chamber is overfilled with air, and the expansion of this air can continue to accelerate the carriage even if additional flow has stopped. Although this complicates the proposition at hand, it can be compensated. Consider the following routine for carriage acceleration:

- 56 -

1. Apply a high pressure for a brief time.
2. Seal the home chamber and allow the compressed air therein to expand.
3. As the carriage speed peaks at the desired steady value, apply the pressure necessary to maintain that speed.

The net result of this procedure is extremely rapid acceleration followed by steady speed. This has been performed in simulation using the techniques and values described in Chapter 4:Dynamic Pneumatic Simulation and Chapter 5:Condition for Steady Speed. The initial applied pressure is 7.905 E5 Pa (114.6 psi) (absolute scale).

Speed vs Time
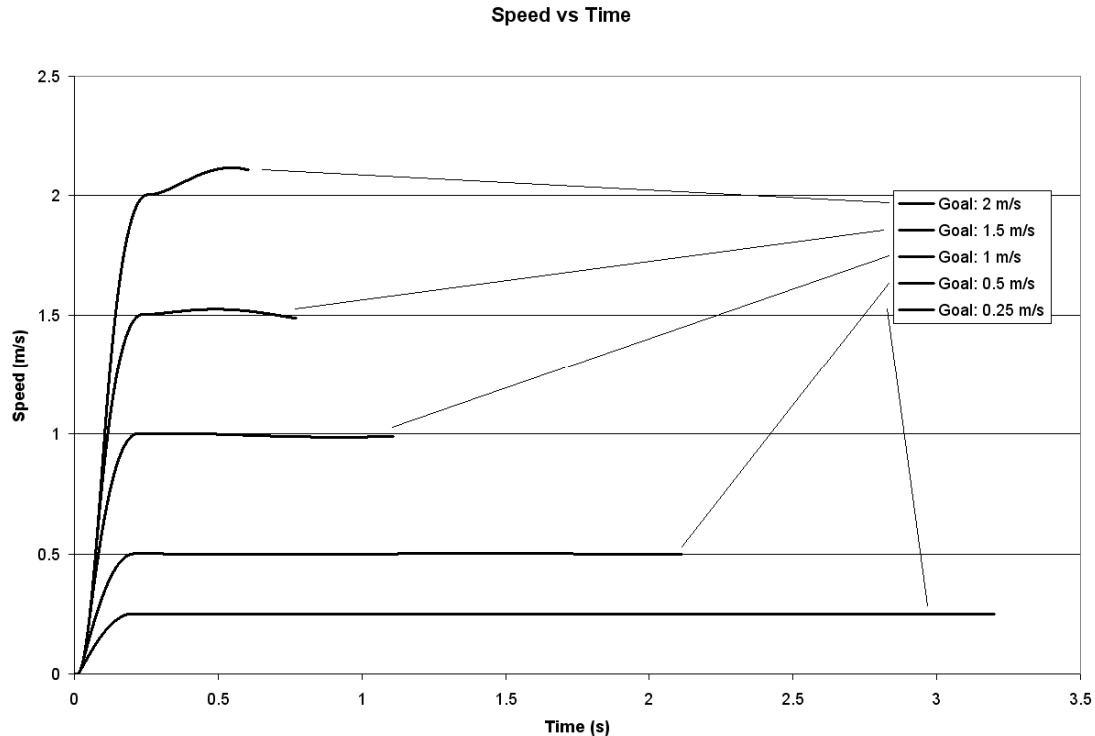
Figure 41: High performance carriage movement

Figure 41 displays the velocity of the carriage during and after acceleration. Note that the acceleration phase is short and transitions smoothly into the steady speed for the lower speeds. To determine the time at which to seal off the high pressure, the simulation was run using different seal times until the carriage's speed peaked at the desired steady speed. Then, the steady pressure was applied at the time of peak speed in order to maintain it. A trend may be observed as the desired speed increases; namely, the speed fluctuates instead of being steady. This phenomenon may be observed for 1.5 m/s (3.4 mph) and 2.0 m/s (4.5 mph). This occurs because the pressure in the far chamber has not built up to its steady value when the steady pressure is applied. Thus, the steady pressure is actually excessive and increases the carriage's speed past the desired value. This effect can be compensated, perhaps by applying a lower pressure to achieve semi-steady speed. However, since the effect is only significant at higher speeds, it may be neglected initially.

- 57 -
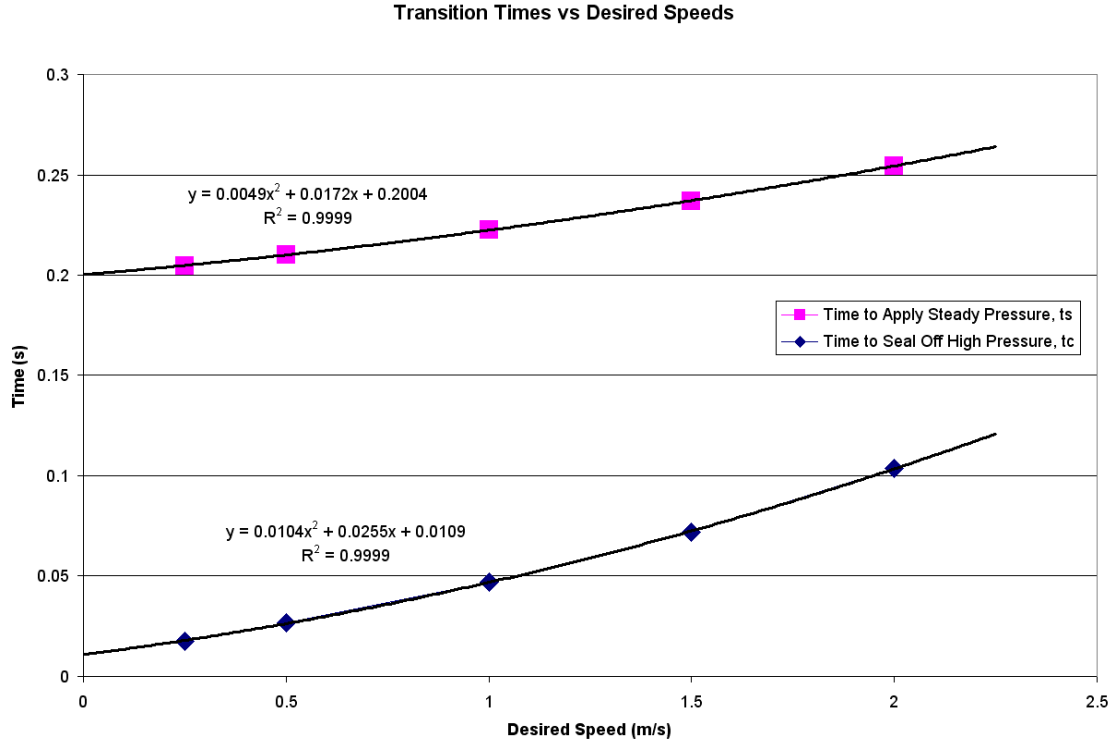
Figure 42: Transition times vs. desired speeds for high-performance acceleration

Figure 42 presents the transition times to accomplish high-performance acceleration. For any desired speed, the high pressure should be sealed off at the lower time, and the steady pressure should be applied at the greater time. Both times are measured relative to the moment of acceleration initiation, marked by the first application of the high pressure. The procedure for determining these times has been described, but the process is relatively troublesome. To aid in the determination of times to achieve other speeds, an empirical curve fit is appropriate. The time at which to seal off the high pressure is

$$t_c = 0.0104x^2 + 0.0255x + 0.0109, \tag{113}$$

and the time at which to apply the steady pressure is

$$t_s = 0.0049x^2 + 0.0172x + 0.2004. \tag{114}$$

Both of these empirical curve fits have R^2 values of 0.9999, and thus are very representative of the data. They should therefore be able to accurately predict time values appropriate to different desired speeds. With these equations, it is a simple matter to achieve high performance acceleration for any speed.

The addition of a variable pressure source is all that is necessary to allow the current prototype to match road speed without using the foot. Indeed, speed-matching should be possible even without the variable pressure source, although the home end of the band cylinder must be manually adjusted to supply the two appropriate pressures for a specific speed. If the foot is ultimately unnecessary, its removal will reduce the weight and length of the carriage, allowing for faster acceleration and longer travel respectively.

- 58 -

Chapter Summary

This chapter discussed the possibility of having the carriage match road speed through purely pneumatic means, instead of using the foot to secure the carriage to the road. If the foot were unnecessary it could be removed from the carriage, resulting in weight reduction, which would lead to faster acceleration times, which would increase the output rate of the RPM machine.

Applying a certain pressure at the home end of the band cylinder will maintain a steady carriage speed. However, the method by which the carriage is accelerated will affect the stability of the final speed. Thus there are two separate stages to consider: acceleration and steady speed. During acceleration, a very high pressure is briefly applied, compressing air in the home chamber. The high pressure is sealed off for a time, giving the air an opportunity to expand. The carriage speed peaks at the desired value, at which time the steady speed pressure is applied to maintain the speed indefinitely.

Whether it is ultimately worthwhile to remove the foot remains to be seen. However, it is assuredly possible according to the described routine. Future work will determine the final course of action.

CHAPTER 6

CONCLUSIONS AND RECOMMENDATIONS

Conclusions

This report has presented the description and justification of a device for the automated placement of raised pavement markers. The premise for ultimate completion has been outlined, and complete details for the current stage of the project. Currently, there is a laboratory prototype of the main functional elements. The prototype is such that it can be transplanted onto a moving vehicle for field testing.

All information currently available indicates that the final product is feasible and will result in numerous benefits, the most notable of which are cost efficiency and safety.

Recommendations for Future Work

Having tested the current prototype in the laboratory, the next step in the product's development is to make a version that is more complete, to be used in more realistic conditions. This involves construction and operation similar to that described in Chapter 2.

Adhesive Dispensing

A major advantage of field deployment is the ability to use adhesive. The current prototype cannot dispense adhesive because doing so would damage the conveyor belt that simulates the road surface. Moving the device on a vehicle, on the experimental road surfaces available, allows for hot-melt bituminous adhesive to be dispensed without harm. Only then can the adhesive system be verified and refined.

Better Foot Performance

In the laboratory, the prototype's foot cannot be supplied with too great a pressure, or the resulting force will interfere with the movement of the conveyor belt. That is, a high foot force pinches the belt against its sliding surface, halting its movement. This restriction is completely artificial and irrelevant to final product concerns, as it is generally desirable to supply the foot with higher pressure. Higher pressure causes the foot to actuate more quickly for the advantage of efficient and predictable timing. Higher pressure also results in greater foot force, making slippage of the carriage less likely once it is secured to the road.

Lateral Targeting

The current prototype tests longitudinal positioning only. The proposed field deployment prototype is an opportunity to test the lateral targeting system as well, as it can be equipped with the lateral array of dot sensors and the lateral actuator. This will complete the two-dimensional targeting of the new dot, and will furthermore demonstrate the targeting in a realistic environment for utmost relevancy.

REFERENCES

1. Health, C.O.o.S.a., *Caltrans Maintenance Program Injuries and Costs by Maintenance Activity 1/1/02 - 1/1/03 (Statewide)*. 2003.
2. Bennett, D. Personal Interview. 5 April 2007.
3. Rihani, R.A., and Leonhard E. Bernold, *Telerobotics for Infrastructure Maintenance: Safe Raised Pavement-Marker Application.* Transportation Research Record, 1997(1585): p. 48-52.
4. MRL. [cited 9 April 2007]; Available from: http://www.markritelines.com/pavement-markers-truck-mounted.php.
5. *Pavement Marking: Automated System Installs Pavement Markers, Improving Safety For Road Crews and Drivers*. Georgia Tech Research News 2007 9 April 2007 [cited; Available from: http://gtresearchnews.gatech.edu/newsrelease/rpm.htm.
6. Young, W.C., *Roark's Formulas for Stress and Strain*. 1989: McGraw-Hill.

APPENDIX A

GLOSSARY OF TERMS

AHMCT	Advanced Highway Maintenance and Construction Technology (Research Center)
dot	See raised pavement marker.
far end	The end of the linear slide opposite the home end.
home end	The end of the linear slide at which the carriage typically resides. It is also toward the front of the vehicle.
lateral	The side-to-side dimension relative to the vehicle's heading.
longitudinal	The forward-and-back dimension relative to the vehicle's heading.
marker	See raised pavement marker.
overfill	The excessive pressure buildup that occurs when a high flow is applied to accelerate the carriage.
raised pavement marker	A small object placed on a roadway to delineate traffic lanes and provide enhanced visual, auditory, and tactile feedback to drivers.
RPM	See raised pavement marker.

APPENDIX B

PNEUMATIC DYNAMIC ACCELERATION C# SIMULATION CODE

```csharp
//all units are SI

double x = .145;

double v = 0;

double a = 0;

double P1 = 1.01e5;

double P2 = 1.01e5;

double Pout1 = 3.77e5;

double Pout2 = 1.01e5;

double Pup1;

double Pup2;

double t = 0;

double tf = 1;

double dt = .0001;

double A = .00114;

double L = 1.524;

double T1 = 298;

double T2 = 298;

const double R = 8.314;

double n1 = P1 * A * x / R / T1;

double n2 = P2 * A * (L - x) / R / T2;

double dn1;

double dn2;

double dv;

double dx;

double FfStatic = 53;

double FfKinetic = 44;
```

- 63 -

```csharp
//the following values are only guesses

double C1 = 3.6e-7;

double C2 = 1.5e-6;

double m = 16;

FileInfo dataFile = new FileInfo(@"C:\Documents and
Settings\pssherrill\Desktop\dataFile.csv");

StreamWriter outStream = dataFile.CreateText();

outStream.WriteLine("t,x,v,a,P1,P2");

while (t < tf)

{

    outStream.WriteLine(Convert.ToString(t) + "," + Convert.ToString(x)
+ "," + Convert.ToString(v) + "," + Convert.ToString(a) + "," +
Convert.ToString(P1) + "," + Convert.ToString(P2));

    Pup1 = Math.Max(P1, Pout1);

    Pup2 = Math.Max(P2, Pout2);

    dn1 = C1 * Math.Sqrt(Pup1) * Math.Sign(Pout1 - P1) *
Math.Sqrt(Math.Abs(Pout1 - P1)) * dt;

    dn2 = C2 * Math.Sqrt(Pup2) * Math.Sign(Pout2 - P2) *
Math.Sqrt(Math.Abs(Pout2 - P2)) * dt;

    n1 = n1 + dn1;

    n2 = n2 + dn2;

    P1 = n1 * R * T1 / A / x;

    P2 = n2 * R * T2 / A / (L - x);

    if (Math.Abs((P1 - P2) * A) < FfStatic && v == 0)

        a = 0;

    else if (v == 0)

    {

        a = ((P1 - P2) * A - FfStatic * Math.Sign(P1 - P2)) / m;

        if (a < 0 && x == .145)

            a = 0;
```

- 64 -

```
        }

        else

            a = ((P1 - P2) * A - FfKinetic * Math.Sign(v)) / m;

        dv = a * dt;

        v = v + dv;

        dx = v * dt;

        x = x + dx;

        t = t + dt;

    }
```

APPENDIX C

BILL OF MATERIALS FOR CURRENT PROTOTYPE

Linear Slide

Part design and drawing by George Burkett.

Part List			
Index	Part Number	Description	Material	Qty.
1	RPH-ASV-0001	Test Stand	NA	1
2	RPH-PC-0001-00	Carriage Plate	ALUMINUM	1
3	RPH-PC-1005	Cylinder Mount	ALUMINUM	2
4	RPH-PC-1006	Brass Nut	MILD STEEL	2
5	RPH-PC-0007	Test Stand End Plate	MILD STEEL	2
6	RPH-PC-1005	Bearing Rail	ALUMINUM	2
7	RPH-PC-1006	Pneu. Cyl. Mt. Plate	ALUMINUM	1
8	RPH-PC-0005	Cylinder Face Plate	CAST AL. TOOLING PLATE	1
9	RPH-PC-0021	Steel Cap	STEEL	2
10	RPH-PC-1022	Rear CMM plate	ALUMINUM	2
11	RPH-PC-1025	mmra Base Plate	ALUMINUM	4
12	RPH-PC-1006	Support Brkct	STEEL	2
13	RPH-PC-1008	Upper Weld Sup. Plate	MILD STEEL	1
14	RPH-PC-0008B	Test Stand End Plate	STEEL	1
15	10GUMATIC	Band Cylinder	NA	1
16	P-WHEEL	P Guide Wheel	NA	4

Test Stand

RPH-ATS-0001

RPH

	5/14/07
DRWN	
CHKD	

Front Plate

Part design and drawing by George Burkett.

Cylinder Face Plate

NOTES: UNLESS OTHERWISE SPECIFIED
1) BREAK ALL SHARP EDGES.
2) HIDDEN LINES NOT NECESSARILY SHOWN.
3) MATERIAL : CAST AL. TOOLING PLATE
4) FINISH: NA

SCALE 0.100

DETAIL A
SCALE 0.250

SEE DETAIL A

.375

R.250

⌀.201 THRU
62 X

⌀.266 THRU
22X

80.000
79.750
79.000
77.000
75.000
72.000
70.000
68.000
42.000
40.000
38.000
12.000
10.000
8.000
5.750
5.000

1.000
.250
2.250
1.750
2.500 3 X
3.000
6.250
5.750

7.813
.188
1.500

GREASE OTHERWISE NOTED:
TOLERANCES
.XX ± 0.01
.XXX ±0.005
ANGLES ±0.5°

SCALE 1.000   DRAWING NO.   RPM-PC-0020
SIZE B   SHT 33 of 30 RPM

DATE 5/11/07
DESIGN GMB
DRAWN   GMB
APPROV
RELEASE

AHMCT Advanced Highway Maintenance and Construction Technology Research Center
University of California, Davis

Rails

Part design and drawing by George Burkett.

NOTES: UNLESS OTHERWISE SPECIFIED
1) BREAK ALL SHARP EDGES.
2) HIDDEN LINES NOT NECESSARILY SHOWN.
3) MATERIAL : 1045 STEEL
4) FINISH: NA

SEE DETAIL A

SCALE 0.188

SEE DETAIL B

78.00

DETAIL B
SCALE 1.000

Ø 10-32 UNF
CLASS 2B
THRU
THD ALL
31 X

2.500 30 X

1.500

.250

DETAIL A
SCALE 0.500

STARTING MATERIAL:
VENDOR: STOCK DRIVE PRODUCTS
PART NUMBER: A 7C15-2065

AHMCT Advanced Highway Maintenance and Construction
Technology Research Center
University of California, DAVIS

TITLE
Bearing Rail

UNLESS OTHERWISE NOTED:
TOLERANCES
.XX ± 0.01
.XXX ±0.005

ANGLES ±0.5°

DESIGN	GMB	DATE 9/24/06
DRAWN	GMB	
APPRV		
RELEASE		

DRAWING NO. NA

SCALE 1.000   SHT 31 of PROJECT RPM

SIZE B

Back Plate

Part design and drawing by George Burkett.

NOTES: UNLESS OTHERWISE SPECIFIED
1) BREAK ALL SHARP EDGES.
2) HIDDEN LINES NOT NECESSARILY SHOWN.
3) MATERIAL : ALUMINUM
4) FINISH: NA

Rear RPM plate

TITLE

SCALE 1.000   DRAWING NO.   RPM-PC-0022
SIZE B   SHT 35 of 35   PROJECT   RPM

Ø.266
THRU
34 X

R.250 TYP

Top End Plates

Part design and drawing by George Burkett.

NOTES: UNLESS OTHERWISE SPECIFIED
1) BREAK ALL SHARP EDGES.
2) HIDDEN LINES NOT NECESSARILY SHOWN.
3) MATERIAL : ALUMINUM
4) FINISH: NA

∅1/4-20 UNC
CLASS 2B
↧0.750 MAX
THD 0.5 MIN
3 X/VIEW

.500

5.000

3.000

1.000

.250

6.000

4.250

R.250
2X

R.500
2 X

3.000

1.250

∅.266
↧THRU

4.250

2.125

.250

3.000

5.000

3.000

1.000

.250

UNLESS OTHERWISE NOTED:
TOLERANCES
.XX ± 0.01   ANGLES ±0.5°
.XXX ±0.005

DESIGN   DWB   DATE 9/11/07
DRAWN   DWB
APPROV
RELEASE

TITLE
Horse Shoe Plate

DRAWING NO.   PRM-PC-0023

SCALE 1.000   SHT 36 of 36 PROJECT   RPM
SIZE B

Bridge Plates

Part design and drawing by George Burkett.

NOTES: UNLESS OTHERWISE SPECIFIED

1) BREAK ALL SHARP EDGES.
2) HIDDEN LINES NOT NECESSARILY SHOWN.
3) MATERIAL : ALUMINUM
4) FINISH: NA

Ø1/4-20 UNC
▽ 0.75 MAX
THD 0.50 MIN
3 X

Ø1/4-20 UNC
▽ 0.75 MAX
THD 0.50 MIN
3 X

5.000

3.000

1.000

.250

6.000

4.250

.500

1.000

3.000

5.000

.250

TITLE

Support Block

DRAWING NO.   RPM-PC-0024

SCALE 1.000

SIZE B   SHT 37 of PROJECT

AHMCT   Advanced Highway Maintenance and Construction
Technology Center
University of California, Davis

UNLESS OTHERWISE NOTED:
TOLERANCES
.XX ± 0.01
.XXX ±0.005

ANGLES ±0.5°

DATE 5/11/07

DESIGN
DRAWN   GMB
APPROV   GMB
RELEASE

- 80 -

Copyright 2011, AHMCT Research Center, UC Davis

End Caps

Part design and drawing by George Burkett.

NOTES: UNLESS OTHERWISE SPECIFIED
1) BREAK ALL SHARP EDGES.
2) HIDDEN LINES NOT NECESSARILY SHOWN.
3) MATERIAL: STEEL
4) FINISH: NA

Ø 1/4-20 UNC
⌴ 0.75 MAX
THD 0.50 MIN
2 X

Ø 3/8-16 UNC
THD ALL
4 X

Ø 1/4-20 UNC
⌴ 0.75 MAX
THD 0.50 MIN
2 X

3.750
.250
.250
4.250
3.000
1.000
1.500
3.500
4.500
.500
3.500
.500
.250

TITLE
Steel Cap

AHMCT Advanced Highway Maintenance and Construction Technology Research Center
University of California, Davis

UNLESS OTHERWISE NOTED:
TOLERANCES
.XX ± 0.01
.XXX ±0.005
ANGLES ±0.5°

DESIGN
DRAWN
APPRV
RELEASE

DATE 5/11/07

DRAWING NO.
RPM-PC-0021

PROJECT
RPM

SCALE 1.000
SHT 34 of 34
SIZE B

End Supports

Part design and drawing by George Burkett.

ALL TRIANGLES ARE ISOCELES

.38

2.250 TYP

R.50 TYP

18.000

53.1°

126.9°

126.9°

53.1°

33.000

36.000

53.1°

12.000

14.000

12.000

6.300

1.700

15.000

2.000

24.000

25.72

NOTES: UNLESS OTHERWISE SPECIFIED

1) BREAK ALL SHARP EDGES.
2) HIDDEN LINES NOT NECESSARILY SHOWN.
3) MATERIAL :: MILD STEEL
4) FINISH: NA

UNLESS OTHERWISE NOTED:
TOLERANCES
.XX ± 0.01
.XXX ±0.005

ANGLES ±0.5°

DESIGN | GMB
DRAWN | GMB
APPRV
RELEASE

DATE 6/20/06

Test Stand End Plate

DRAWING NO. RPM-PC-0007

PROJECT RPM

SCALE 1.000 | SHT 24 of 24

SIZE B

AHMCT Advanced Highway Maintenance and Construction Technology | University of California, DAVIS

Test Stand End Plate

DETAIL A
SCALE 0.375

NOTES: UNLESS OTHERWISE SPECIFIED
1) BREAK ALL SHARP EDGES.
2) HIDDEN LINES NOT NECESSARILY SHOWN.
3) MATERIAL : MILD STEEL
4) FINISH: NA

SEE DETAIL A

- 85 -

Test Stand End Plate

DETAIL A
SCALE 0.375

NOTES: UNLESS OTHERWISE SPECIFIED
1) BREAK ALL SHARP EDGES.
2) HIDDEN LINES NOT NECESSARILY SHOWN.
3) MATERIAL : MILD STEEL
4) FINISH: NA

SEE DETAIL A

- 85 -

ALL TRIANGLES ARE ISOCELES

NOTES: UNLESS OTHERWISE SPECIFIED
1) BREAK ALL SHARP EDGES.
2) HIDDEN LINES NOT NECESSARILY SHOWN.
3) MATERIAL : MILD STEEL
4) FINISH: NA

Test Stand End Plate

RPM-PC-0007

NOTES: UNLESS OTHERWISE SPECIFIED
1) BREAK ALL SHARP EDGES.
2) HIDDEN LINES NOT NECESSARILY SHOWN.
3) MATERIAL : MILD STEEL
4) FINISH: NA

SEE DETAIL A

Ø.313 THRU
THD 3/8 - 16 UNC THD ALL
4 X

Ø1.500 THRU

5.800
5.000
4.000
3.000
2.200

.500
1.375
2.250
3.375
5.375

Ø.386 THRU
THRU 3/8 -16
4 X
FOR Ø3/8 -16

Ø.397 thru
8 x

16.500
11.500
6.500
1.500

.750
11.250
13.750

9.750
7.250

DETAIL A
SCALE 0.375

Ø1.500 THRU

Test Stand End Plate

RPM-PC-0007   RPM
SCALE 1.000 DRAWING NO.
SIZE B   SHT 27 of 28PROJECT

ANGLES ±0.5°
UNLESS OTHERWISE NOTED:
TOLERANCES
.XX ± 0.01
.XXX ±0.005

DESIGN
DRAWN   GMB
APPROV   GMB
RELEASE

DATE 3/28/06
BY

- 87 -

Copyright 2011, AHMCT Research Center, UC Davis

Upper Weld Support Plate

Part design and drawing by George Burkett.

NOTES: UNLESS OTHERWISE SPECIFIED
1) BREAK ALL SHARP EDGES.
2) HIDDEN LINES NOT NECESSARILY SHOWN.
3) MATERIAL : STEEL
4) FINISH: NA

⌀ .397
▽ THRU
3 X

2.000
1.000
4.500
9.000
13.500
18.000
.375

UNLESS OTHERWISE NOTED:
TOLERANCES
.XX ± 0.01
.XXX ±0.005
ANGLES ±0.5°

DESIGN
DRAWN
APPROV
RELEASE

TITLE
Upper Weld Sup. Plate
SCALE 1.000   DRAWING NO. RPM-PC-0026
SIZE B   SHT 38 of PROJECT   RPM

- 89 -

Copyright 2011, AHMCT Research Center, UC Davis
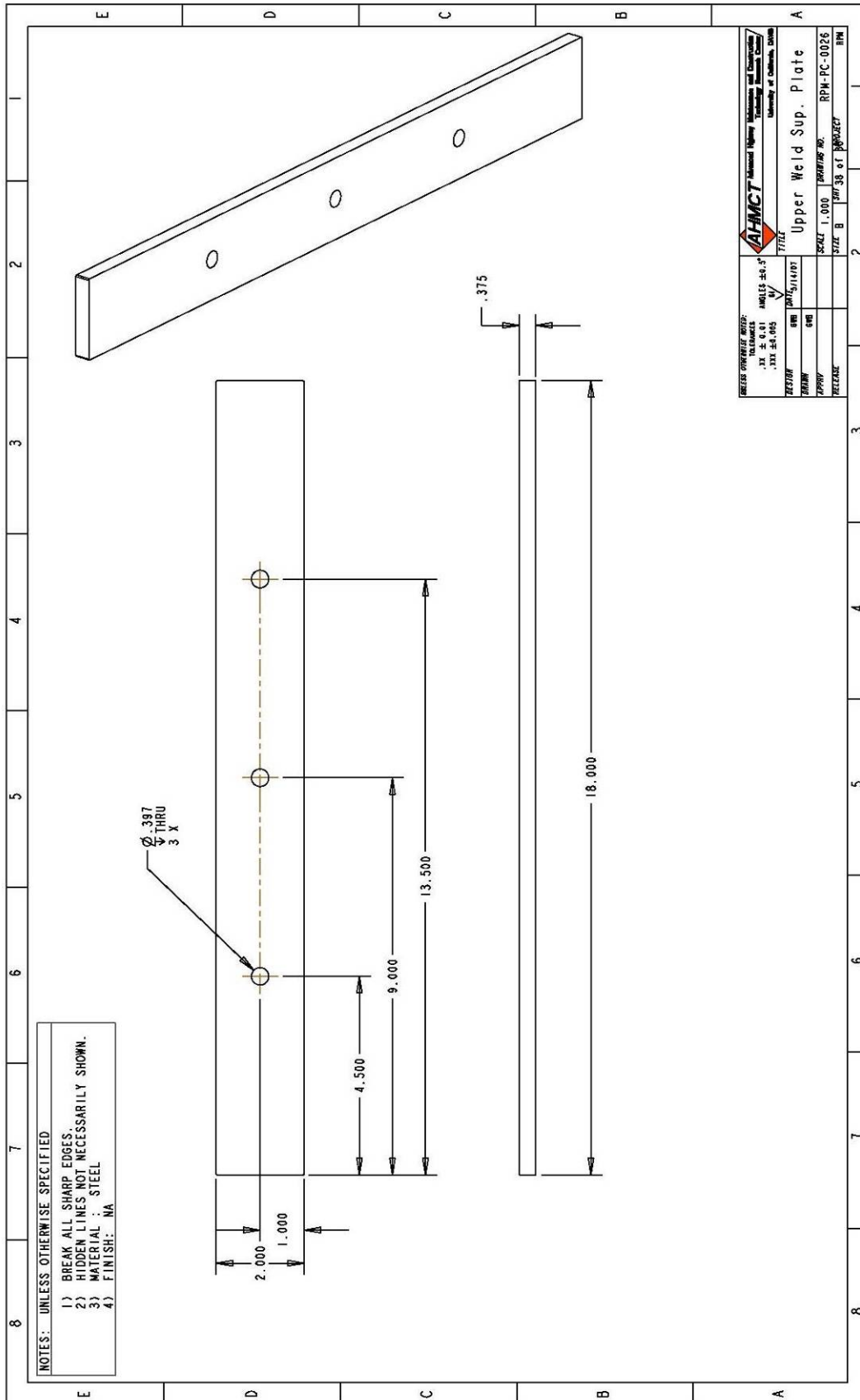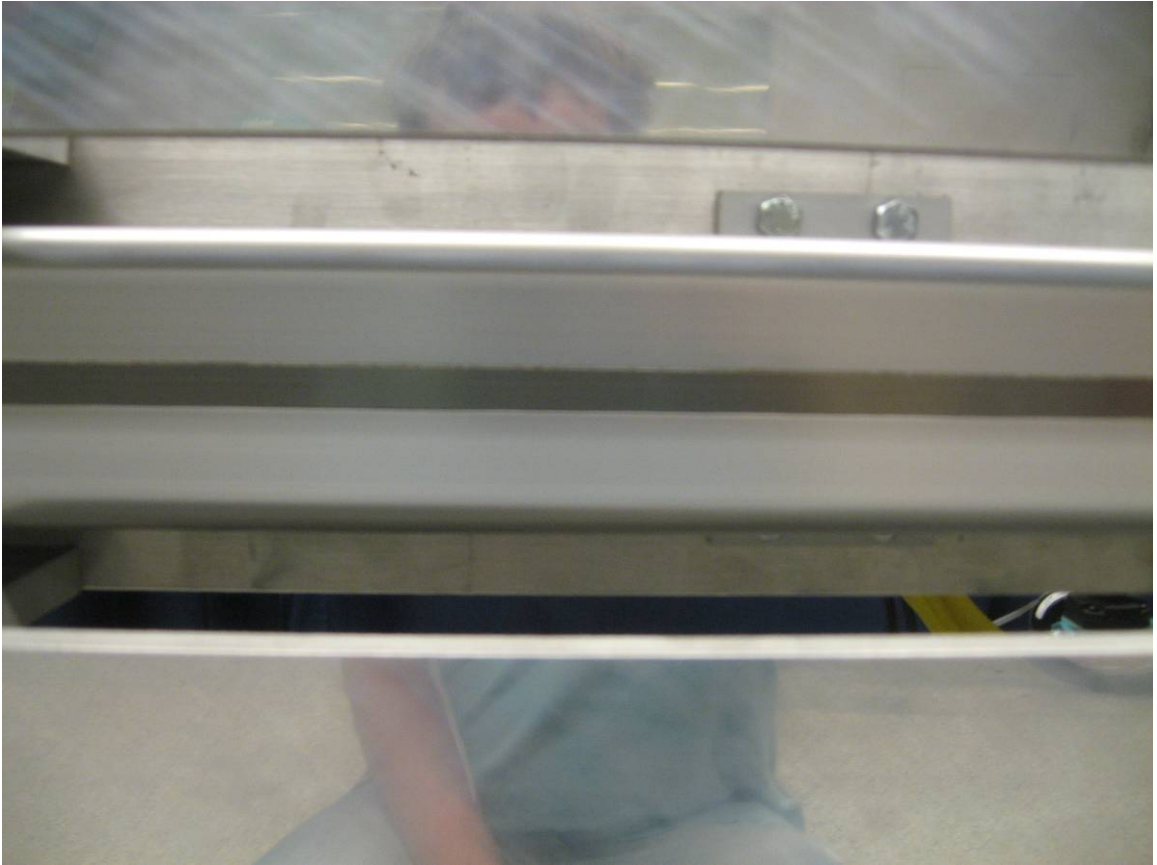
Band Cylinder

End Cylinders

Mounting Plates

Part design and drawing by George Burkett.

NOTES: UNLESS OTHERWISE SPECIFIED
1) BREAK ALL SHARP EDGES.
2) HIDDEN LINES NOT NECESSARILY SHOWN.
3) MATERIAL : ALUMINUM
4) FINISH: NA

∅ 1.51 THRU

∅ .386 THRU 4 X

2.75
2.250
1.375
.500
.500
2.300
4.100
4.60

.31

- 93 -
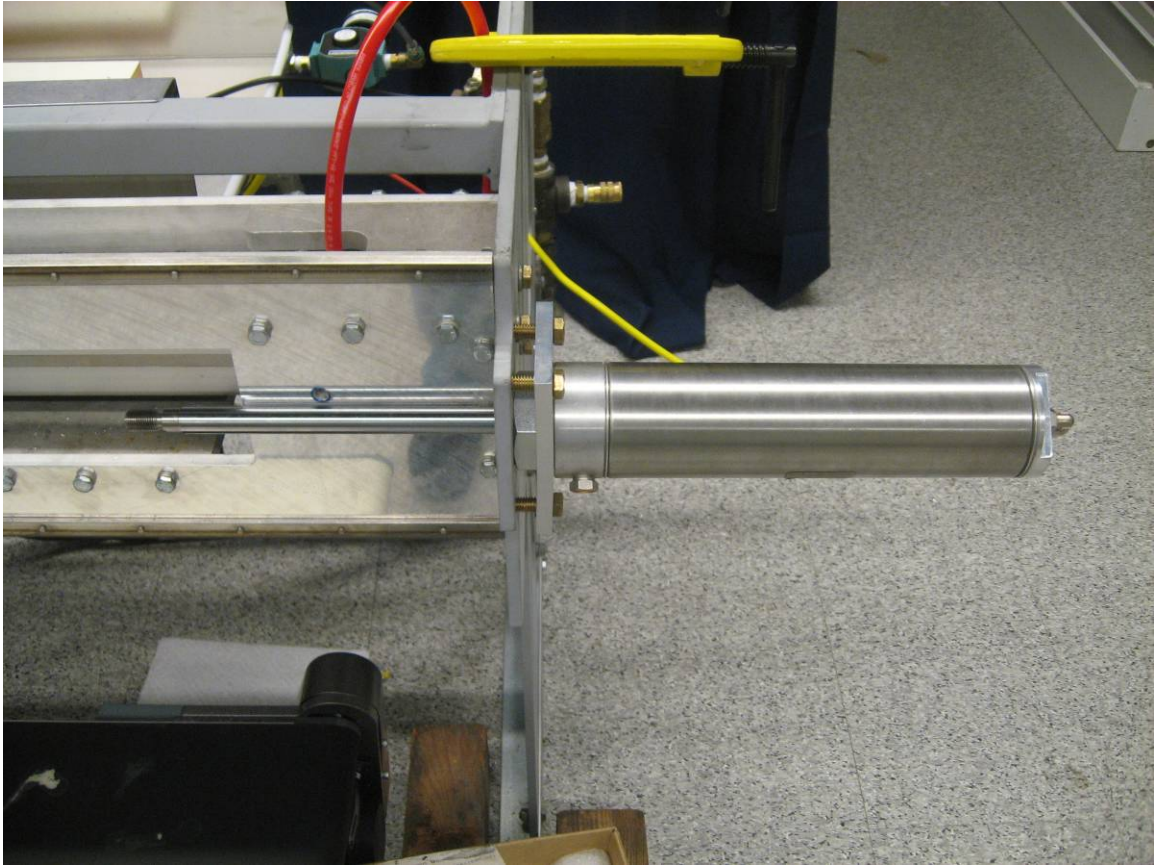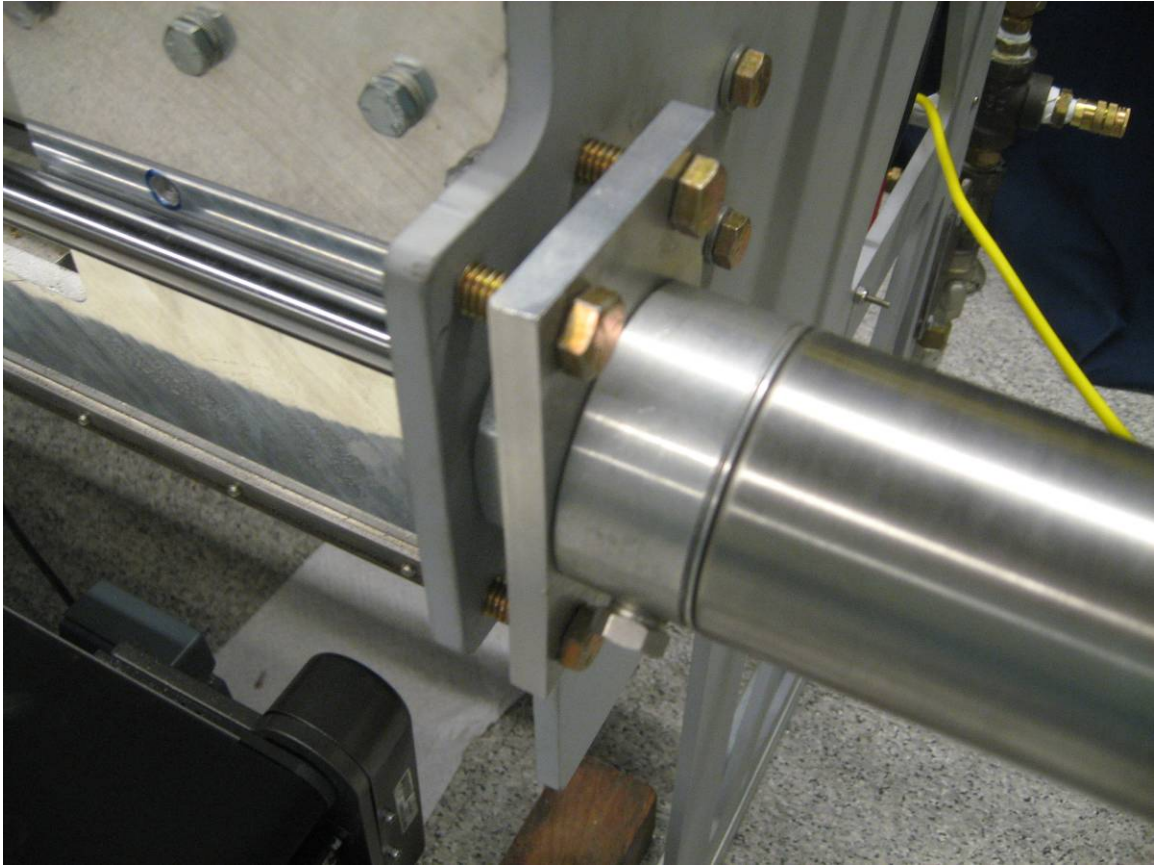
Carriage

Dot Placer

Cylinder

Magnetic Sensor

Upper Standoffs

NOTES: UNLESS OTHERWISE SPECIFIED

1) BREAK ALL SHARP EDGES.
2) HIDDEN LINES NOT NECESSARILY SHOWN.
3) MATERIAL : ALUMINUM
4) FINISH: NA

1/4-20 UNC - 2B
▽ .75
▽ THD .50 MIN
(BOTH SIDES)

1.94

Ø .63

UNLESS OTHERWISE NOTED:
TOLERANCES
.XX ± 0.01
.XXX ±0.005

ANGLES ±0.5°

DESIGN   PS   DATE 1/25/06
DRAWN   PS
APPRV
RELEASE

AHMCT Advanced Highway Maintenance and Construction
Technology Research Center
University of California, Davis

TITLE
UPPER_CANT_MCM6750K171

DRAWING NO.

SCALE 1.500   SHT 1 of 1 PROJECT
SIZE A

Back Plate

Part design and drawing by George Burkett.

NOTES: UNLESS OTHERWISE SPECIFIED
1) BREAK ALL SHARP EDGES.
2) HIDDEN LINES NOT NECESSARILY SHOWN.
3) MATERIAL : ALUMINUM
4) FINISH: NA

Ø.27 ⌄THRU
82.00° x Ø.51
4 X

15.00
14.000
7.000
7.000
5.63
2.25
.25
.281
.99
.63
1.26
1.625
1.969

TITLE
Plac. Cyl. Mt. Plate
DRAWING NO.
RPM-PC-0010
SCALE 1.000   SHT 32 of   PROJECT
SIZE B   RPM

UNLESS OTHERWISE NOTED:
TOLERANCES   ANGLES ±0.5°
.XX ± 0.01
.XXX ±0.005

Lower Standoffs

NOTES: UNLESS OTHERWISE SPECIFIED

1) BREAK ALL SHARP EDGES.
2) HIDDEN LINES NOT NECESSARILY SHOWN.
3) MATERIAL : ALUMINUM
4) FINISH: NA

1/4-20 UNC - 2B
↧ 0.75
▽ THD .50 MIN

10-24 UNC - 2B
↧ 0.75
▽ THD .50 MIN

1.82

Ø .63

UNLESS OTHERWISE NOTED:
TOLERANCES
.XX ± 0.01   ANGLES ±0.5°
.XXX ±0.005   64/

DESIGN	PS	DATE 7/25/06
DRAWN	PS	
APPRV		
RELEASE		

AHMCT Advanced Highway Maintenance and Construction Technology Research Center
University of California, Davis

TITLE LOWER_CANT_MCM6750K171

DRAWING NO.

SCALE 1.500   SHT 1 of 1   PROJECT
SIZE A

BPM

Upper Tube Bracket

NOTES: UNLESS OTHERWISE SPECIFIED

1) BREAK ALL SHARP EDGES.
2) HIDDEN LINES NOT NECESSARILY SHOWN.
3) MATERIAL : ALUMINUM
4) FINISH: NA

.75

.38

∅ .27
⤓ THRU
2 X

2.25

1.688

.28

.06

UNLESS OTHERWISE NOTED:
TOLERANCES
.XX ± 0.01   ANGLES ±0.5°
.XXX ±0.005   64/

DESIGN	PS	DATE 7/25/06
DRAWN	PS	
APPRV		
RELEASE		

AHMCT Advanced Highway Maintenance and Construction
Technology Research Center
University of California, DAVIS

TITLE
Plate_MCM9516k162

SCALE 2.000   DRAWING NO.
SIZE A   SH 1 of 1   PROJECT

RPW

- 105 -

Copyright 2011, AHMCT Research Center, UC Davis

Nose Mount

Pipe Tee

Compression Sensor

SECTION A-A

8-32 UNC
4 PLACES

ID .19

SLIP FIT OVER RPM-PPL-0001
(APPROX Ø .88)

A

A

.23

.40

Ø .30

Ø .24

Ø .24

.15 x 45°
4 PLACES

1.00

1.00

.19

.38

NOTES: UNLESS OTHERWISE SPECIFIED
1) BREAK ALL SHARP EDGES.
2) HIDDEN LINES NOT NECESSARILY SHOWN.
3) MATERIAL : ALUMINUM
4) FINISH: NA

UNLESS OTHERWISE NOTED:
TOLERANCES
.XX ± 0.01
.XXX ±0.005
ANGLES ±0.5°
64/

DESIGN	PS	
DRAWN	PS	
APPRV		
RELEASE		

DATE 8/14/06

AHMCT Advanced Highway Maintenance and Construction Technology Research Center
University of California, DAVIS

TITLE SENSOR_COLLAR_MCM6023K181

DRAWING NO. RPM-PPL-0004
PROJECT RPM

SCALE 1.500   SHT 1 of 1
SIZE A

NOTES: UNLESS OTHERWISE SPECIFIED

1) BREAK ALL SHARP EDGES.
2) HIDDEN LINES NOT NECESSARILY SHOWN.
3) MATERIAL : ALUMINUM
4) FINISH: NA

∅ .88

3/8-16 UNC - 2B TAP   THRU
5/16 DRILL (0.31) THRU   -(1) HOLE

∅ .20

∅ .75

2.18

UNLESS OTHERWISE NOTED:
TOLERANCES
.XX ± 0.01
.XXX ±0.005

ANGLES ±0.5°
64√

DESIGN
DRAWN   PS
APPRV
RELEASE

DATE 8/14/08

AHMCT Advanced Highway Maintenance and Construction
Technology Research Center
University of California, Davis

TITLE HOLLOW_CYLINDER_MCM8861SK411

DRAWING NO.

SCALE 1.000   SHT 1 of 1 PROJECT
SIZE A

NOTES: UNLESS OTHERWISE SPECIFIED

1) BREAK ALL SHARP EDGES.
2) HIDDEN LINES NOT NECESSARILY SHOWN.
3) MATERIAL : ALUMINUM
4) FINISH: NA

0.05 x 45° CHAMFER

3/8 - 16 UNC
THRU

AHMCT Advanced Highway Maintenance and Construction Technology Research Center
University of California, DAVIS

TITLE
HOLLOW_CYLINDER_MCM88615K411

UNLESS OTHERWISE NOTED:
TOLERANCES
.XX ± 0.01   ANGLES ±0.5°
.XXX ±0.005   64/

DESIGN
DRAWN   PS   DATE 8/14/06
APPRV
RELEASE

SCALE 1.000   DRAWING NO.
SIZE A   SHT 1 of 1 | PROJECT

NOTES: UNLESS OTHERWISE SPECIFIED
1) BREAK ALL SHARP EDGES.
2) HIDDEN LINES NOT NECESSARILY SHOWN.
3) MATERIAL : DELRIN
4) FINISH: NA

$\emptyset$ .20
∇ THRU

.50

SLIP FIT INTO RPM-PPL-0001
(APPROX $\emptyset$ .75)

UNLESS OTHERWISE NOTED:
TOLERANCES
.XX ± 0.01
.XXX ±0.005
ANGLES ±0.5°
64/

		DATE
DESIGN	PS	8/14/06
DRAWN	PS	
APPRV		
RELEASE		

AHMCT Advanced Highway Maintenance and Construction Technology Research Center
University of California, Davis

TITLE
DELRIN_BEARING_MCM2610T25

DRAWING NO. RPM-PPL-0002
RPM

SCALE 2.000   SHT 1 of 1   PROJECT
SIZE A

- 113 -

NOTES: UNLESS OTHERWISE SPECIFIED

1) BREAK ALL SHARP EDGES.
2) HIDDEN LINES NOT NECESSARILY SHOWN.
3) MATERIAL : STAINLESS STEEL
4) FINISH: NA

.40

.50

Ø .50

(INITIAL OD MAY NEED TO BE
BIGGER FOR NPT THREADS)

Ø .20
THRU

Ø .26
.15

1.75

.20

.40

1/4 NPT
.40 THREAD ENGAGEMENT
(MAY REQUIRE OD GREATER THAN .5)

AHMCT Advanced Highway Maintenance and Construction
Technology Research Center
University of California, DAVIS

TITLE
SMALLER_ROD.MCM88915K821

SCALE 1.500   SHT 1 of 1 PROJECT
SIZE A   DRAWING NO. RPM-PPL-0003   RPM

UNLESS OTHERWISE NOTED:
TOLERANCES
.XX ± 0.01
.XXX ±0.005   ANGLES ±0.5°
                64

DESIGN   PS   DATE 3/14/06
DRAWN   PS
APPRV
RELEASE

- 114 -

Copyright 2011, AHMCT Research Center, UC Davis

Hex Nipple

Vacuum Cup

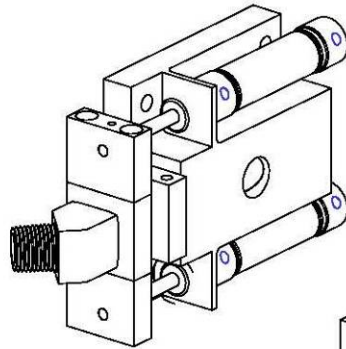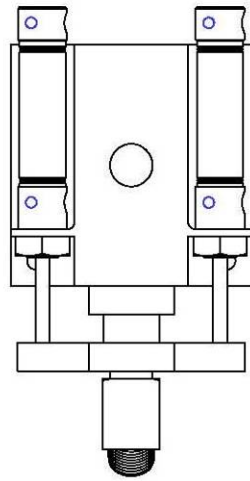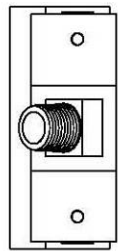# Adhesive Dispenser

Part design and drawing by George Burkett.

Part List				
Index	Part Number	Description	Material	Qty.
1	RPM-AAD-0002	Main Piston	NA	1
2	RPM-TLD-0041	Dispenser Cylinder Unit	Aluminum STEEL	1
3	RPM-TLD-0006	AAP Washer	STEEL	4
4	RPM-TLD-0037	3/8-16 UNC 3/4-1/4 Bolt	STEEL	4
5	RPM-TLD-0006	3"X10" Plex, Sealer (Omega.com)	NA	1
6	RPM-TLD-0043	Dispenser Mounting Plate	Aluminum	1

Adhesive Dispenser
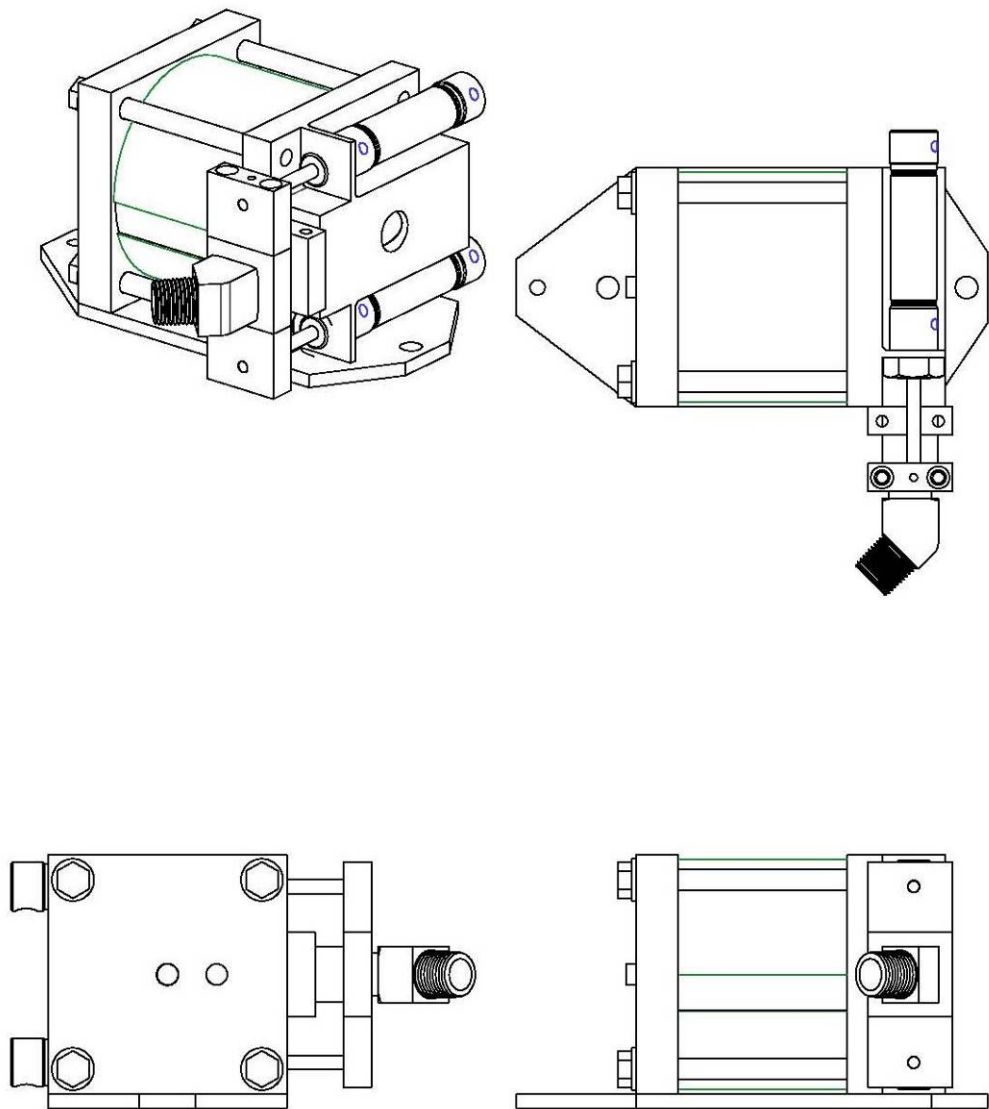
RPM-AAD-0001

RPM

GMB 7/26/05

GMB

GMB

- 118 -

Part List				
Index	Part Number	Description	Material	Qty.
1	RPM-AAD-0002	Main Plates	NA	1
2	RPM-AAD-0003	Twin Plates	NA	2
3	RPM-PAD-0001	Adhesive Dispenser Cap	6061 ALUMINUM	1
4	RPM-PAD-0002	Dispenser Cylinder Wall	STAINLESS STEEL	1
5	RPM-PAD-0003	Dispenser Bottom Plate	STAINLESS STEEL	1
6	RPM-PAD-0004	3/8" Washer	STEEL	4
7	RPM-PAD-0005	3/8-16 UNC 3x-1/2 Bolt	STEEL	4
8	RPM-PAD-0006	3" 316 Stea. Heater (Emerg.com)	NA	1
9	RPM-PAD-0001	1/8" NPT Pipe Fitting	Brass	1
10	RPM-PAD-0002	Dispenser Moving Plate	ALUMINUM	1
11	RPM-PAD-0004	Lower Piston Drive Block	ALUMINUM	2
12	RPM-PAD-0003	Slide Valve Ami.	STAINLESS STEEL	2
13	RPM-PAD-0004	1/2"100X0*50 O-Ring	Rubber	1

Adhesive Dispenser

RPM-AAD-0001

RPM

DWN 7/26/05

CHK

- 119 -
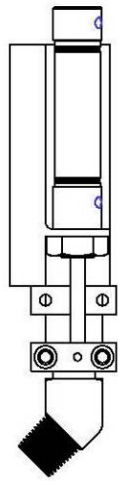
ASSEMBLY INSTRUCTIONS:
1) SLIDE ITEM 1 INTO ITEM 2
2) ATTACH ITEM 4 (2X) TO ITEM 1
3) PLACE ITEM 5 (2 X) THROUGH ITEM 2 AND MOUNTING NUT
4) THREAD ITEM 5 INTO ITEM 2 (2 X)
5) LOCK CYLINDER ROD IN PLACE USING SET SCREWS IN ITEM 4 (2 X -SET SCREWS NOT SHOWN)
6) TIGHTEN MOUNTING NUT ON AIR CYLINDER TO ORIENT AIR PORTS TO DESIRED ORIENTATION
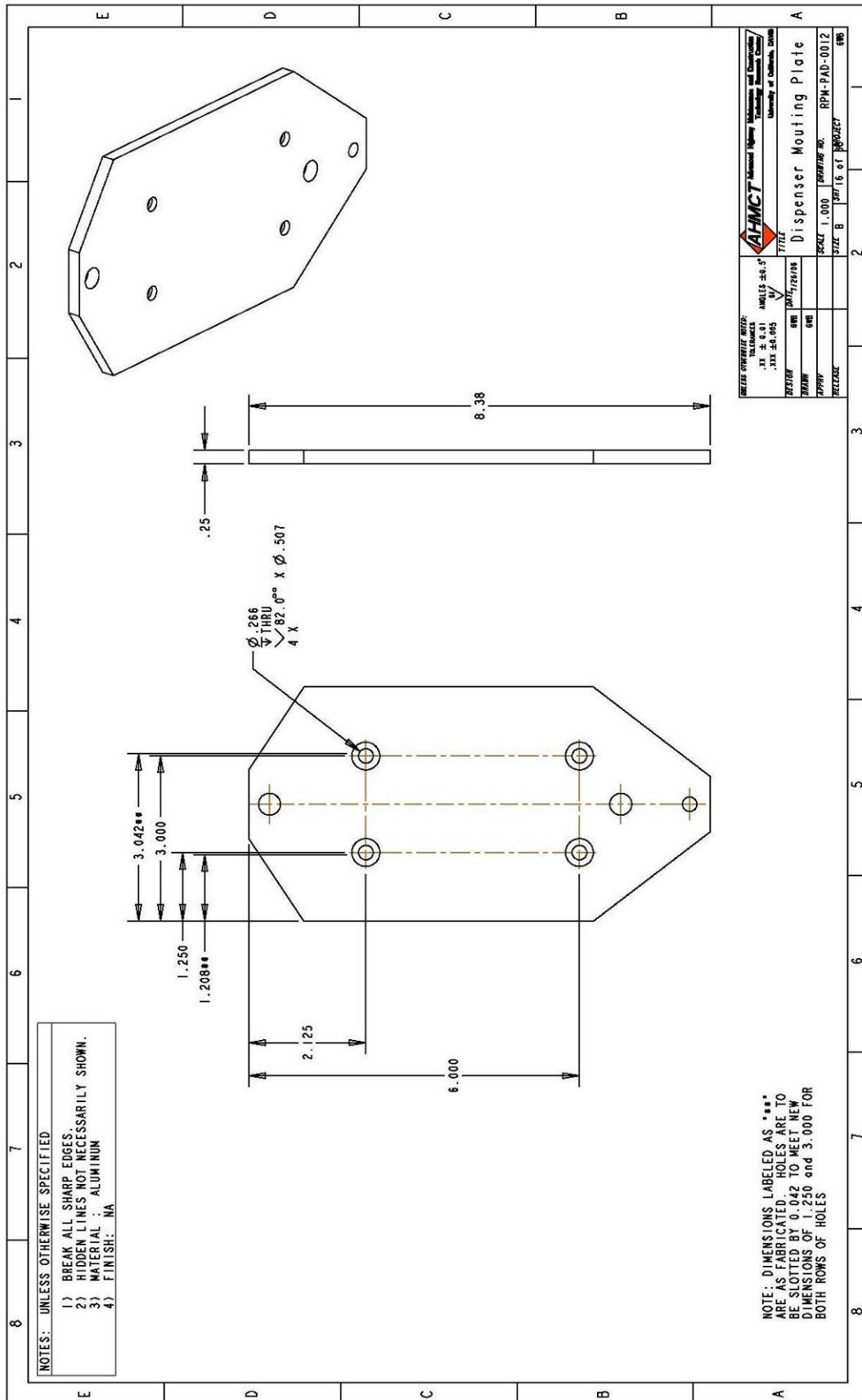*MAY HAVE TO ITTERATE IN ORDER TO PROPERLY ADJUST CYLINDER CUSHIONS

- 120 -

Back Plate

Part design and drawing by George Burkett.

NOTES: UNLESS OTHERWISE SPECIFIED
1) BREAK ALL SHARP EDGES.
2) HIDDEN LINES NOT NECESSARILY SHOWN.
3) MATERIAL : ALUMINUM
4) FINISH: NA

NOTE: DIMENSIONS LABELED AS "**"
ARE AS FABRICATED. HOLES ARE TO
BE SLOTTED BY 0.042 TO MEET NEW
DIMENSIONS OF 1.250 and 3.000 FOR
BOTH ROWS OF HOLES

TITLE
Dispenser Mouting Plate

⌀ .266 THRU
⌵ 82.0°° X ⌀ .507
4 X

8.38

.25

3.042**
3.000

1.250
1.208**

2.125

6.000

Main Cylinder

Part design and drawing by George Burkett.

NOTES: UNLESS OTHERWISE SPECIFIED
1) BREAK ALL SHARP EDGES.
2) HIDDEN LINES NOT NECESSARILY SHOWN.
3) MATERIAL : STAINLESS STEEL
4) FINISH: NA

3.19

45° X .03
2X

Ø4.00

Ø3.760±.002

TITLE
Dispenser Cylinder Wall

DRAWING NO. RPM-PAD-0002

SCALE 1.000   SHT 7 of 3   PROJECT RPM

SIZE B

UNLESS OTHERWISE NOTED:
TOLERANCES
.XX ± 0.01   ANGLES ±0.5°
.XXX ±0.005

DESIGN   GMB   DATE 7/26/06
DRAWN   GMB
APPRV
RELEASE

Main Cylinder Piston

Part design and drawing by George Burkett.

NOTES: UNLESS OTHERWISE SPECIFIED
1) BREAK ALL SHARP EDGES.
2) HIDDEN LINES NOT NECESSARILY SHOWN.
3) MATERIAL : ALUMINUM
4) FINISH: NA

SEE DETAIL A

SEE DETAIL B

1.495

.188

Ø3.750

R.13 TYP

Ø3.25

Ø.75

Ø5/16-18 UNC
CLASS 2B
▽1.000 MAX
▽THD .750 MIN

1.81

1.50

45° X .13

SECTION A-A

DETAIL A
SCALE 8.000
LOWER EDGE AT 1.495

.010 +.002 -.000

DETAIL B
SCALE 8.000
LOWER EDGE AT .188

.005 +.001 -.000

UNLESS OTHERWISE NOTED:
TOLERANCES
.XX ± 0.01
.XXX ±0.005

ANGLES ±0.5°

DESIGN   DATE 7/26/06
DRAWN   GWB
APPROV   GWB
RELEASE

TITLE
Main Dispenser Piston

DRAWING NO.   RPM-PAD-0004

SCALE 1.000   SHT 11 of 204

SIZE B   PROJECT   RPM

DETAIL A
SCALE 3.000

.037

3.460

SEE DETAIL A

NOTES: UNLESS OTHERWISE SPECIFIED
1) BREAK ALL SHARP EDGES.
2) HIDDEN LINES NOT NECESSARILY SHOWN.
3) MATERIAL :: ALUMINUM
4) FINISH: NA

UNLESS OTHERWISE NOTED:
TOLERANCES
.XX ± 0.01   ANGLES ±0.5°
.XXX ±0.005

DESIGN   GMB   DATE 7/24/06
DRAWN   GMB
APPRV
RELEASE

TITLE
Main Dispenser Piston
MOD

DRAWING NO.
AHM-FAB-0804

PROJECT

SCALE 1.000
SIZE B   SHT 10 of 1

AHMCT Advanced Highway Maintenance and Construction Technology
University of California, Davis

- 128 -

NOTES: UNLESS OTHERWISE SPECIFIED
1) BREAK ALL SHARP EDGES.
2) HIDDEN LINES NOT NECESSARILY SHOWN.
3) MATERIAL : ALUMINUM
4) FINISH: NA

1.62

Ø3.460

.037±.001
2 X

.28

TITLE Main Dispenser Piston
MOD

DRAWING NO. RPM-PAD-0004

PROJECT RPM

SCALE 1.000   SIZE B   SHT 1 of 3

Main Piston Flag

Part design and drawing by George Burkett.

NOTES: UNLESS OTHERWISE SPECIFIED
1) BREAK ALL SHARP EDGES.
2) HIDDEN LINES NOT NECESSARILY SHOWN.
3) MATERIAL : STAINLESS STEEL
4) FINISH: NA

Ø 5/16-18 UNC
THD 0.5"

2.738

.500

.313
FLATS

Ø .375

TITLE
Main Piston Flag

DRAWING NO.
RPM-PAD-0013

SCALE 1.000   SIZE B   SHT 17 of   PROJECT RPM

Main Piston Ring

Part design and drawing by George Burkett.

.016

Ø3.520

.030

Ø3.780±.002

NOTES: UNLESS OTHERWISE SPECIFIED
1) BREAK ALL SHARP EDGES.
2) HIDDEN LINES NOT NECESSARILY SHOWN.
3) MATERIAL : PHOSPHOR BRONZE
4) FINISH: NA

UNLESS OTHERWISE NOTED:
TOLERANCES
.XX ± 0.01
.XXX ±0.005

ANGLES ±0.5°

DESIGN GMB DATE 10/12/06
DRAWN GMB
APPROV
RELEASE

TITLE
Large Piston Ring
V2

DRAWING NO. RPM-PAD-0020

SCALE 1.000

SIZE B   SHT 29 of 1   PROJECT RPM

Top Plate

Part design and drawing by George Burkett.

DETAIL A
SCALE 2.000
SEAT FOR Ø1/2 x Ø3/8 O-RING

SECTION A-A

SEE DETAIL A

NOTES: UNLESS OTHERWISE SPECIFIED
1) BREAK ALL SHARP EDGES.
2) HIDDEN LINES NOT NECESSARILY SHOWN.
3) MATERIAL : 6061 ALUMINUM
4) FINISH: NA

TITLE
Adhesive Dispenser Cap

DRAWING NO.
RPM-PAD-0001

SCALE 1.000   SHT 6 of 39
SIZE B   PROJECT RPM

- 134 -

Copyright 2011, AHMCT Research Center, UC Davis

Bottom Plate

Part design and drawing by George Burkett.

NOTES: UNLESS OTHERWISE SPECIFIED
1) BREAK ALL SHARP EDGES.
2) HIDDEN LINES NOT NECESSARILY SHOWN.
3) MATERIAL : STAINLESS STEEL
4) FINISH: NA

SECTION A-A

R.13
2X

R.13
2X

∅1/4-20 UNC
CLASS 2B
▽THD .750 MAX
▽.500 MIN
2 X

∅3/8-16 UNC
CLASS 2B
▽THRU
THD ALL
4 X

∅.75 ▽THRU ▽.13
45.0° X ∅1.00
4.000

∅1.000±.002
▽THRU

∅.625 +.010 -.000
▽THRU
2X

4.250
3.804
2.125
3.000
1.250
.375
.63
.446
.446
2.125
3.804
.563
.562
3.688
1.13
3.13

TITLE
Dispenser Bottom Plate

DRAWING NO.
RPM-PAD-0003

UNLESS OTHERWISE NOTED:
TOLERANCES
.XX ± 0.01
.XXX ±0.005
ANGLES ±0.5°

DATE 7/26/06

SCALE 1.000   SHT 8 of 3   PROJECT   RPM
SIZE B

National Highway Maintenance and Construction Technology Research Center
University of California, Davis

DESIGN
DRAWN
APPRV
RELEASE

NOTES: UNLESS OTHERWISE SPECIFIED
1) BREAK ALL SHARP EDGES.
2) HIDDEN LINES NOT NECESSARILY SHOWN.
3) MATERIAL : STAINLESS STEEL
4) FINISH: NA

$\emptyset 1.000 \pm .002$
THRU

$\emptyset .625^{+.010}_{-.000}$
THRU
2X

.563

.562

3.688

TITLE
Dispenser Bottom Plate

Advanced Highway Maintenance and Construction
Technology Research Center
University of California, DAVIS

DRAWING NO.   RPM-PAD-0003

SCALE 1.000   SHT 9 of 39 PROJECT RPM
SIZE B

DESIGN
DRAWN   GMB
APPRV   GMB
RELEASE

UNLESS OTHERWISE NOTED:
TOLERANCES
.XX ± 0.01
.XXX ±0.005
ANGLES ±0.5°

DATE 7/26/06

- 137 -

Copyright 2011, AHMCT Research Center, UC Davis

Lower Dispenser Piston

Part design and drawing by George Burkett.

FILL PASSAGE

SECTION A-A

DISPENSER OUTLET

∅1/2-14 NPT
THD MAX

∅.50
⩗.75

2.125

1.125

∅.75
⩗THRU

A

A

∅1/4-20 UNC
CLASS-2B
⩗THRU
⩗THD 0.5 MIN
(BOTH SIDES)
2 X

.500

SEE DETAIL A

5.375

4.75

4.500

4.25

∅.990

1.500

.750

.750

1.500

∅.38
⩗3.38

.010⁺·⁰⁰²₋·⁰⁰⁰
2X

2.63

.25

DETAIL A
SCALE 1.500
PISTON RING CONFIGURATION

NOTES: UNLESS OTHERWISE SPECIFIED
1) BREAK ALL SHARP EDGES.
2) HIDDEN LINES NOT NECESSARILY SHOWN.
3) MATERIAL : ALUMINUM
4) FINISH: NA

- 139 -

Lower Piston Ring

Part design and drawing by George Burkett.

.016

Ø1.010±.002

Ø.800

.020

UNLESS OTHERWISE NOTED:
TOLERANCES
.XX ± 0.01
.XXX ±0.005

ANGLES ±0.5°

		DATE
DESIGN	BMB	6/12/06
DRAWN	BMB	
APPROV		
RELEASE		

AHMCT Advanced Highway Maintenance and Construction / Technology Research Center
University of California, Davis

TITLE
Small Piston Ring
V2

DRAWING NO.
RPM-PAD-0021

PROJECT
RPM

SCALE 1.000 SHT 2 of 3

SIZE B

- 143 -

Center Moving Plate

Part design and drawing by George Burkett.

Side Moving Plates

Part design and drawing by George Burkett.

NOTES: UNLESS OTHERWISE SPECIFIED
1) BREAK ALL SHARP EDGES.
2) HIDDEN LINES NOT NECESSARILY SHOWN.
3) MATERIAL : ALUMINUM
4) FINISH: NA

Ø .266
▽ THRU
⌴ Ø0.397
▽ 0.250
2X

Ø 6-32 UNF
▽ THRU TO ORTHOGONAL HOLE

Ø 10-32 UNF
▽ THRU
▽ THD ALL

1.250

.250

.500

.688

.250

.688

1.250

.813

1.500

TITLE
Lower Piston Drive Block

DRAWING NO.
RPM-PAD-0014

SCALE 1.000   SHT 18 of
SIZE B

UNLESS OTHERWISE NOTED:
TOLERANCES
.XX ± 0.01   ANGLES ±0.5°
.XXX ±0.005

DATE 7/26/06
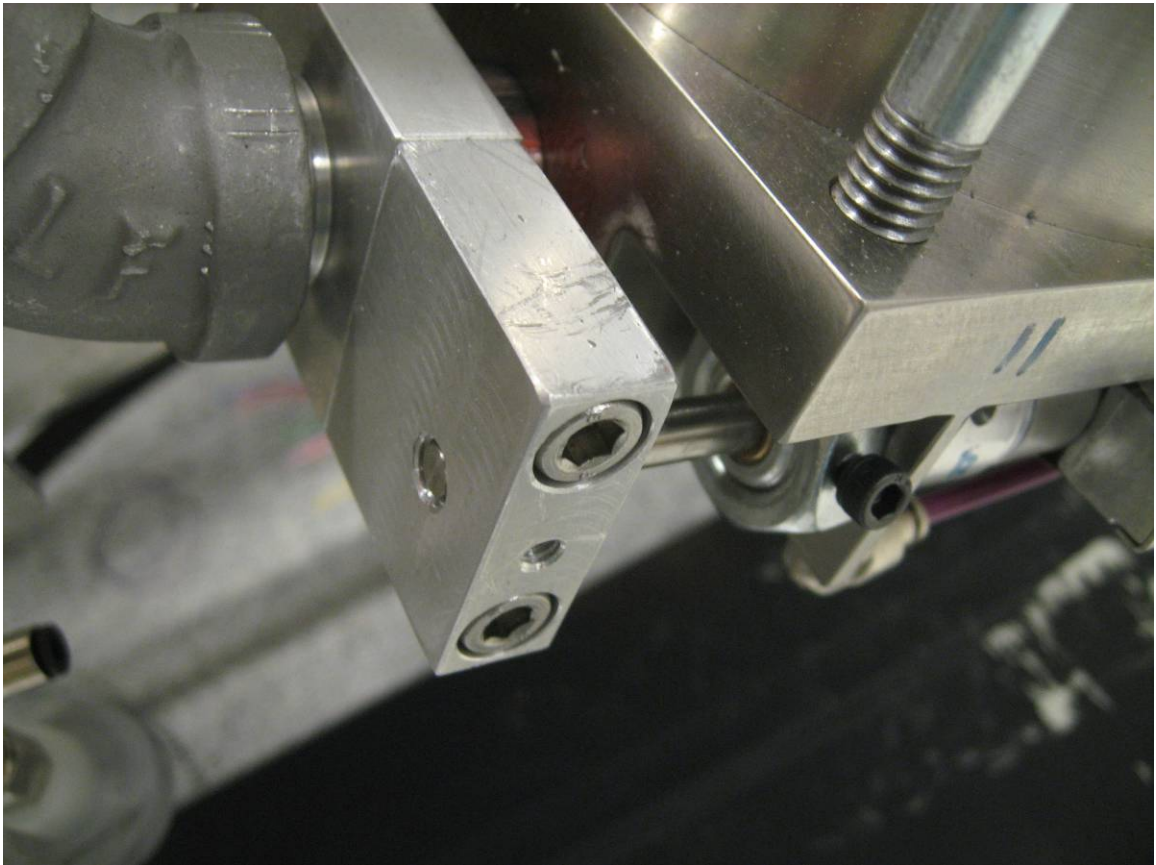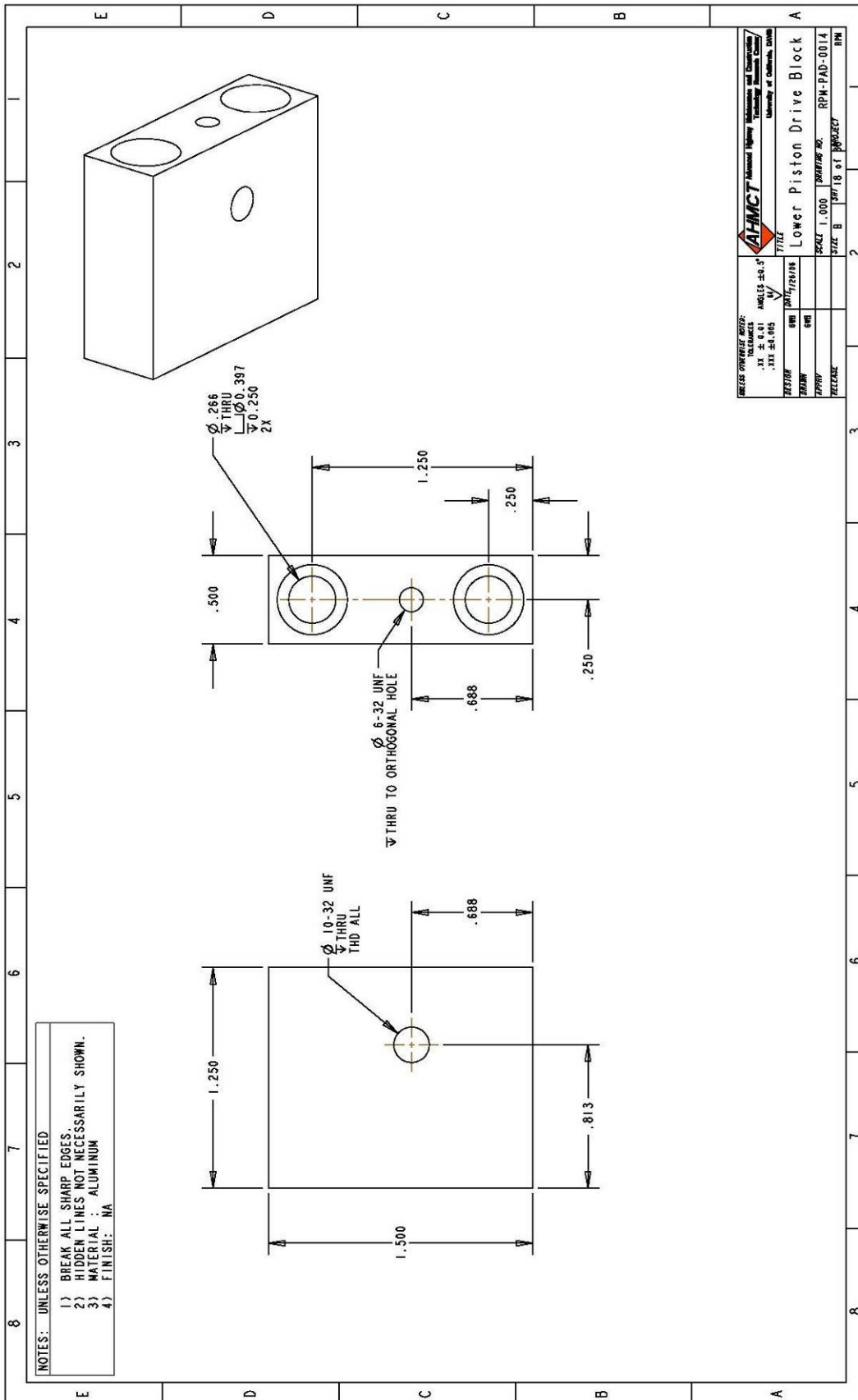
Hose
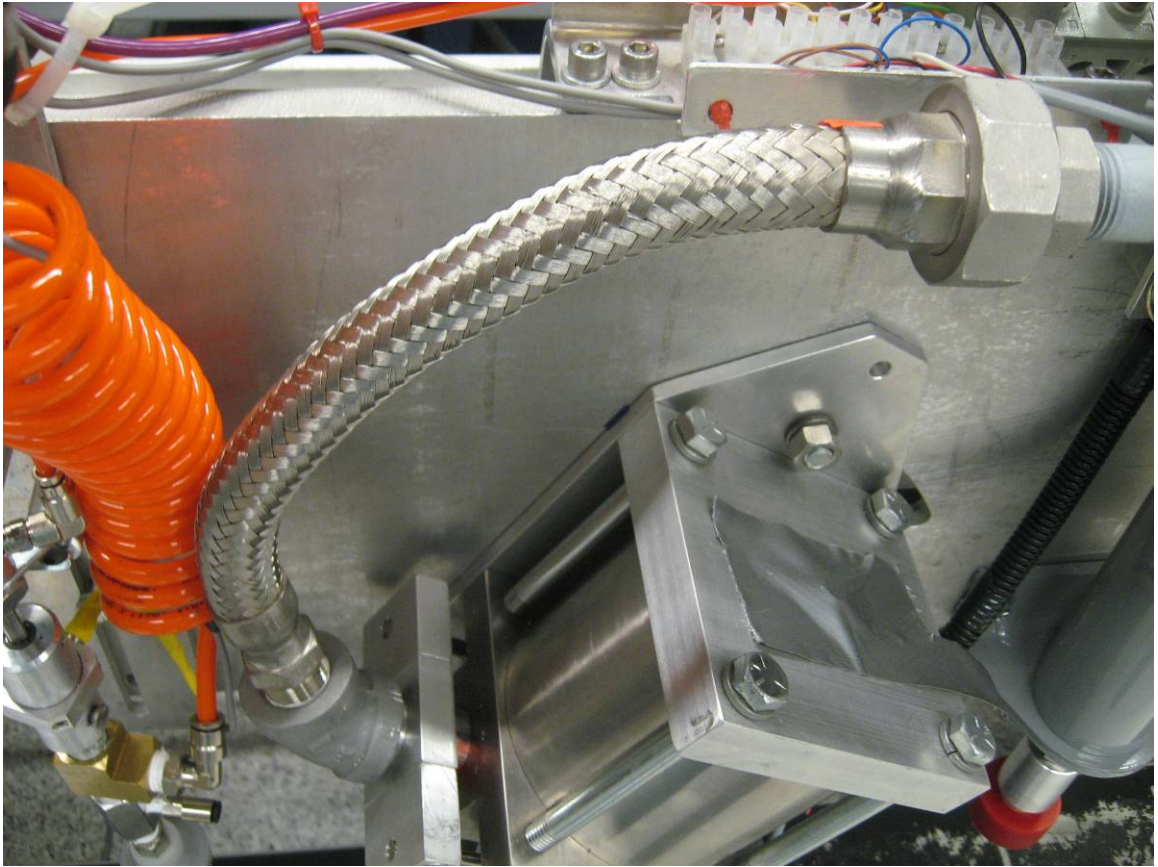
Pneumatic Cylinders
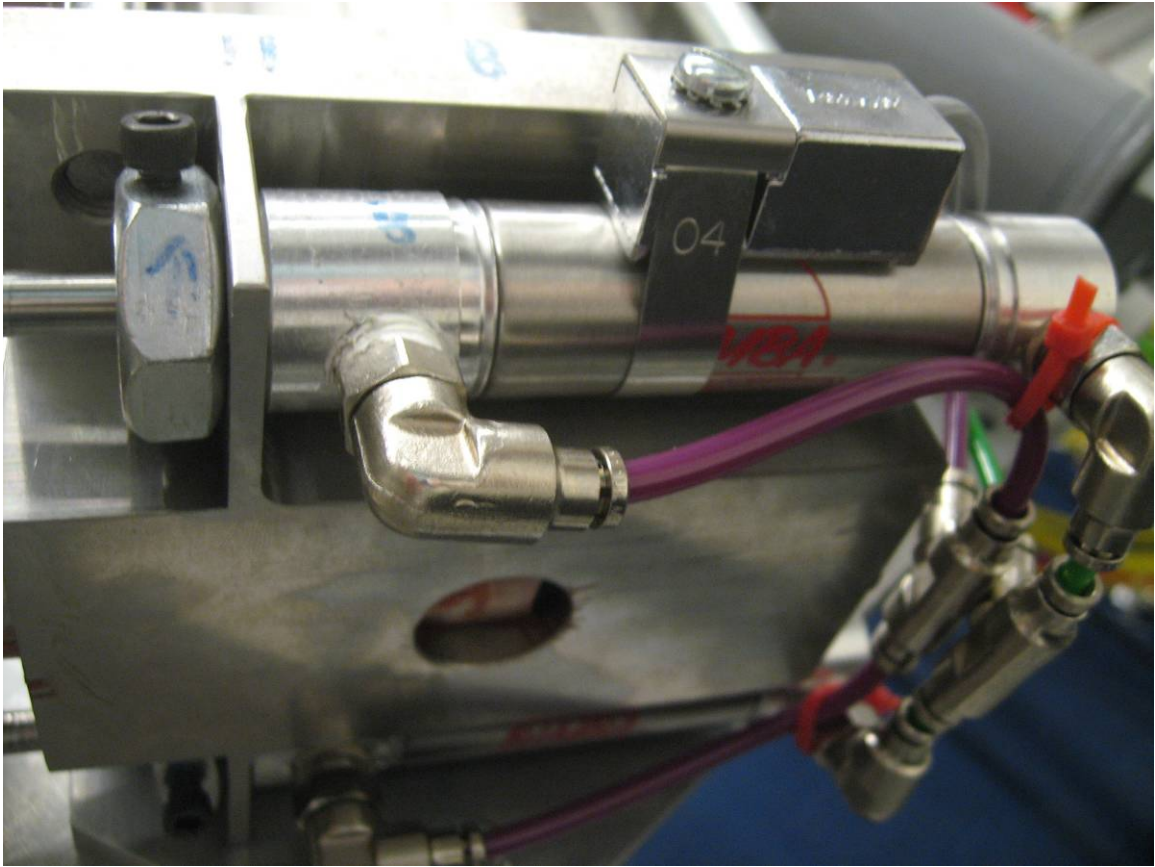
Elbow with Bracket
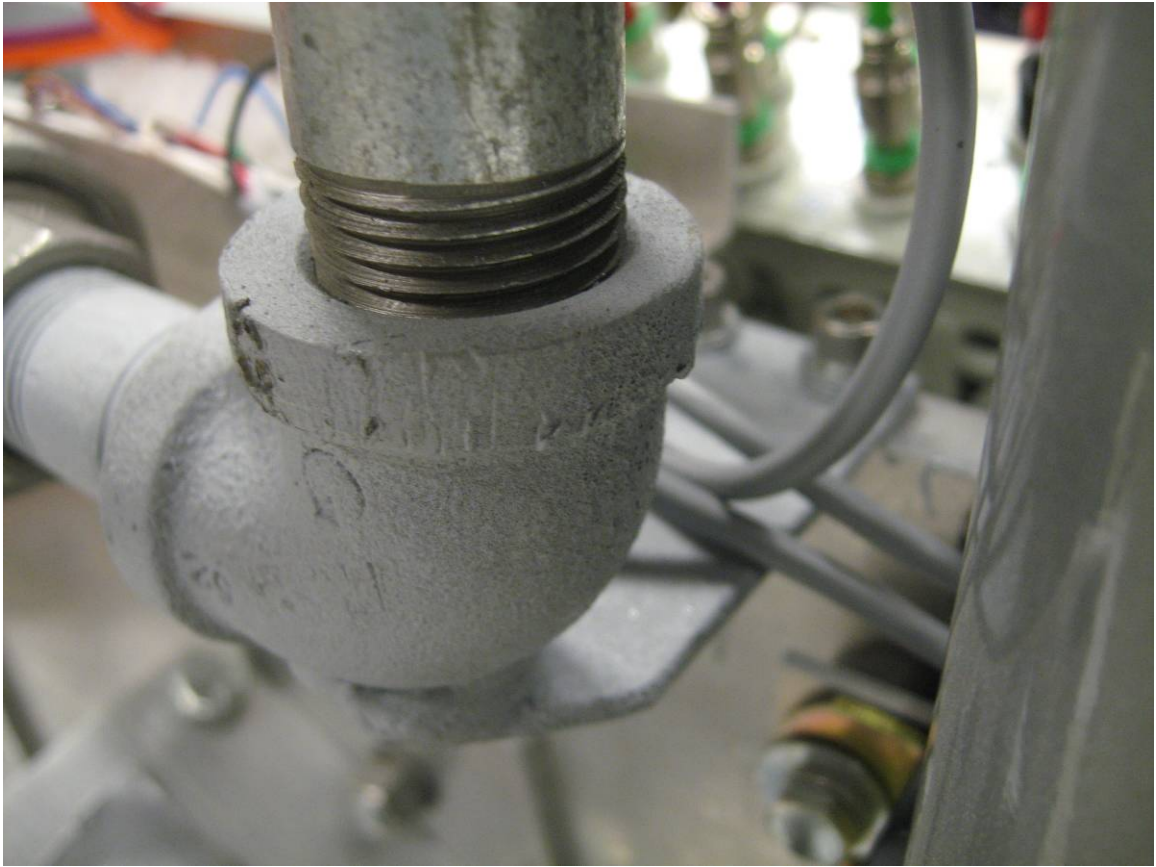
Foot
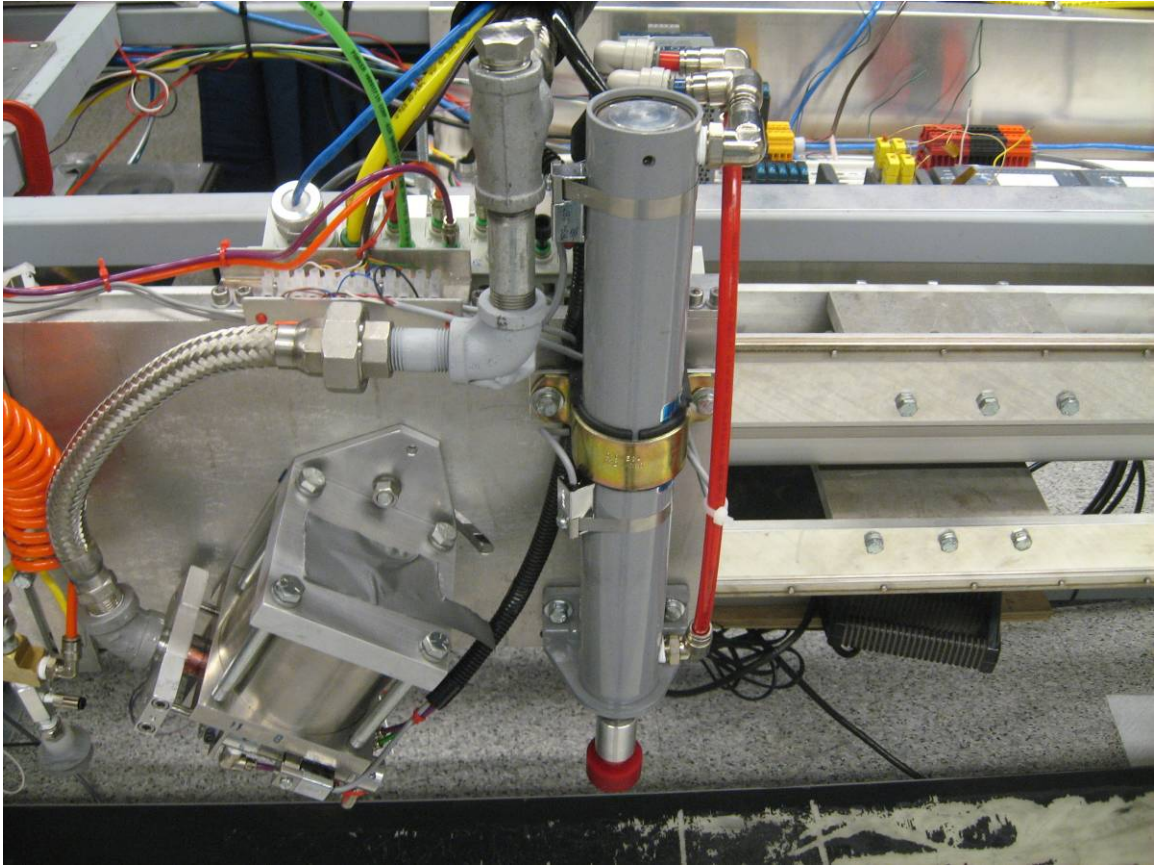
Pneumatic Cylinder
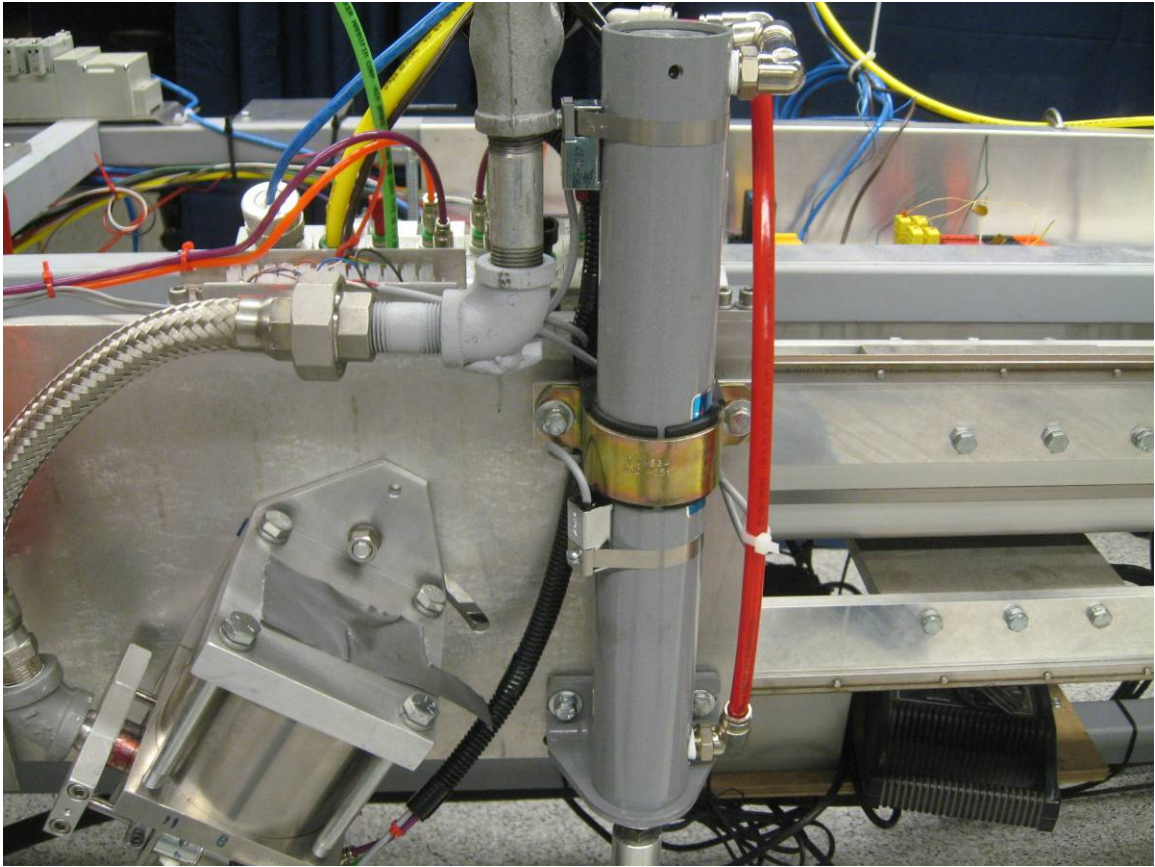
Tube Bracket

Bracket Back

NOTES: UNLESS OTHERWISE SPECIFIED

1) BREAK ALL SHARP EDGES.
2) HIDDEN LINES NOT NECESSARILY SHOWN.
3) MATERIAL : ALUMINUM
4) FINISH: NA

.13

Ø .33
▽ THRU
2 PLACES

1.25

.63

3.37

4.19

.41

AHMCT Advanced Highway Maintenance and Construction
Technology Research Center
University of California, Davis

TITLE
BRIDGE_PLATE_ALUMINUM

DRAWING NO.   RPM-PBR-0002

SCALE 1.000   SHT 1 of 1   PROJECT   RPM

SIZE A   2

UNLESS OTHERWISE NOTED:
TOLERANCES
.XX ± 0.01
.XXX ±0.005

ANGLES ±0.5°

DESIGN   PS   DATE 8/14/06
DRAWN   PS
APPRV
RELEASE

Magnetic Sensors

Nose Mount

Standoffs
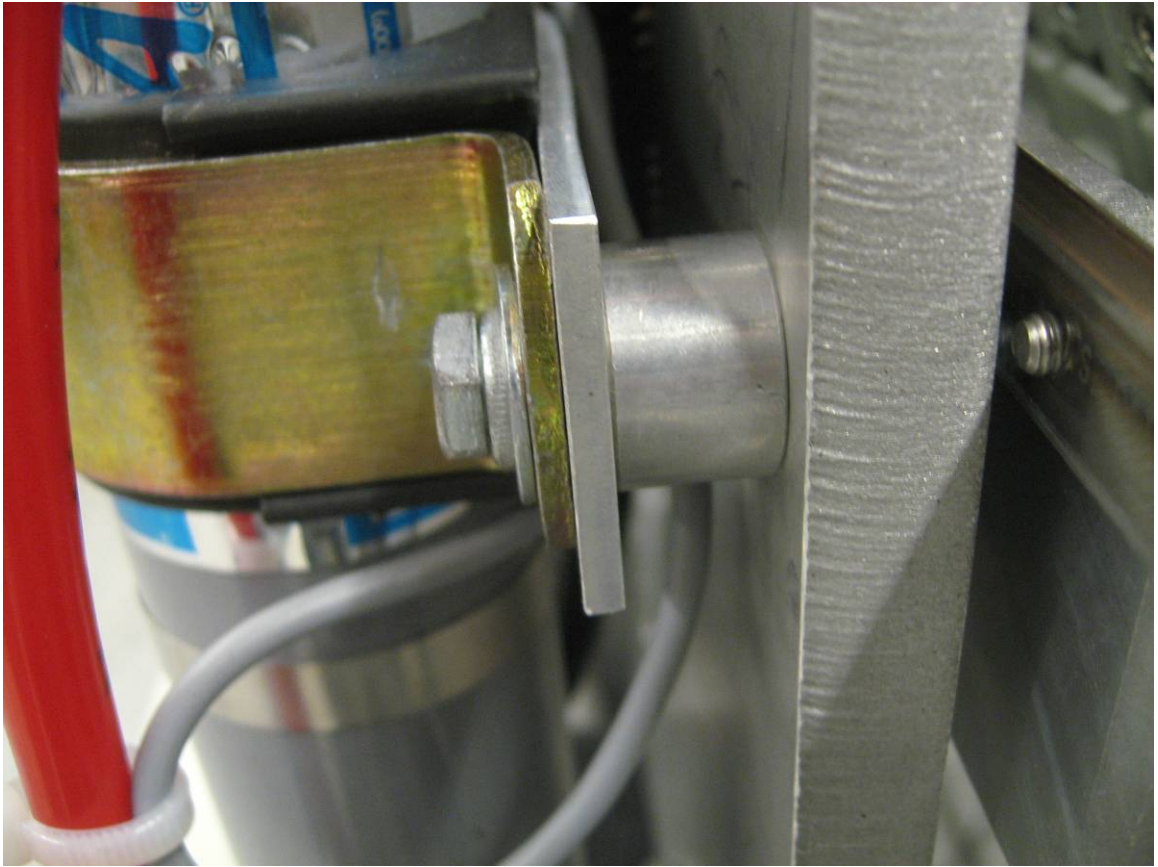
Coupler
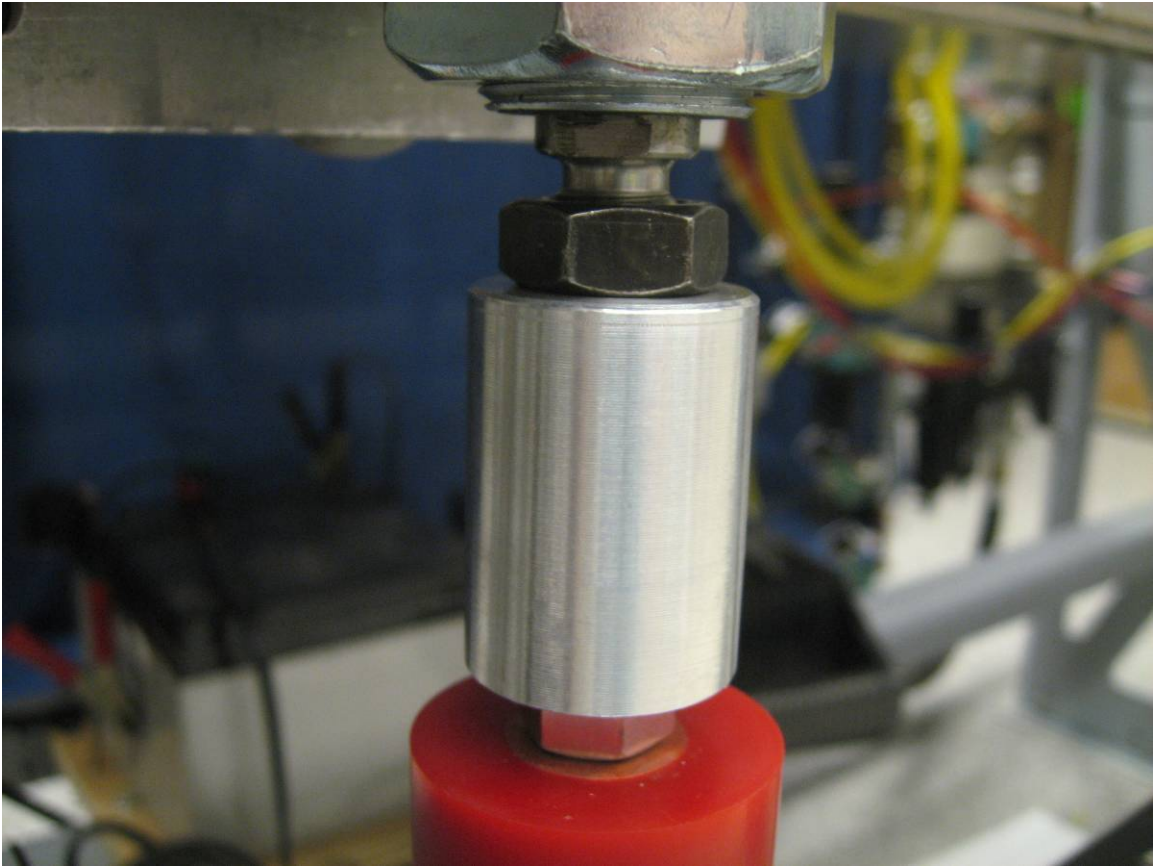
Pad
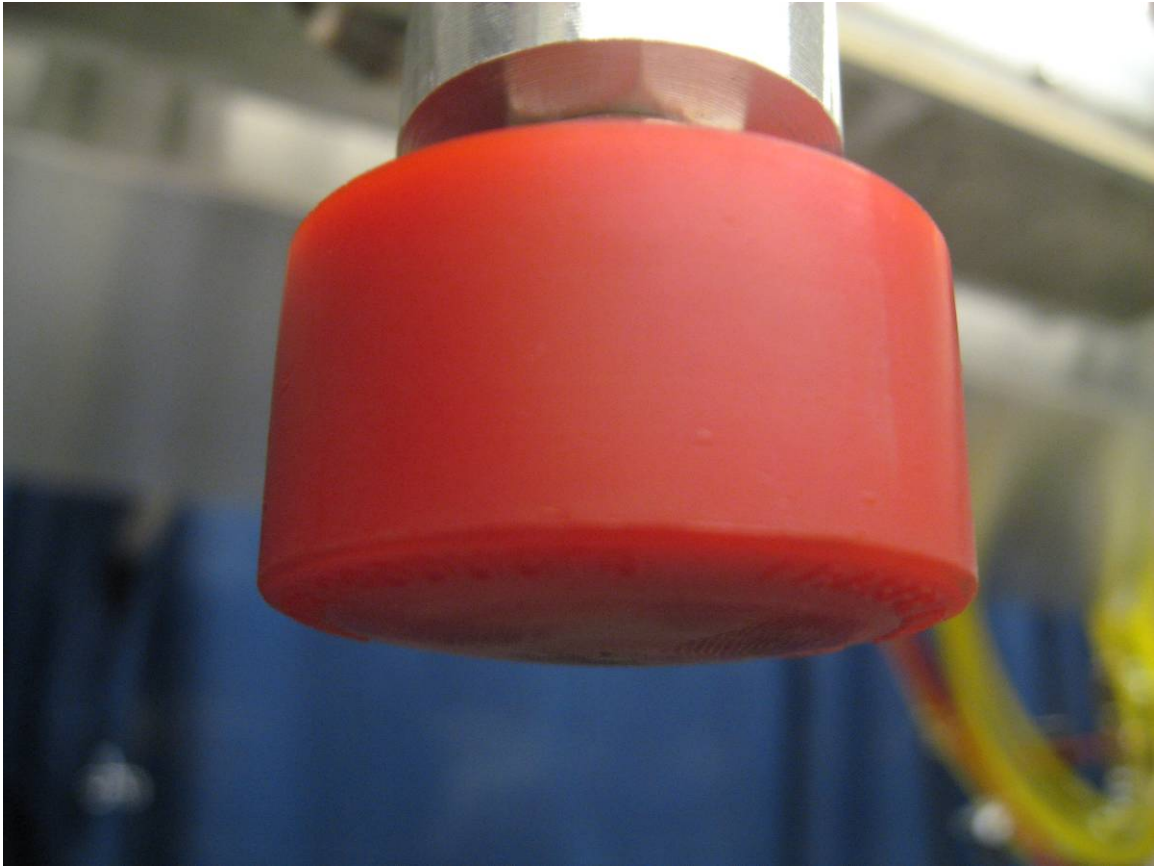
Carriage Mechanism
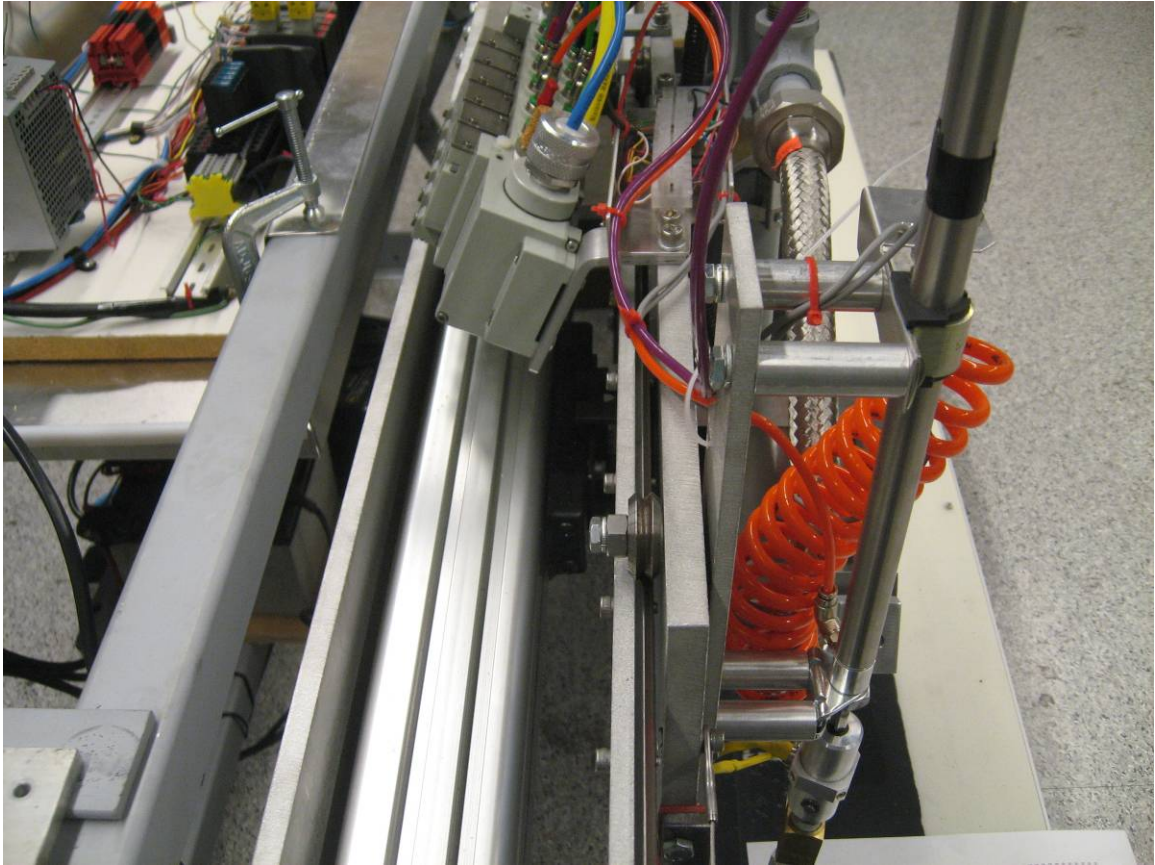
Main Plate

Part design and drawing by George Burkett.

- 163 -
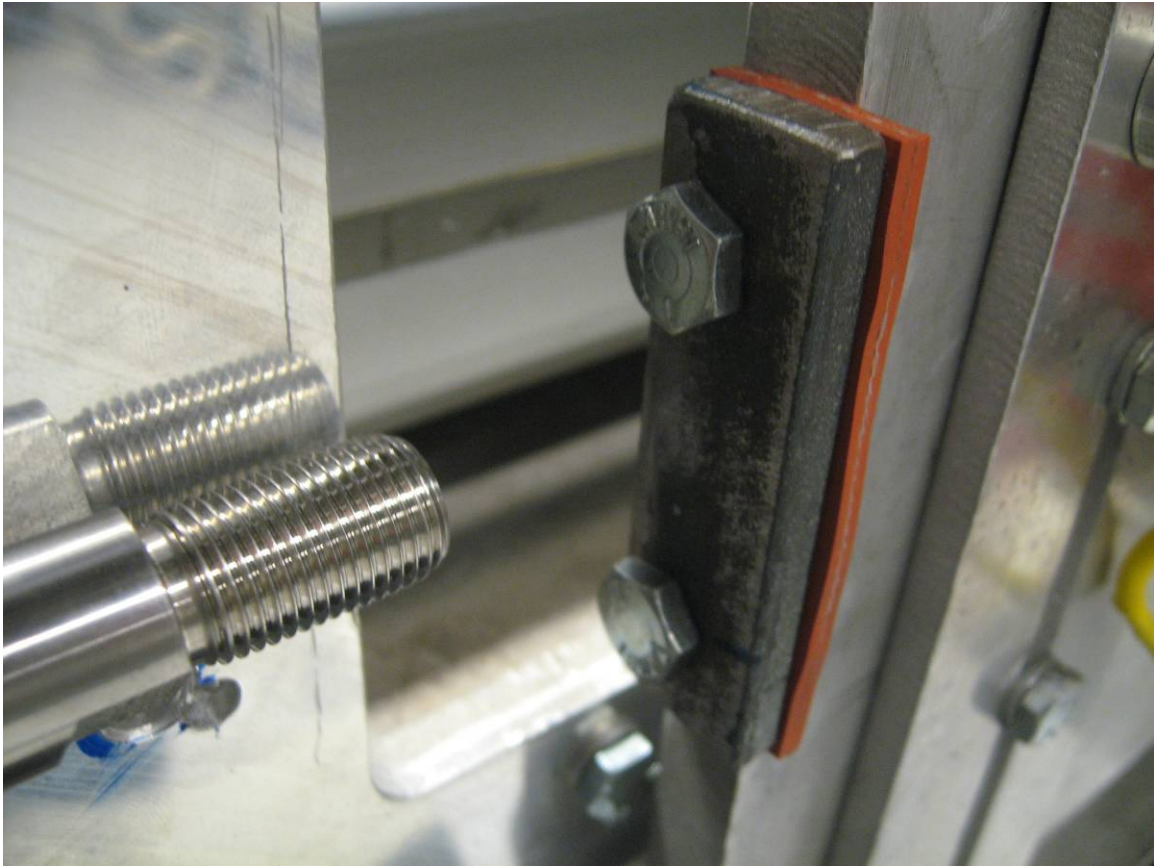
Rollers
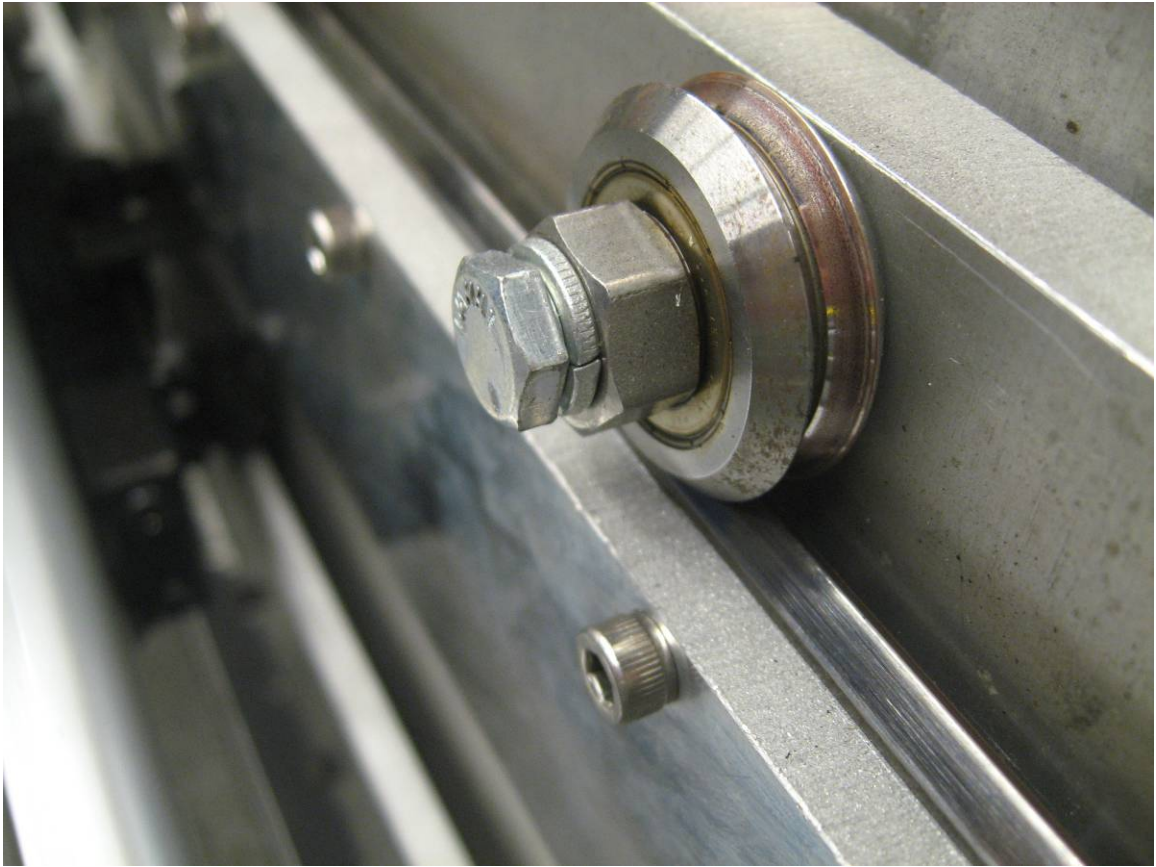
Conveyor
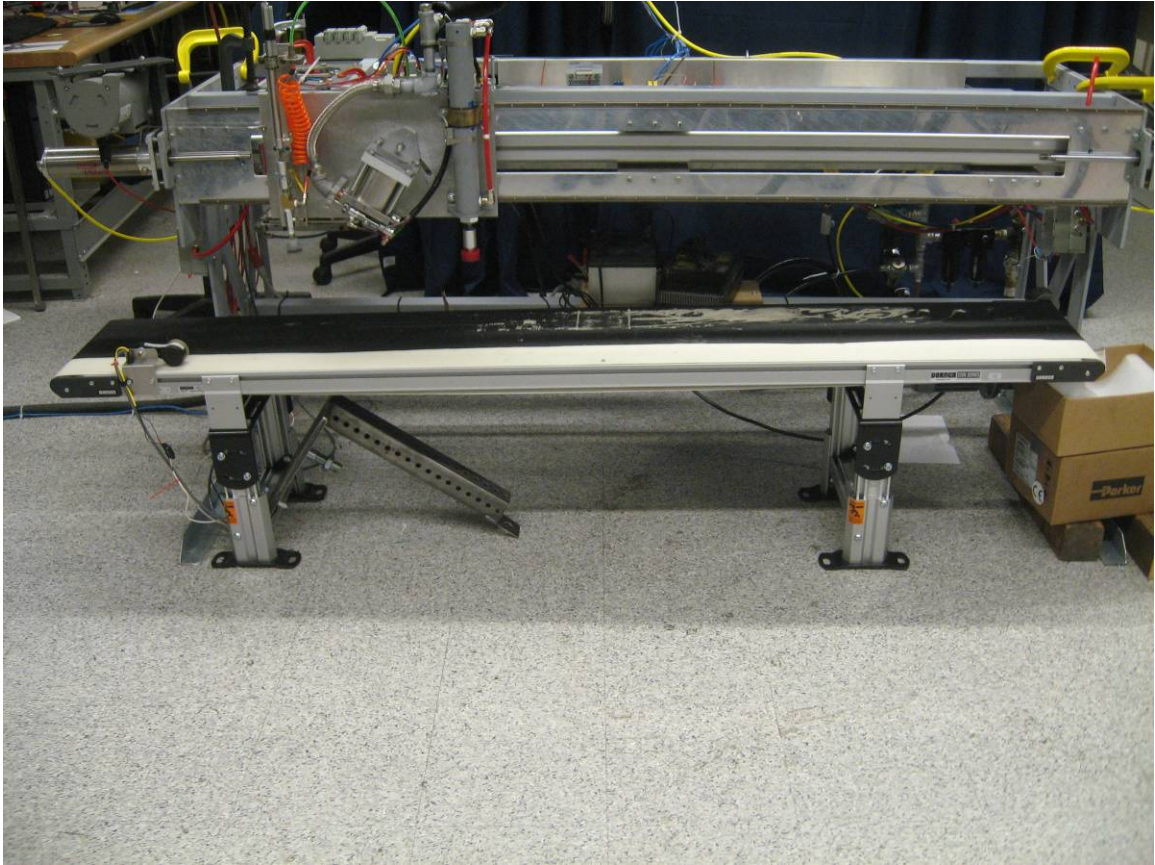
Bracket
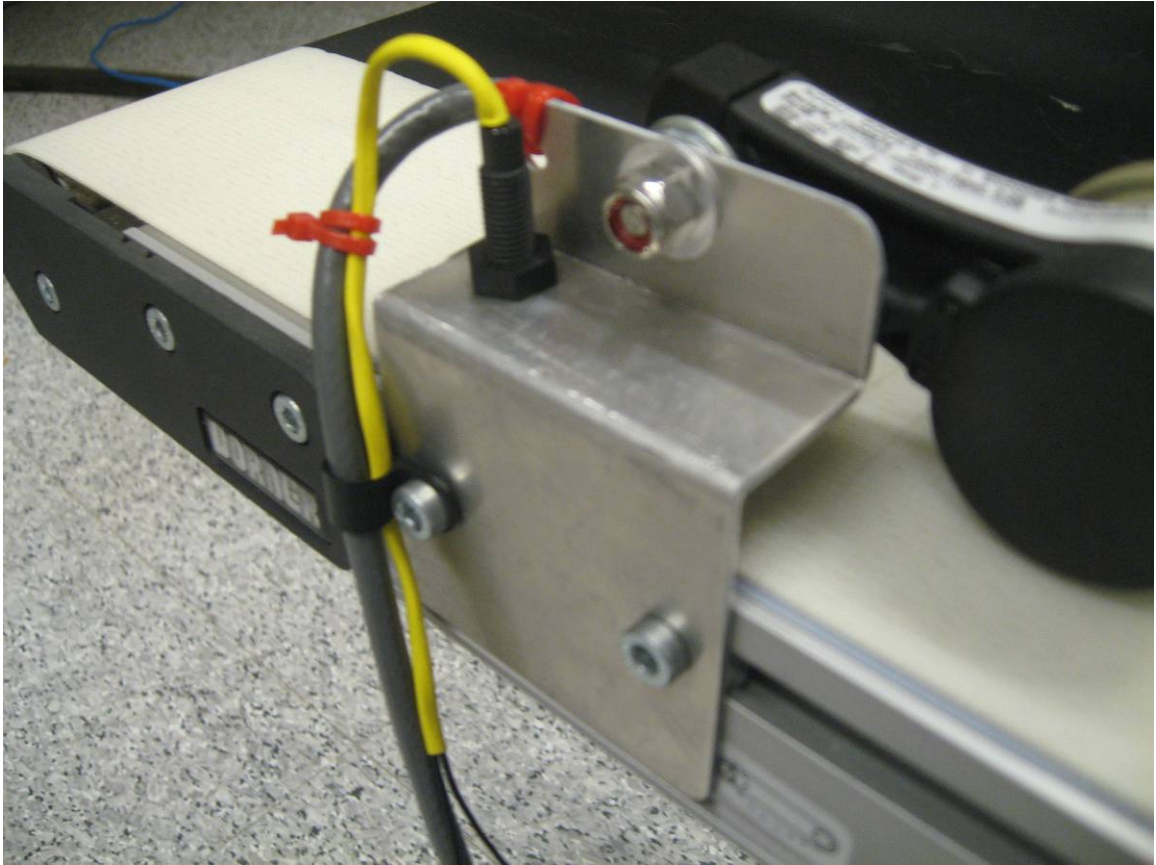
Measurement Wheel

Magnetic Sensor

APPENDIX D

CONTROL CODE

- 169 -

Top State Diagram

Front Panel

Dot Type

Please Select Type ▼

Error? Status Message

Conveyor Speed (mph)

0

Initial Position (in)

0

Vac enabled?

stop machine

STOP

Emergency Stop

STOP

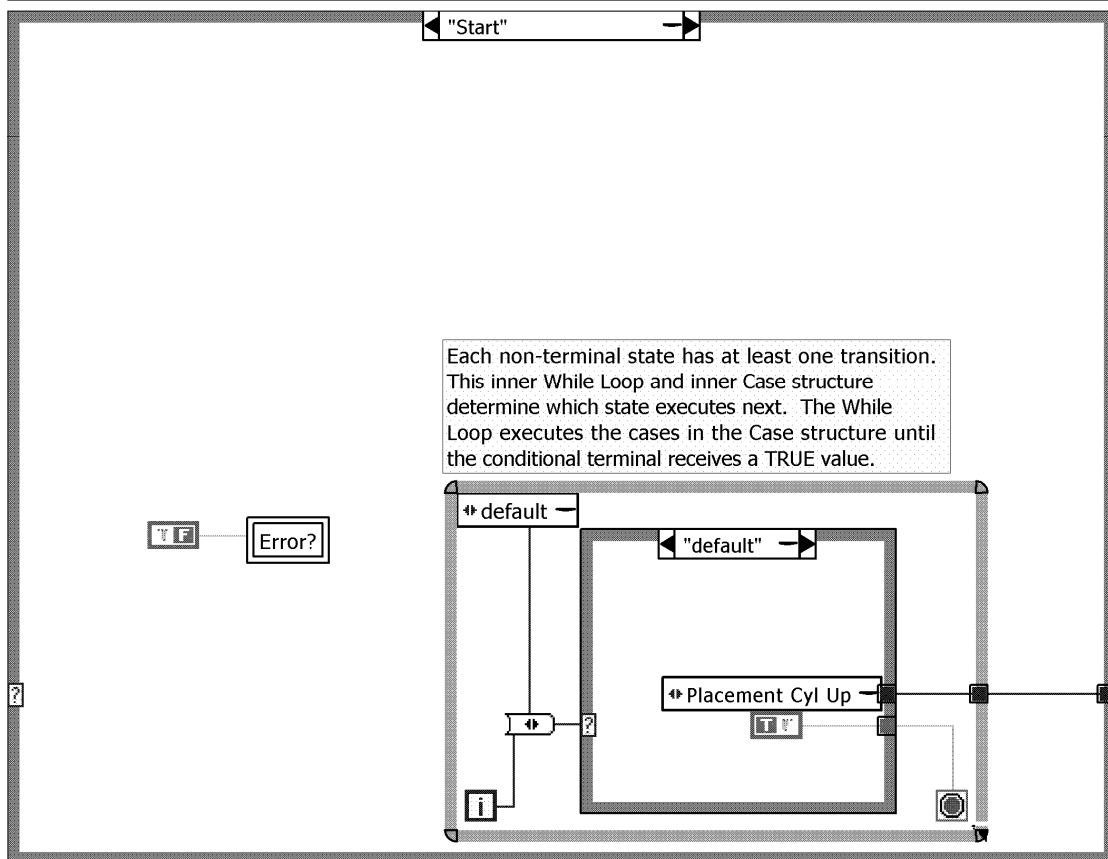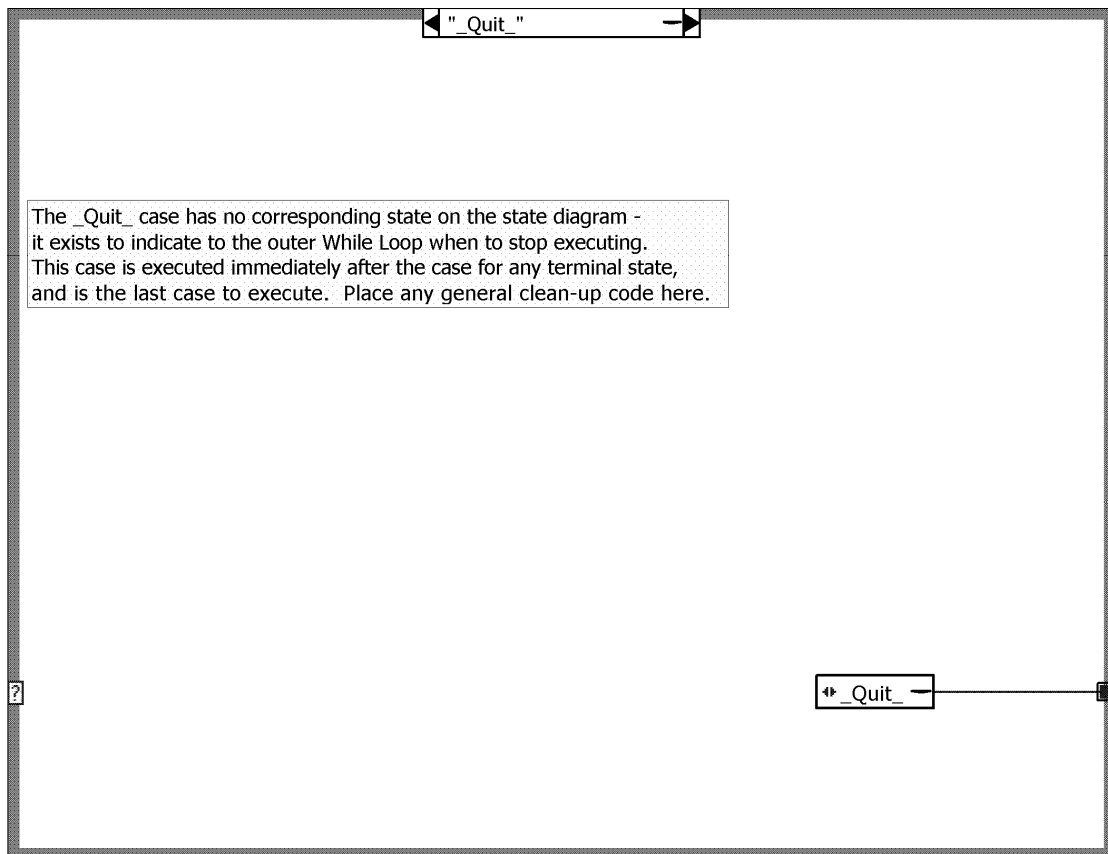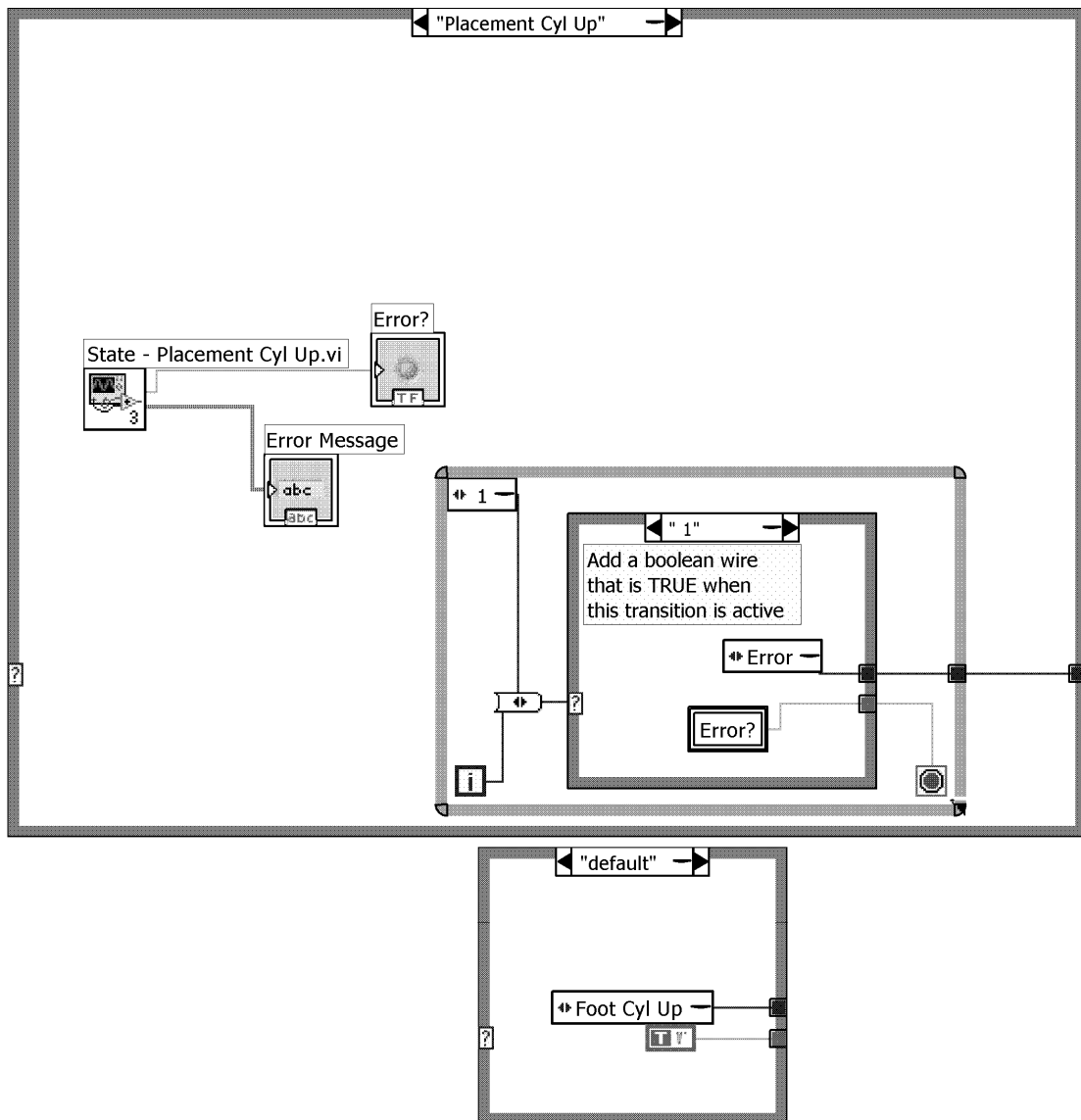# State Diagram

Block Diagram

Warm Up

Dot Type Selection
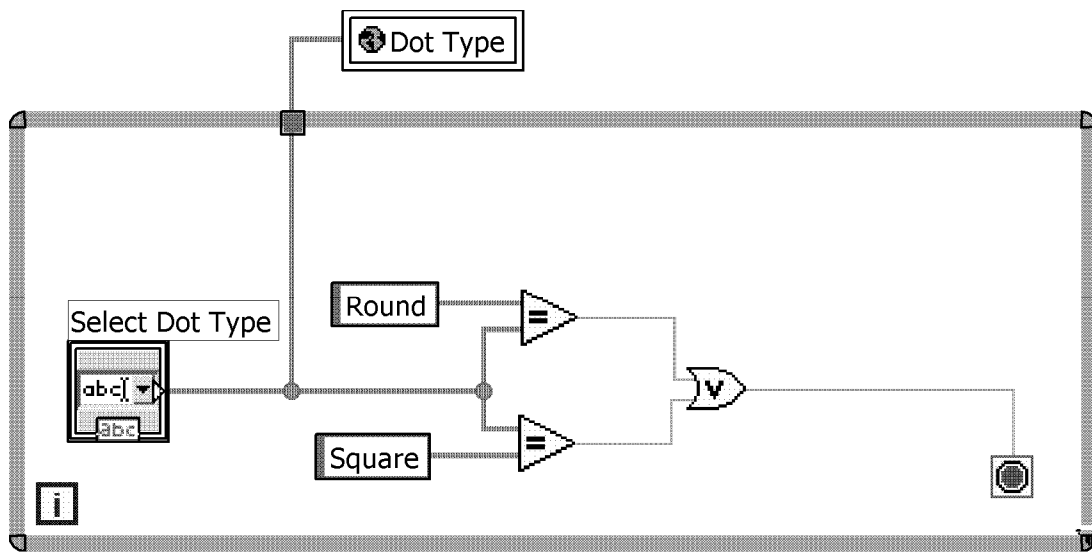
Ready Check

State Diagram

Block Diagram

This outer Case structure contains cases that correspond to the states in the state diagram.
Configure each case to reflect the actions you want each state to perform.

◄ "Pickup_Dot" ►

State - Pick Up Dot.vi

◄► default ►

◄ "default" ►

◄► Start ►

◄► Retract Tray ►

◄► _Quit_ ►

"_Quit_"

The _Quit_ case has no corresponding state on the state diagram -
it exists to indicate to the outer While Loop when to stop executing.
This case is executed immediately after the case for any terminal state,
and is the last case to execute. Place any general clean-up code here.

Quit

"Start"

Each non-terminal state has at least one transition.
This inner While Loop and inner Case structure
determine which state executes next. The While
Loop executes the cases in the Case structure until
the conditional terminal receives a TRUE value.

Error?

default

"default"

Placement Cyl Up

i

- 177 -

"Foot Cyl Up"

State - Foot Cyl Up.vi

4

Error?

Error Message

1

" 1"

Add a boolean wire
that is TRUE when
this transition is active

Error

Error?

i

?

"default"

Dispenser Set to Fill

T F

?

- 179 -

"Dispenser Set to Fill"

State - Dispenser Set to Fill.vi

Error?

Error Message

1

"default"

Deploy_tray

i

" 1"

Add a boolean wire
that is TRUE when
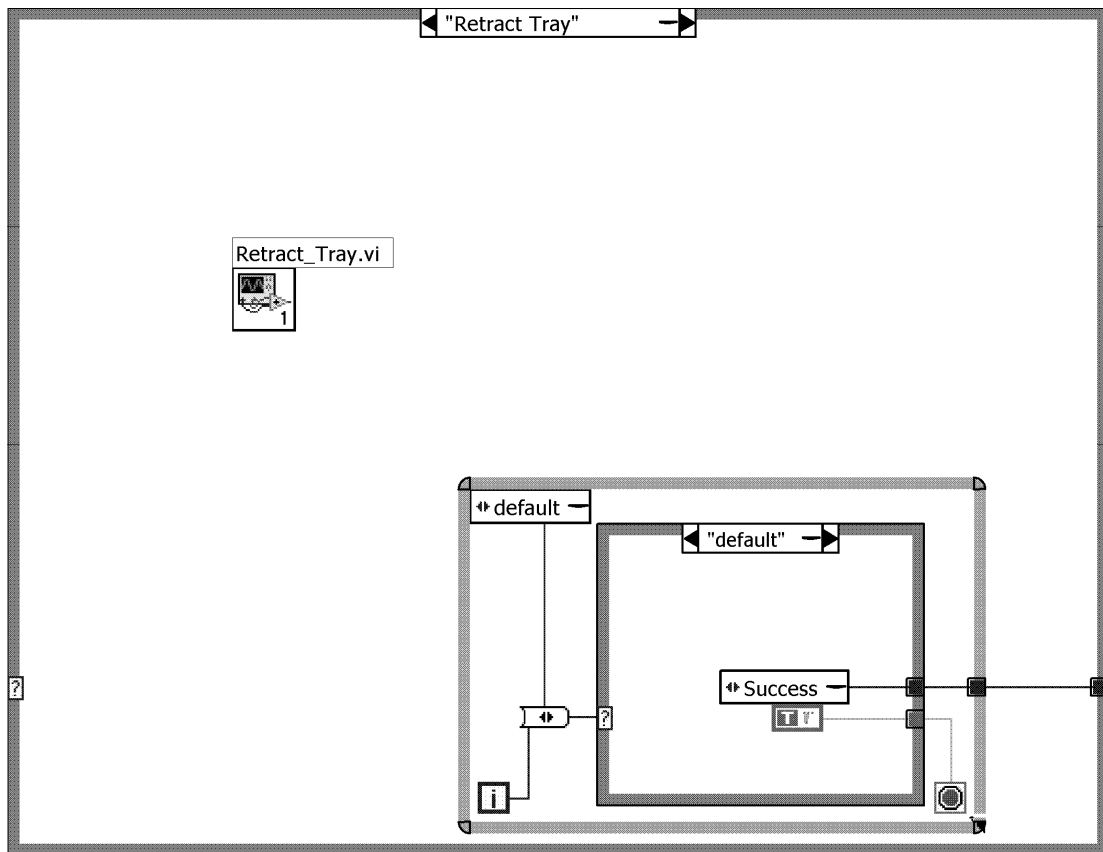this transition is active

Error

Error?

- 180 -

"Error"

default

"default"

Quit

i

"Success"
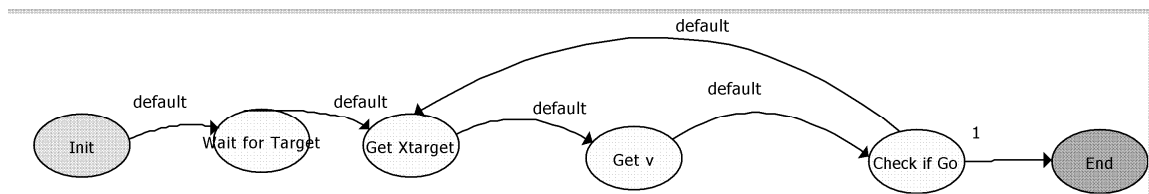
all checks successful   Error Message

default

"default"

Quit

i
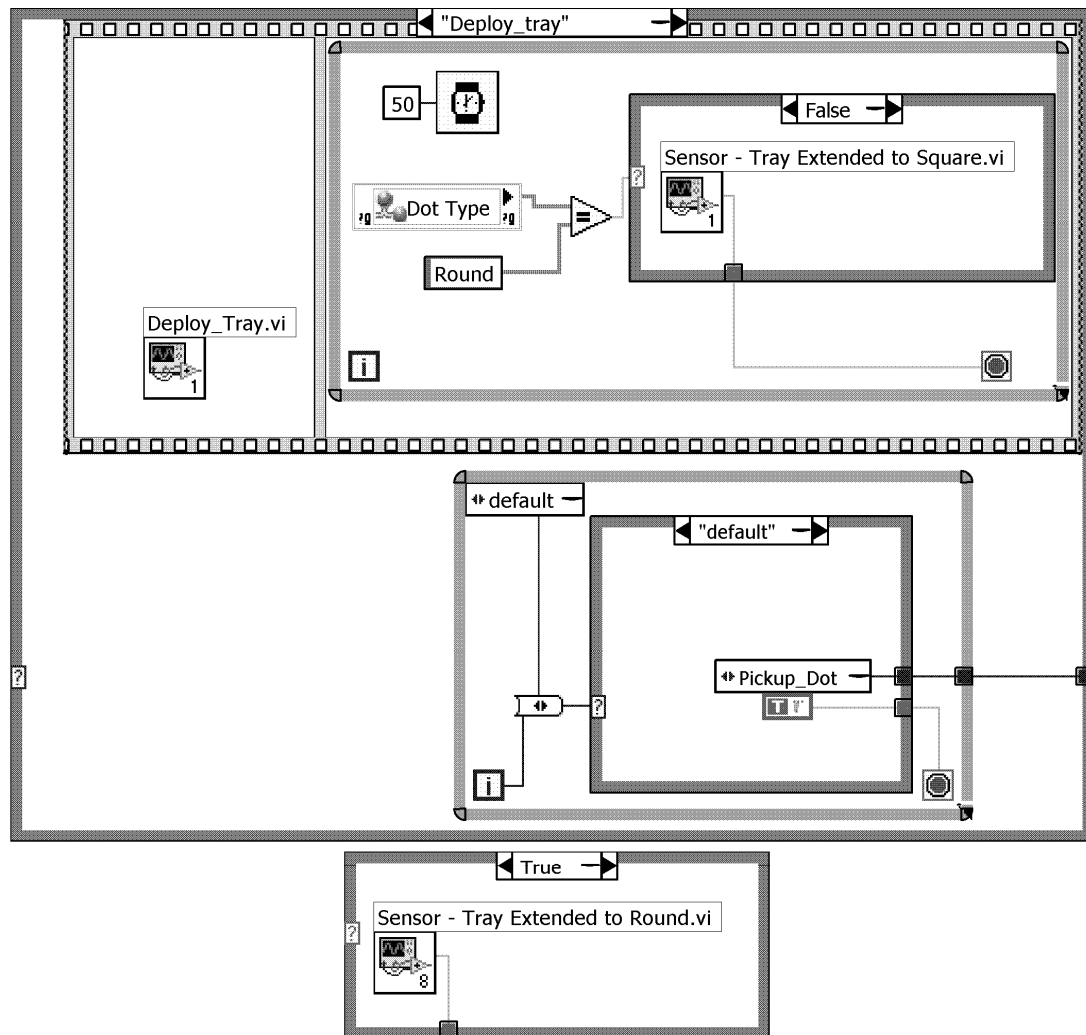
Targeting

State Diagram

- 183 -

Block Diagram

Right-click the border of this outer While Loop and select Edit State Diagram to open the State Diagram Editor Window.

This outer Case structure contains cases that correspond to the states in the state diagram.
Configure each case to reflect the actions you want each state to perform.

◀ "Get Xtarget" ▶

◀▶ default ─

"default" ▶

◀▶ Init ─

◀▶ Get v ─

i

◀▶ _Quit_ ─

You only can edit certain parts of the State Machine. Right-click the While Loop and select
Unlock Code From State Diagram to unlock the state machine from the State Diagram Editor.

- 184 -

"_Quit_"

The _Quit_ case has no corresponding state on the state diagram -
it exists to indicate to the outer While Loop when to stop executing.
This case is executed immediately after the case for any terminal state,
and is the last case to execute. Place any general clean-up code here.

Quit

"Init"

Each non-terminal state has at least one transition.
This inner While Loop and inner Case structure
determine which state executes next. The While
Loop executes the cases in the Case structure until
the conditional terminal receives a TRUE value.

default

"default"

Wait for Target

- 185 -

"Get v"

default

"default"

Check if Go

i

"Check if Go"

Initial Magnet Position (in)

State - Check if Go.vi

Sensor - Position.vi

Initial Position at Touchdown (in)

1

" 1"

Add a boolean wire
that is TRUE when
this transition is active

End

i

Check If Go

- 189 -
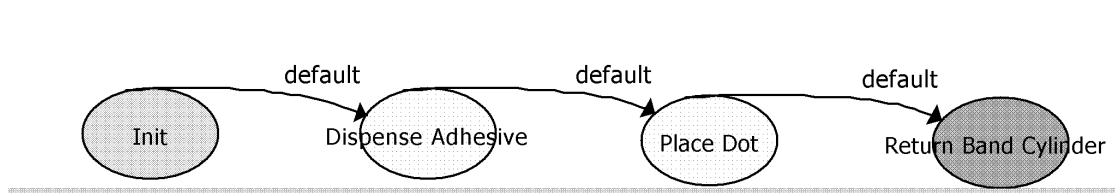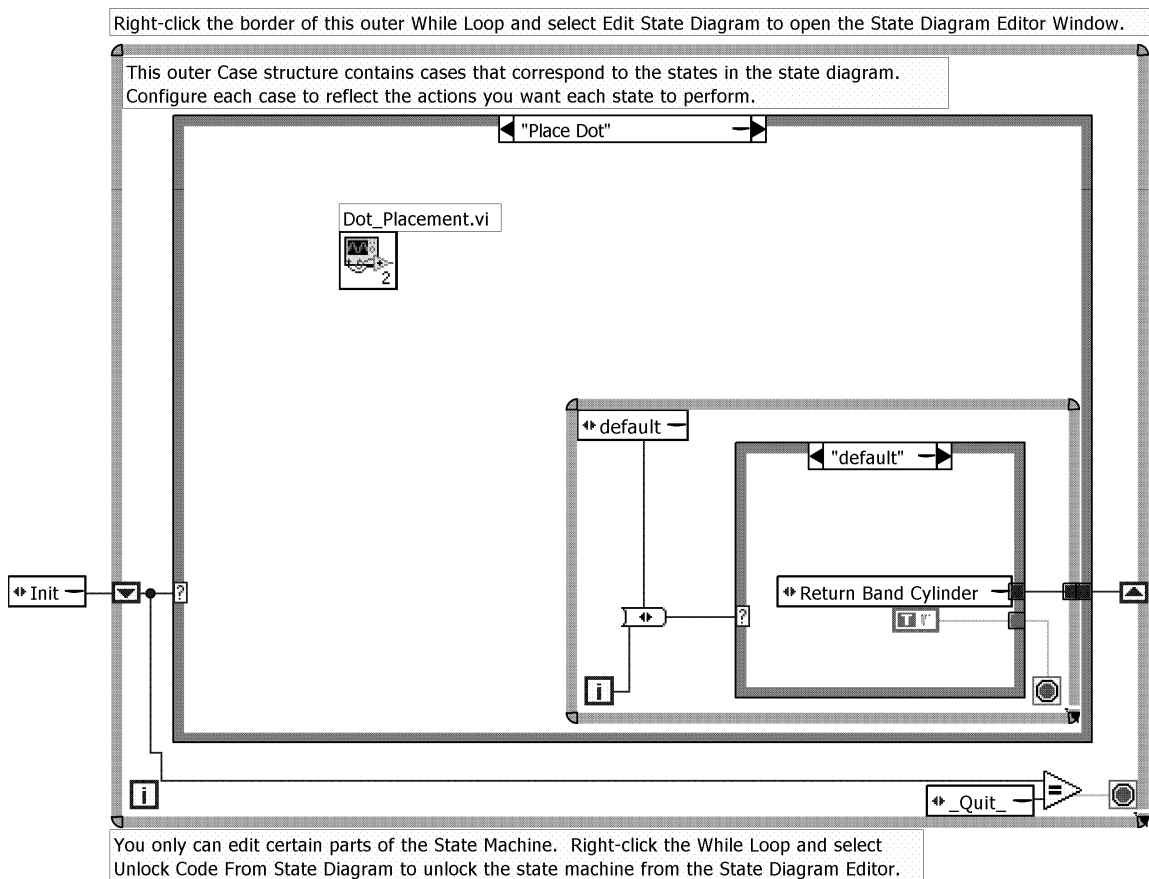
Band Cylinder Execution

State Diagram

Block

"_Quit_"

The _Quit_ case has no corresponding state on the state diagram -
it exists to indicate to the outer While Loop when to stop executing.
This case is executed immediately after the case for any terminal state,
and is the last case to execute. Place any general clean-up code here.

Quit

"Init"

Each non-terminal state has at least one transition.
This inner While Loop and inner Case structure
determine which state executes next. The While
Loop executes the cases in the Case structure until
the conditional terminal receives a TRUE value.

default

"default"

Dispense Adhesive

- 192 -

"Dispense Adhesive"

State - Dispense Adhesive.vi

default

"default"

Place Dot

"Return Band Cylinder"

Initial Position (in)

State - Return Band Cylinder.vi

default

"default"

Quit

Dispense Adhesive

Place Dot

Return Band Cylinder